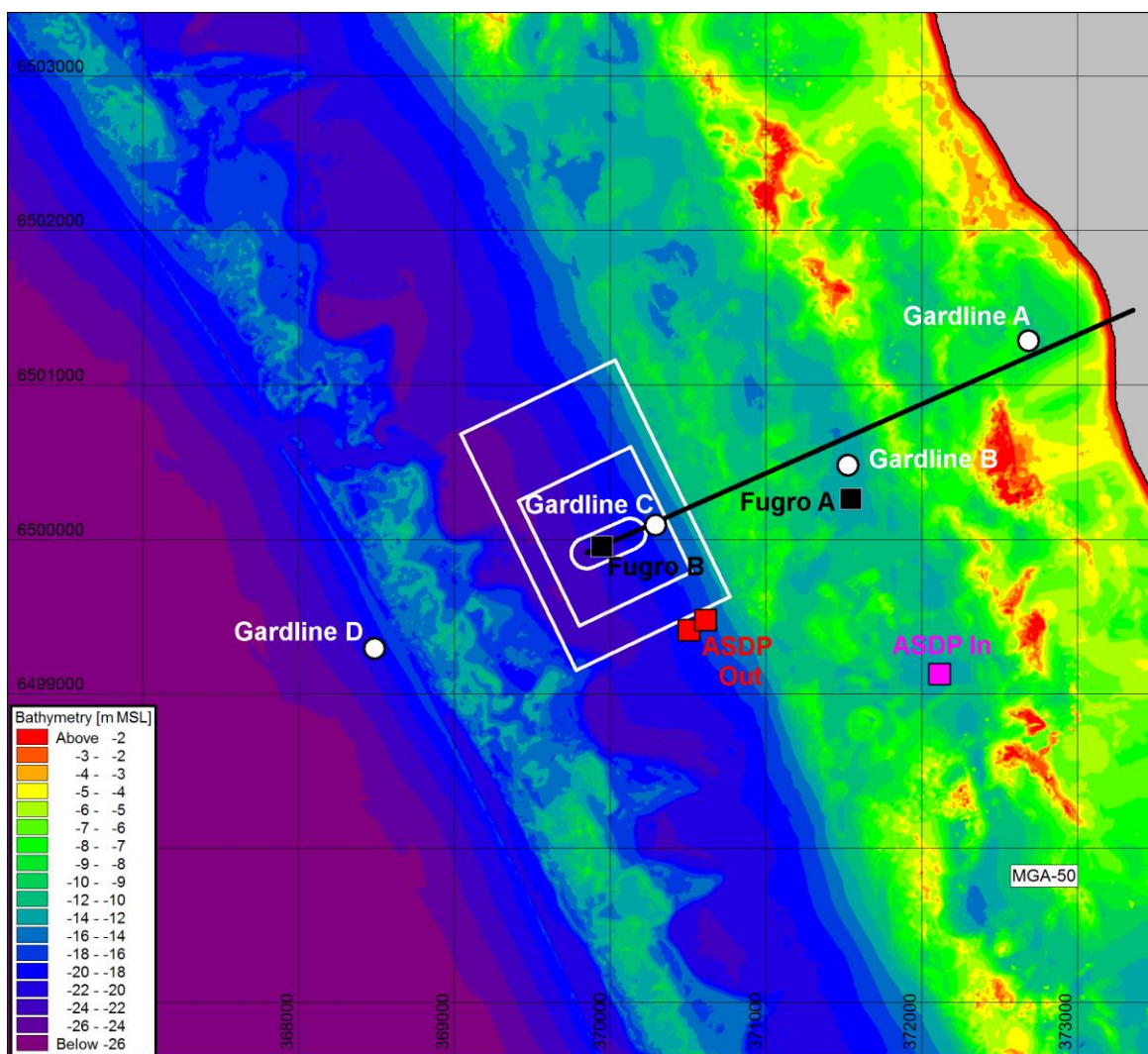


Alkimos Hydrodynamic Modelling

Scenario Report



This report has been prepared under the DHI Business Management System certified by Bureau Veritas to comply with ISO 9001 (Quality Management)

ISO 9001
Management System Certification
BUREAU VERITAS
Certification Denmark A/S



Alkimos Hydrodynamic Modelling

Scenario Report

Prepared for Water Corporation

Represented by Bree Atkinson

Project manager	Jason Antenucci
Author	Andrew Driscoll
Project number	43802755
Approval date	20 February 2019
Revision	Rev. 0
Classification	Confidential

CONTENTS

Executive Summary	i
1 Introduction	1
1.1 Background	1
1.2 Report Structure	1
1.3 Conventions	1
2 Project Overview	3
2.1 High-Level Site Characterisation	3
2.2 Overview of Modelling Approach	6
2.3 Summary of Local 3D Hydrodynamic Model	6
2.3.1 Introduction	6
2.3.2 Model System	7
2.3.3 Model Setup	8
2.3.4 Simulation Periods	12
3 Scenario Configuration.....	13
3.1 General	13
3.2 Development Overview - WWTP	14
3.3 Development Overview - ASDP	16
3.4 Near-field Dilution and Far-field Coupling	19
3.4.1 General	19
3.4.2 WWTP Near-field Characterisation	19
3.4.3 ASDP Near-field Characterisation	21
3.5 Dissolved oxygen	22
3.6 Fecal Indicator Bacteria	23
4 Results and Discussion	25
4.1 General	25
4.2 ASDP Wastefield.....	25
4.3 WWTP Wastefield	26
4.4 ASDP Seawater Intake	26
4.5 Dissolved Oxygen Saturation.....	33
5 References.....	34
APPENDIX A: Scenario Screening Design Periods	
APPENDIX B: ASDP Excess Salinity Fields	
APPENDIX C: WWTP S2 (Seafood Consumption) and S3 (Recreational) Mapping	
APPENDIX D: Dissolved Oxygen Saturation Fields	

FIGURES

Figure 2-1	Map indicating locations of Fugro (2005) and Gardline (2017-2018) instrumentation installed on behalf of Water Corporation. Graticules of overlain MGA grid are 1km squares.	4
Figure 2-2	Flowchart of models applied in the present work.....	6
Figure 2-3	Unstructured mesh applied for the Local 3D Hydrodynamic Model (full area).	10
Figure 2-4	Unstructured mesh applied for the Local 3D Hydrodynamic Model (detail), showing the preferred ASDP intake and outfall locations.	11
Figure 3-1	Candidate development plans for the Alkimos site. The combination of Intake A / Outfall B has been carried forward for the detailed assessment reported here. Image adapted from Water Corporation (2018), with updated coordinates.	13
Figure 3-2	Diurnal variation in WWTP discharge flowrate as applied in scenario testing, extrapolated based on 11 months of observed operational flows at existing Alkimos WWTP facility.	15
Figure 3-3	Annual variation in WWTP discharge temperature as applied scenario testing, based upon measured discharge temperatures from the existing Alkimos WWTP facility.	15
Figure 3-4	Assembly of ambient salinity measurements from multiple sources plotted onto a common generic 12 month time axis, superimposed by the sine curve used as a conservative estimate of the upper salinity envelope for the calculation of ASDP discharge salinity.....	18
Figure 3-5	Network of lateral sources applied to describe the WWTP linear diffuser (upper left, where diffuser endpoints are indicated with black squares) and ASDP rosette diffusers (lower right, where red squares denote rosette locations).	21
Figure 3-6	Definition sketch for near-field behaviour of a dense discharge from a single port diffuser (after Roberts, 1997).	22
Figure 4-1	Vertical cross-shore section AB through ASDP rosettes – annual 95 th percentile excess salinity.	28
Figure 4-2	Vertical cross-shore section AB through ASDP rosettes – annual 95 th percentile WWTP tracer concentration (= 5 th percentile WWTP dilution).....	28
Figure 4-3	Vertical cross-shore section CD through WWTP diffuser line – annual 95 th percentile excess salinity.	29
Figure 4-4	Vertical cross-shore section CD through WWTP diffuser line – annual 95 th percentile WWTP tracer concentration (= 5 th percentile WWTP dilution).....	29
Figure 4-5	Annual time series plot of ASDP instantaneous excess salinity at the ASDP intake location.	30
Figure 4-6	Annual time series plot of ASDP instantaneous FIB bacterial counts at the ASDP intake location.	30
Figure 4-7	Annual percentile plot of ASDP instantaneous excess salinity at the ASDP intake location.	31
Figure 4-8	Annual percentile plot of ASDP instantaneous FIB bacterial counts at the ASDP intake location. Note that the focussing of the y-axis on 95 th percentile and above to facilitate viewing.	31

TABLES

Table 2-1	Details of dedicated fixed instrumentation established at the Alkimos WWTP/ASDP site, as locations indicated in Figure 2-1. Gardline particulars as shown pertain specifically to Deployment 1. Minor shifts to positioning, ambient depth and vertical bin elevations are seen between deployments.	5
Table 2-2	Summary of Regional and Local MIKE3 hydrodynamic model configurations as applied.....	9
Table 2-3	Vertical discretisation applied in Local 3D Hydrodynamic Model.	12

Table 3-1	Particulars for the Alkimos WWTP outfall as simulated. Environmental loads as specified in Water Corporation (2018).	14
Table 3-2	Particulars for the preferred candidate Alkimos ASDP rosette outfall as simulated.	16
Table 3-3	Representative background salinity and temperature conditions as applied for previous modelling of the Alkimos WWTP in WP (2005).	17
Table 4-1	Water quality performance statistics at the ASDP intake. Results are colour coded with green comfortably within modelled criteria, yellow also within the criteria modelled however is encroaching towards the criteria, and red signals exceedance of the criteria (of which there are none).	32

GLOSSARY

2DV	Two Dimensional, in Vertical plane
ABSLMP	Australian Baseline Sea Level Monitoring Project
ADCP	Acoustic Doppler Current Profiler (TRDI Branded wave/current meter)
AHD	Australian Height Datum
AHS	Australian Hydrographic Service
ANTT	Australian National Tide Tables
ASB	Above Sea Bed
ASDP	Alkimos Seawater Desalination Plant
AWAC	Acoustic Wave and Current Profiler (Nortek branded wave/current meter)
BoM	Australian Bureau of Meteorology
CD	Chart Datum
C-MAP	Commercial package of digital navigation charting by Jeppesen
CTD	Conductivity Temperature Depth instrument
DoT	Western Australian Dept. of Transport
FIB	Fecal Indicator Bacteria
HYCOM	Hybrid Coordinate Ocean Model
IMOS	Integrated Marine Observing System
LAT	Lowest Astronomical Tide
LEPA	Low Ecological Protection Area
LIDAR	Light Detection and Ranging
MSL	Mean Sea Level
NOAA	US National Oceanographic and Atmospheric Administration
PRP	(Alkimos) Peer Review Panel
UNESCO	United Nations Educational, Scientific and Cultural Organization
WP	WorleyParsons
WWTP	(Alkimos) Wastewater Treatment Plant
Zone S2	Environmental quality guideline for Consumption of Seafood
Zone S3	Environmental quality guideline for Primary or Secondary Recreational Contact

Executive Summary

DHI Water and Environment (DHI) has been contracted by the Water Corporation to perform a numerical modelling assessment of hydrodynamics, plume transport and dilution for the discharge of brine effluent from the proposed Alkimos Seawater Desalination Plant (ASDP). The intake and outfall structures of the ASDP will be located amidst or offshore of a highly complex reef system (Figure 2-1).

Previous works to date have included a model calibration report (DHI, 2018a) as well as a conceptual design report for the ASDP diffuser (DHI, 2018b). A screening study considering various combinations of intake/outfall locations and concepts has been completed by DHI and will be reported under a separate cover. The present report describes the results of a 12-month simulation assessing the environmental performance of the preferred ASDP design alternative featuring approximately 300 ML/d of potable water production, in combination with expansion of the existing WWTP facility to its permitted capacity of 80 ML/d.

The overall objective of the study is to develop a local validated model that supports the design process, environmental approvals, and stakeholder engagement. Model outputs are used to assess both environmental and public health related criteria, as well as being used to provide an assessment of the possible microbiological challenge posed by the treated wastewater from the WWTP outfall on the ASDP intake. The interrogation of the model outputs consider:

- the near-bottom excess salinity footprint of the ASDP output
- concentrations at the ASDP intakes of excess salinity originating from the ASDP outfall
- concentrations at the ASDP intakes of fecal indicator bacteria (FIB) originating from the WWTP outfall
- mapping of environmental quality guideline zones for Consumption of Seafood (Zone S2) and for Primary or Secondary Recreational Contact (Zone S3)
- the related dissolved oxygen (DO) response of the above near-bottom footprint, considering atmospheric input and sediment oxygen demand

The brine discharge, following dilution within the near field to an excess salinity of approximately 1.1 ppt above ambient, is seen to descend perpendicularly downslope to the deep portion of the channel between the outer and second reef lines where the existing WWTP diffuser is located (Figure 2-1). This behaviour is a near-permanent feature, and is only minimally affected by the behaviour of the water column above it. The descending brine wastefield then bifurcates as it approaches the barrier of the outer reefline and spreads at reduced velocity in both shore-parallel directions and forms a semi-permanent, kilometre-scale near-bed stratified feature within the channel. The brine layer shows variability from month to month depending on hydrographic conditions, but does not (within the year simulated) demonstrate major changes in dimensions by season.

At the ASDP intakes, water quality performance criteria relating to the ASDP and WWTP discharges are met throughout the 12-month simulation. Concentrations of fecal indicator bacteria (FIB) at the ASDP intakes were assessed against 95% concentration criteria for both Thermotolerant Coliforms (TTC) and Enterococci spp., and found to be within acceptable limits. Similarly, ASDP tracer concentrations at the ASDP intakes were also

within acceptable limits, indicating that recirculation of the desalination facility is not a significant concern.

Dissolved oxygen (DO) impacts have been assessed using a simple model which considers atmospheric input in combination with sediment oxygen demand, which leads to a reduction in DO as a result of the longer near-bed residence time associated with the near-bottom footprint of the negatively buoyant diluted ASDP wastefield. The model results were interrogated against a criterion that DO saturation should not fall below 90% for a running median calculated over a 7-day window. This interrogation resulted in several patches of exceedances occurring within three of the simulation months.

However, the violations of the median 90% DO saturation criterion were only slightly below this threshold. The minimum 7-day median DO saturation percentage over the year was 88%. Further, sensitivity tests have shown that exceedances of the criterion are extremely sensitive to the modelled vertical dispersion. Even small departures from the conservatively small dispersion applied in the present assessment results in the disappearance of all exceedances of the criterion. For this reason, it is considered highly unlikely that sediment oxygen demand in combination with the additional residence time imposed by the ASDP plume would in practice result in exceedances of the specified DO criterion within the area of interest.

DO impacts associated with biological and chemical oxygen demand have not been considered in the present work.

1 Introduction

1.1 Background

DHI Water and Environment (DHI) has been contracted by the Water Corporation to perform a numerical modelling assessment of hydrodynamics, plume transport and dilution for the discharge of brine effluent from the proposed Alkimos Seawater Desalination Plant (ASDP). The intake and outfall structures of the ASDP will be located amidst or offshore of a highly complex reef system.

The proposed ASDP will be co-located with the existing Alkimos Wastewater Treatment Plant (WWTP), which was commissioned in 2010 and discharges buoyant treated wastewater through a linear offshore diffuser. A previous modelling study (WP, 2005) was prepared in support of submittals for regulatory approval of the WWTP. The marine monitoring program has found the WWTP plant to be compliant to date in relation to the marine discharge and there is no indication of any adverse marine impacts. The minimisation of potential impacts to the reef system is a priority for the development of the ASDP, as is the maintenance of the level of dilution which has already been permitted for the existing WWTP.

Previous works to date have included a model calibration report (DHI, 2018a) as well as a conceptual design report for the ASDP diffuser (DHI, 2018b). A screening study considering various combinations of intake/outfall locations and concepts has been completed by DHI and will be reported under a separate cover. The present report describes the results of a 12-month simulation assessing the environmental performance of the preferred ASDP design alternative, in combination with expansion of the existing WWTP facility to its permitted capacity of 80 ML/d.

Model outputs are used to assess both environmental and public health related criteria, as well as being used to provide an assessment of the possible microbiological challenge posed by the treated wastewater from the WWTP outfall on the ASDP intake.

1.2 Report Structure

The remainder of the report is structured as follows:

- Section 2 describes a scope overview and a high level site characterisation
- Section 3 presents an overview of the proposed WWTP expansion and ASDP development, as well as describing how these facilities are incorporated into the Local 3D Hydrodynamic Model
- Section 4 presents results and discussion from the models described in Section 3.
- Section 5 provides a list of references cited.

1.3 Conventions

Unless otherwise stated, the following conventions prevail within the report:

- The local models have been constructed and reported using horizontal positioning in the MGA-50 projection using the GDA94 coordinate datum.
- The models have been constructed using a vertical datum of mean sea level (MSL), and this is used throughout except where otherwise noted.
- Wind and wave directions are reported as "from", while current directions are "to".
- Except where noted, time references denote Greenwich Mean Time (GMT).

2 Project Overview

2.1 High-Level Site Characterisation

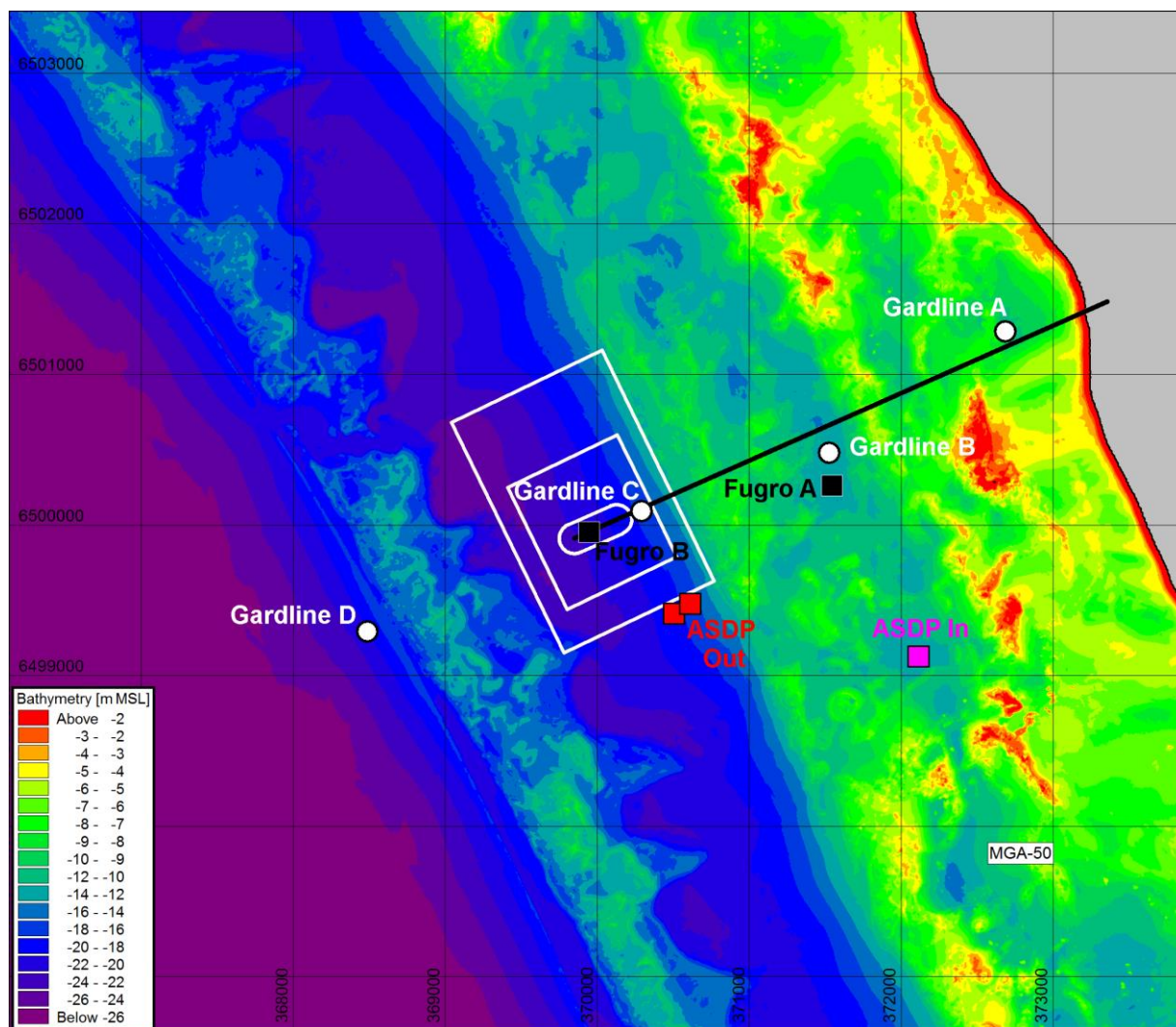
The study area features weak, dominantly diurnal tidal forcing with a mean daily range on the order of 0.7m. Wind driven processes predominate, particular in summer due to land-sea breeze cycles commonly reaching speeds greater than 15 m/s. Wind stresses are at their lowest typically in late autumn (Apr/May). Median depth-averaged current speeds range from 9.9 cm/s in 21m water depth immediately offshore of the outer reef to 7.8 cm/s at the existing WWTP outfall to 4.3 cm/s in 10m depth within the inshore reef.

The broader-scale circulation in the region is dominated by the Leeuwin Current, a warm boundary current flowing southwards along the edge of the continental shelf. Inshore of the Leeuwin Current, the Capes Current flows northward as a result of upwelling and northward wind stresses, and is thus strongest in spring and summer months. Owing to its location on the inner coastal shelf, as well as proximity to the Leeuwin Current and the inshore Capes Current, nontidal residual flows contribute to the current energy on the shelf near the Alkimos site. Continental shelf waves induce long-period modulations in water level which can reach the same order of magnitude as the tide. Further details can be found in Gallop et al (2012), Mihanovic et al (2016), and references therein.

The area is exposed to persistently high swell conditions, despite some sheltering to swell originating in the Southern Ocean from Rottnest Island. Annual mean wave conditions approaching the outer reef have been measured at a significant wave height of $H_s=1.8\text{m}$ with an associated peak period of $T_p=12.2\text{s}$.

Offshore, dominant mechanisms are a combination of meteorological and oceanographic (non-tidal) flows. Over the inner reef, wave-driven currents become important when waves are large. Due to the complexity of the reef structure, wave effects on mean flows tend to be manifested primarily as shoreward-directed flow over shallow areas and offshore-directed return flows in locally deeper areas.

The site includes the existing Alkimos WWTP facility, which incorporates a 300m long linear diffuser located 3.7 km from the shoreline (Figure 2-1). The WWTP and ASDP development scenarios simulation in the present work are described in detail in Sections 3.2 and 3.3.



WWTP diffuser, and WWTP regulatory zones and candidate ASDP intake and outfall locations also shown. Bathymetry shown is 5m resolution to align with the native 5m gridded resolution bathymetric LIDAR datasets (DoT, 2009; 2016). The Local Hydrodynamic Model mesh, per Figure 2 3 and Figure 2 4, is necessarily coarser.

Figure 2-1 Map indicating locations of Fugro (2005) and Gardline (2017-2018) instrumentation installed on behalf of Water Corporation. Graticules of overlain MGA grid are 1km squares.



Table 2-1 Details of dedicated fixed instrumentation established at the Alkimos WWTP/ASDP site, as locations indicated in Figure 2-1. Gardline particulars as shown pertain specifically to Deployment 1. Minor shifts to positioning, ambient depth and vertical bin elevations are seen between deployments.

Station	Coordinates		MGAS0		Instrument Type(s)	Ambient Depth (m MSL)	bin thickness	"Bottom" Data m MSL (m ASB)	"Surface" Data m MSL (m ASB)	Provided Items	Output Time Step
	Long	Lat	E(m)	N(m)							
Fugro A* ¹	115.64558	-31.62563	371,545	6,500,263	Aanderaa RCM9	12m	n/a	-9.0m MSL (+3.0m ASB)	-3.0m MSL (+9.0m ASB)	Directional currents* ²	10min
					Aanderaa RCM7						
Fugro B	115.62857	-31.62832	369,936	6,499,945	Wave-enabled 300 kHz RDI Workhorse ADCP	20m	2m	-15.5m MSL (+4.5m ASB)	-3.5m MSL (+16.5m ASB)	Directional currents, Temperature, Bulk wave parameters* ³	10min (flow) 3hrs (waves)
Gardline A (Deployment 1)	115.65881	-31.61653	372,788	6,501,287	Nortek AWAC	9.5m	1m	-8.1m MSL (+1.4m ASB)	-2.1m MSL (+7.4m ASB)	Directional currents, Temperature, Pressure, Depth (derived), Bulk wave parameters	10min (flow, pressure, water temp) 2hrs (waves)
Gardline B (Deployment 1)	115.64580	-31.62347	371,563	6,500,503	Nortek AWAC	12.7m	1m	-11.3m MSL (+1.4m ASB)	-3.3m MSL (+9.4m ASB)	Directional currents, Temperature, Pressure, Depth (derived), Bulk wave parameters	10min (flow, pressure, water temp) 2hrs (waves)
Gardline C (Deployment 1)	115.63203	-31.62755	370,263	6,500,034	Nortek AWAC	17.9m	1m	-16.5m MSL (+1.4m ASB)	-3.5m MSL (+14.4m ASB)	Directional currents, Temperature, Pressure, Depth (derived), Bulk wave parameters	10min (flow, pressure, water temp) 2hrs (waves)
Gardline D (Deployment 1)	115.61307	-31.63455	368,474	6,499,235	Nortek AWAC	20.7m	1m	-19.3m MSL (+1.4m ASB)	-4.3m MSL (+16.4m ASB)	Directional currents, Temperature, Pressure, Depth (derived), Bulk wave parameters	10min (flow, pressure, water temp) 2hrs (waves)

*1 Instrument was moved by a third party to approx. 120m WNW of this location sometime between 28 May and 26 Jun 2005.

*2 Water temperature provided for provisionally processed versions of both instruments, but not included in final deliverable and some data clearly erroneous. Omitted from present work.

*3 Instrument also records pressure, but this information was not included in data provided to DHI.

2.2 Overview of Modelling Approach

The overall objective is to develop a local validated model that will support the design process, environmental approvals, and stakeholder engagement. The modelling uses a downscaled model ecosystem approach to meet these objectives, in the manner described in Figure 2-2.

The top tier models shown in Figure 2-2 are global in scale. The middle tier model shown in Figure 2-2 is regional in scale, and is a project-tailored derivative of a version originally developed by DHI for the Australian Maritime Safety Authority. The Regional Hydrodynamic Model is applied purely for the purpose of generating boundary data to force the Local Hydrodynamic Model.

The bottom tier model shown in Figure 2-2 was developed specifically for this project, with the Local 3D Hydrodynamic Model being the vehicle applied for the ASDP and WWTP plume assessments.

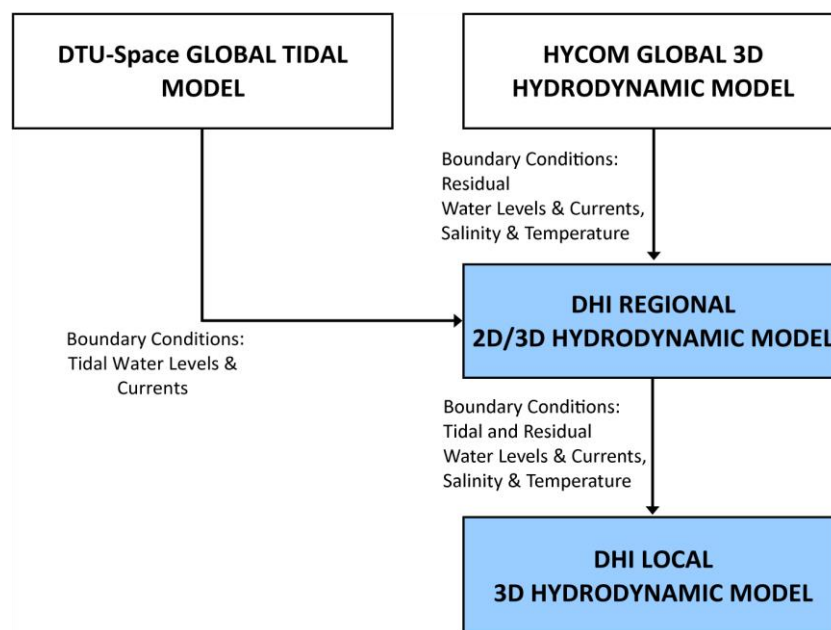


Figure 2-2 Flowchart of models applied in the present work.

2.3 Summary of Local 3D Hydrodynamic Model

2.3.1 Introduction

The Local 3D Hydrodynamic Model is the decision making tool for ASDP intake/outfall assessments. The Local 3D Hydrodynamic Model is forced by the combination of extracted boundary conditions from the Regional Hydrodynamic Model, measured wind records from Ocean Reef, and (when enabled) wave forcing from the Local Wave Model.

The Regional Hydrodynamic Model plays the role of a facilitator for the present work, as it provides no answers itself but provides critical forcing data to drive the Local 3D Hydrodynamic Model. The Regional Hydrodynamic Model incorporates both tidal and

nontidal forcing, as well as describing the fully stratified water column offshore of southwest WA. This ensures that the complex mechanisms that dominate medium-term water levels and flows on the shelf are present in the boundary data which are then fed into the Local 3D Hydrodynamic Model as a one-way nesting. Further details on the setup and calibration of the Regional Hydrodynamic are available in DHI (2018a).

Wave forcing plays a role in driving circulation within the inner portion of the reef when waves are large, but are of minimal importance when waves are smaller. A spectral wave model has been established for the purposes of a) providing direct forcing onto the mean flow via radiation stresses and b) modifying the effective bed roughness felt by the hydrodynamic model via wave-induced roughness calculations. Testing has shown that the inclusion of wave forcing tends to result in modest improvements relative to measurements in the inshore stations, but to reduce model skill in deeper water. The results presented here omit wave forcing.

2.3.2 Model System

MIKE 3 FMHD solves the time-dependent conservation equations of mass and momentum in three dimensions, the Reynolds-averaged Navier-Stokes equations. The flow field and pressure variation are computed in response to a variety of forcing functions, when provided with the bathymetry, bed resistance, hydrographic boundary conditions, etc. The conservation equations for heat and salt are also included. MIKE 3 uses the UNESCO equation for the state of sea-water (1980) as the relation between salinity, temperature and density. The hydrodynamic phenomena included in the equations are:

- Effects of buoyancy and stratification
- Turbulent (shear) diffusion, entrainment and dispersion
- Coriolis forces
- Barometric pressure gradients
- Wind stress
- Variable bathymetry and bed resistance
- Hydrodynamic effects of rivers, outfalls and sediment
- Sources and sinks (both mass and momentum)
- Heat exchange with the atmosphere including evaporation and precipitation
- Wave forcing via radiation stresses

MIKE 3 FM has an advection - diffusion equation solver that simulates the transport of heat and of dissolved and suspended substances subject to the transport processes described by the hydrodynamics. A full heat balance is included in MIKE 3 for the calculation of water temperature.

MIKE 3 FM is based on an unstructured flexible mesh and uses a finite volume solution technique based on linear triangular or quadrilateral elements. This approach allows for a variation of the horizontal resolution of the model grid mesh within the model area to allow for a finer resolution of selected sub-areas.

The vertical dimension in MIKE 3 FM can be discretised either using a sigma grid or a sigma-z grid. This allows for maximum flexibility in model construction depending on the nature of the problem at hand and the simulation domain.

The MIKE 3 FM model allows for consideration of wave radiation stresses, tidal potential, and an array of structures (eg weirs, culverts, piers, gates, turbines). The commercial basis of the model and the large global user base means that new updates are regularly available with additional features and integration with other MIKE models. Integration between MIKE3 FMHD and MIKE21 SW allows for the options of wave action

affecting mean flows in terms of direct forcing (via radiation stresses) as well as via additional effective roughness (wave-induced roughness calculations).

The model is available in hydrostatic and non-hydrostatic versions; the hydrostatic mode has been used in this case.

2.3.3 Model Setup

The spatial extent of the Local 3D Hydrodynamic Model is shown in Figure 2-3, with details shown in Figure 2-4.

The extent of the Local Hydrodynamic Model domain is approximately 40km in the longshore direction and 14km in the cross-shore direction. The offshore boundary terminates at about the -32m MSL depth contour. The nominal mesh resolution varies from 750m at the boundary down to 50m in a high resolution area centred around the Gardline AWAC validation stations as well as the WWTP outfall.

The arrangement of the innermost mesh resolution is tailored to both the model validation of ambient processes and the simulation of effluent plumes. Whilst reef features are present at scales below 50 metres, the key topographical features of relevance to plume dynamics (in particular flow pathways from the lagoon region to offshore) are captured by the 50m resolution as demonstrated in DHI (2018a). In addition, consideration was also made as to the coupling of the near-field with the far-field model for the plume scenarios. The targeted near-field dilutions implemented into the far-field model (~1:30 and ~1:200 for the ASDP and WWTP respectively) were demonstrated to be reproduced accurately at the locations in the mesh where the sources were introduced, confirming that numerical dilution at the source locations does not unduly affect model response and that mesh resolution is also adequate in this regard.

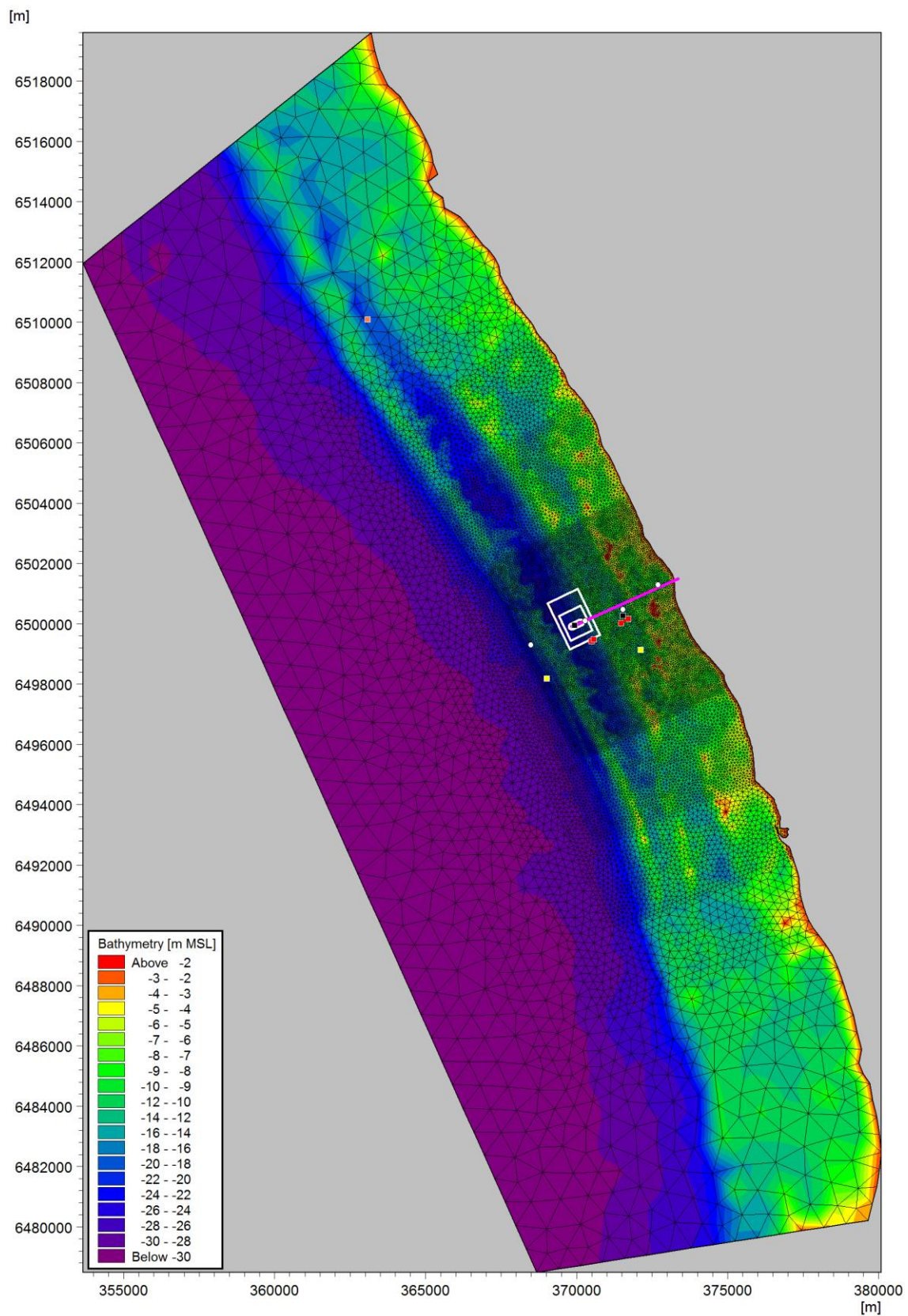
Basic details of the Local Hydrodynamic Model construction are summarised below.

- Constructed in in MGA-50 coordinates, with a vertical datum of mean sea level (MSL).
- Bathymetric data was compiled into a database with the following hierarchy: DoT (2016) LIDAR where available, followed by DoT (2009) LIDAR, and C-MAP (digital navigation charting) data for the remainder of the domain.
- 13 sigma layers over the vertical, with additional resolution at both bottom (for ASDP plumes) and surface (for WWTP plumes), as shown in Table 2-3. The surface resolution is comparable to that applied in WP (2005) for the original permitting of the WWTP.
- Boundary forcing is based on Flather boundary conditions, using water levels, and 2DV fields of velocity, salinity and temperature as extracted from the Regional 3D Hydrodynamic Model.
- Wind forcing is applied using BoM measurements at Ocean Reef. Ancillary meteorological inputs required for heat exchange calculations (air temperature, relative humidity and cloud cover) are taken from CFSR fields (Saha et al, 2011).
- Spatially and temporally varying ambient salinity and temperature are included. A full heat exchange formulation is included in a manner consistent with the Regional 3D Model.
- Wave radiation stresses and wave-induced roughness are excluded

- Bed roughness is imposed in terms of an effective grain diameter for bedforms, which are input as a map to incorporate the significantly higher roughness over the reef.

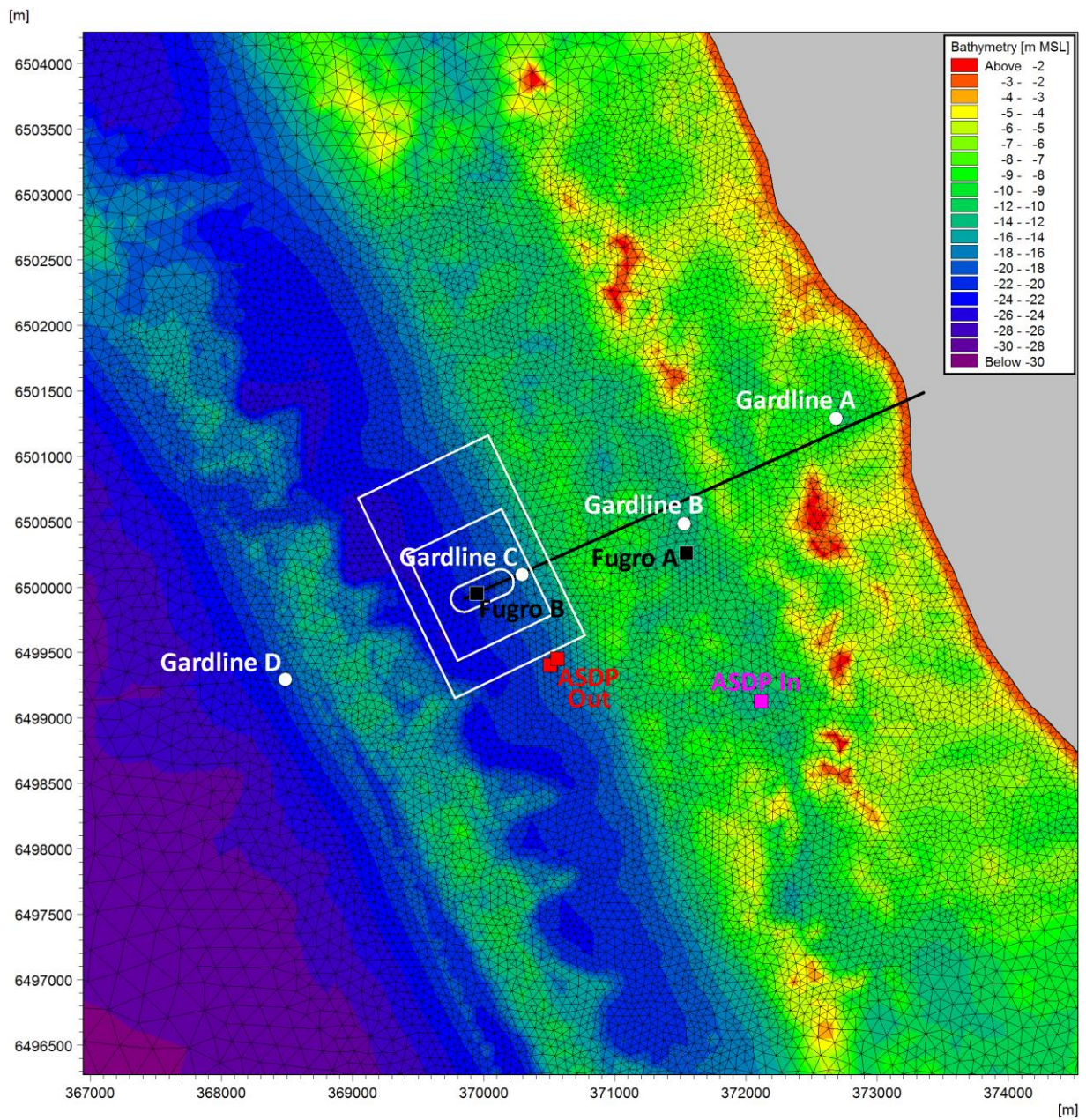
Table 2-2 Summary of Regional and Local MIKE3 hydrodynamic model configurations as applied.

Property	Local 3D Model
Model System	MIKE3FM HD
Nominal Mesh Resolution	750m → 50m
Coordinate System	MGA-50
Bathymetry	C-MAP, DoT LIDAR
Vertical Grid	13 σ layers of variable relative thickness, enhanced at surface (5%) and bottom (2.5%)
Time Step	Dynamic
Hydrodynamic Boundary Conditions	Flather Boundaries, water level + 2DV fields of u,v as extracted from Regional 3D Model
Salinity and Temperature Boundary Conditions	2DV fields of S,T as extracted from Regional 3D Model
Initial 3D Salinity & Temperature Fields	Interpolated from results of Regional 3D Model
Met Forcing	BoM-measured winds at Ocean Reef
Atm. Heat Exchange and Evaporation	Included (CFSR inputs)
Wind Friction	$w_{fc} = 0.00125$
Tidal Potential	Omitted
Roughness	Variable, based on reef mapping
Eddy Viscosity	Smagorinsky (horiz) / k- ϵ (vertical)
Dispersion Factor	1.0 (Horizontal) / 0.1 (Vertical)



White dots = Gardline AWACs, black squares = Fugro stations, orange square = Two Rocks Stn A mooring, magenta line = WWTP outfall pipe, yellow squares = candidate ASDP intakes, red squares = candidate ASDP outfalls.

Figure 2-3 Unstructured mesh applied for the Local 3D Hydrodynamic Model (full area).



White dots = Gardline AWACs, black squares = Fugro stations, black line = WWTP outfall pipe, magenta square = preferred candidate ASDP intake location, red squares = preferred candidate ASDP rosette outfall locations.

Figure 2-4 Unstructured mesh applied for the Local 3D Hydrodynamic Model (detail), showing the preferred ASDP intake and outfall locations.

Table 2-3 Vertical discretisation applied in Local 3D Hydrodynamic Model.

Layer # (from bottom)	Vertical Discretisation of σ -grid (% of water column)	Layer Thickness for Given Water Depth (m)		
		5m	10m	20m
13	5%	0.250	0.500	1.000
12	5%	0.250	0.500	1.000
11	5%	0.250	0.500	1.000
10	5%	0.250	0.500	1.000
9	10%	0.500	1.000	2.000
8	15%	0.750	1.500	3.000
7	15%	0.750	1.500	3.000
6	15%	0.750	1.500	3.000
5	10%	0.500	1.000	2.000
4	5%	0.250	0.500	1.000
3	5%	0.250	0.500	1.000
2	2.5%	0.125	0.250	0.500
1	2.5%	0.125	0.250	0.500

2.3.4 Simulation Periods

The evaluation of scenarios has been performed in two phases.

An initial screening phase (DHI, 2019) addressed a range of candidate scenarios for both WWTP and ASDP facilities, to identify the most appropriate combination to carry forward for a detailed EIA assessment. A review of long-term wind, residual current and wave data (measured and hindcast) was carried out to identify seasonally representative design periods of manageable computational burden (30 days' duration) for the scenario screening exercise. This climatological review is described in Appendix A, and resulted in the identification of the following seasonal 30 day screening periods:

- Autumn: 16 Apr – 15 May 2017
- Winter: 23 Jun – 22 Jul 2017
- Summer: 17 Nov – 16 Dec 2017

The above 30-day periods were also applied for model calibration/validation in DHI (2018a).

A final phase of the scenario assessment consists of a full 12 month simulation for the preferred candidate ASDP arrangement, in combination with the planned expansion of the WWTP facility. The 12 month simulation was performed for the period of 01 April 2017 through 31 March 2018, which approximately aligns with the deployment period for the four Gardline AWACs forming the primary pre-expansion physical baseline dataset at the site.

3 Scenario Configuration

3.1 General

The candidate development scenarios are described in detail in Water Corporation (2018), with relevant aspects summarised here. The candidate development plans for the Alkimos site are shown in Figure 3-1.

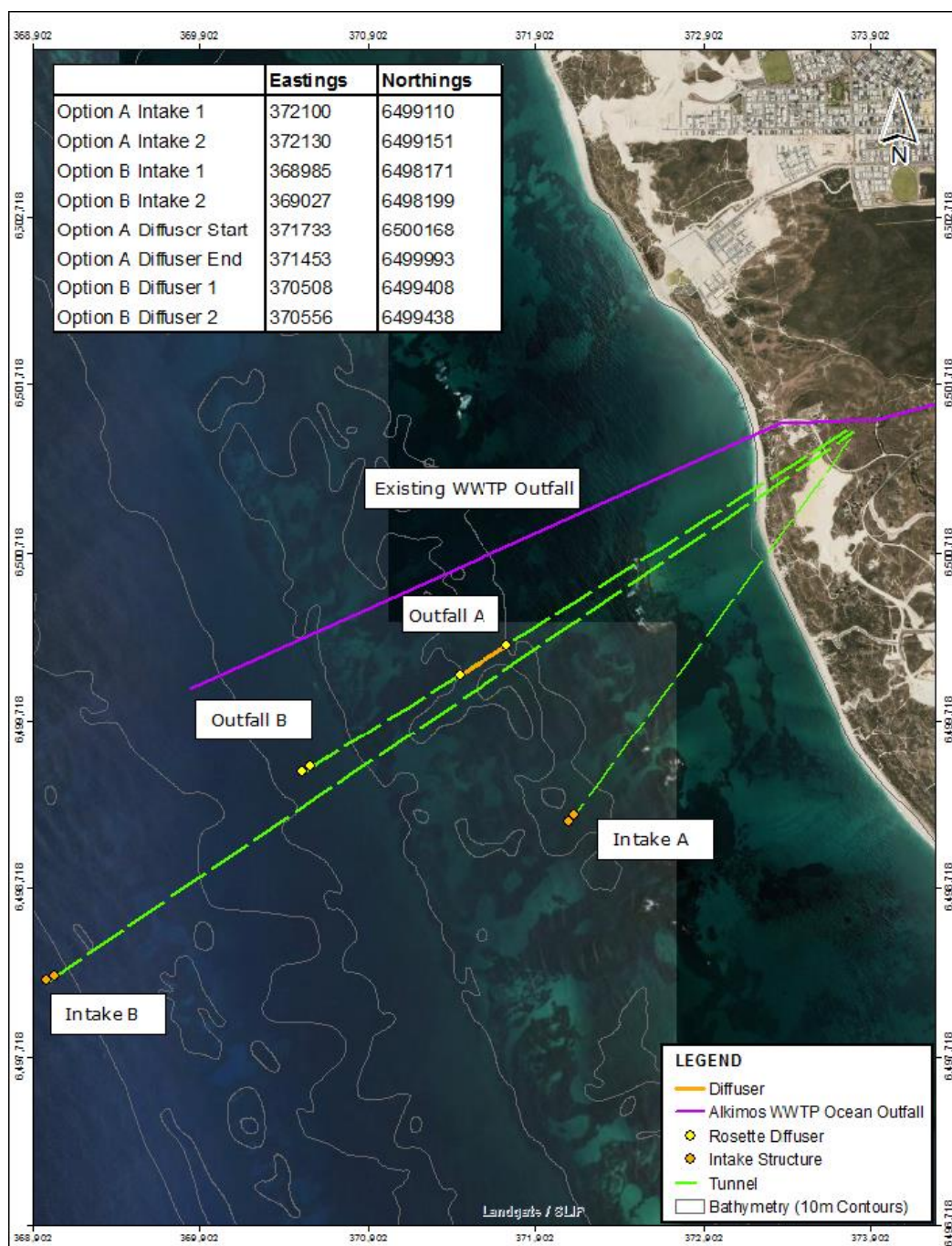


Figure 3-1 Candidate development plans for the Alkimos site. The combination of Intake A / Outfall B has been carried forward for the detailed assessment reported here. Image adapted from Water Corporation (2018), with updated coordinates.

3.2 Development Overview - WWTP

The present Alkimos WWTP outfall includes a staged linear diffuser located approximately 3.7 km offshore of the shoreline as indicated in Figure 3-1 and summarised in Table 2-1. The diffuser was sized for a discharge of 80 ML/d, but presently operates at a fraction of capacity. The existing WWTP discharge condition, per Water Corporation (2016b, 2017), is roughly 11 ML/day being discharged through a limited subset of the 100 total diffuser ports, with the remaining ports being capped.

The WWTP scenario evaluated in the present 12 month simulations includes an expansion of operations to the 80 ML/d permitted level, in conjunction with the uncapping of all diffuser ports. The WWTP discharge incorporates a diurnal variation provided by the Water Corporation based upon the established operating statistics from the existing Alkimos WWTP, which has been upscaled to match the 80 ML/d mean daily flow rate as shown in Figure 3-2.

As the WWTP discharges wastewater originating from a range of terrestrial sources, the WWTP discharge temperature is neither a constant, nor a simple function in relation to ambient seawater. Based upon a review of the measured discharge temperatures at Alkimos WWTP from 2011 to 2017, a characteristic annual profile of the monthly averaged discharge temperature was identified as shown in Figure 3-3. The monthly averaged WWTP discharge temperature is typically on the order of 3 to 5 °C warmer than the equivalent monthly averaged seawater temperature at the site.

The salinity of the WWTP discharge is nearly fresh, at 650 mg/L TDS. For the present assessment, the discharge is assumed here to be devoid of dissolved oxygen.

Table 3-1 Particulars for the Alkimos WWTP outfall as simulated. Environmental loads as specified in Water Corporation (2018).

Parameter	Value
Coordinates (inshore to offshore ends)	(370127,6500036) to (369850,6499911)
Effective diffuser length	300m
Water depth over diffuser length	19.6 to 22.2m; nominally 21m
Number of Ports	100
Port Spacing	3m
Port Diameter	0.1m*
Port Elevations above Seabed	~1.0 m
Port arrangement	Perpendicular to feeder, alternating (155.8°,335.8°)
Vertical discharge angle	Parallel with seabed
Mean Daily Flow Rate	80 ML/day (0.926 m ³ /s)**
Port exit velocity	1.18 m/s
Discharge TDS	650 mg/L
Discharge Temperature	Variable – see Figure 3-3
Discharge DO	0 mg/L
Bacterial load (Total TTC)	100,000 CFU / 100 mL
Bacterial load (Enterococci spp.)	20,000 MPN / 100 mL

*Drawings show slightly larger D=0.106m for offshore 60 ports **with diurnal variation (Figure 3-2).

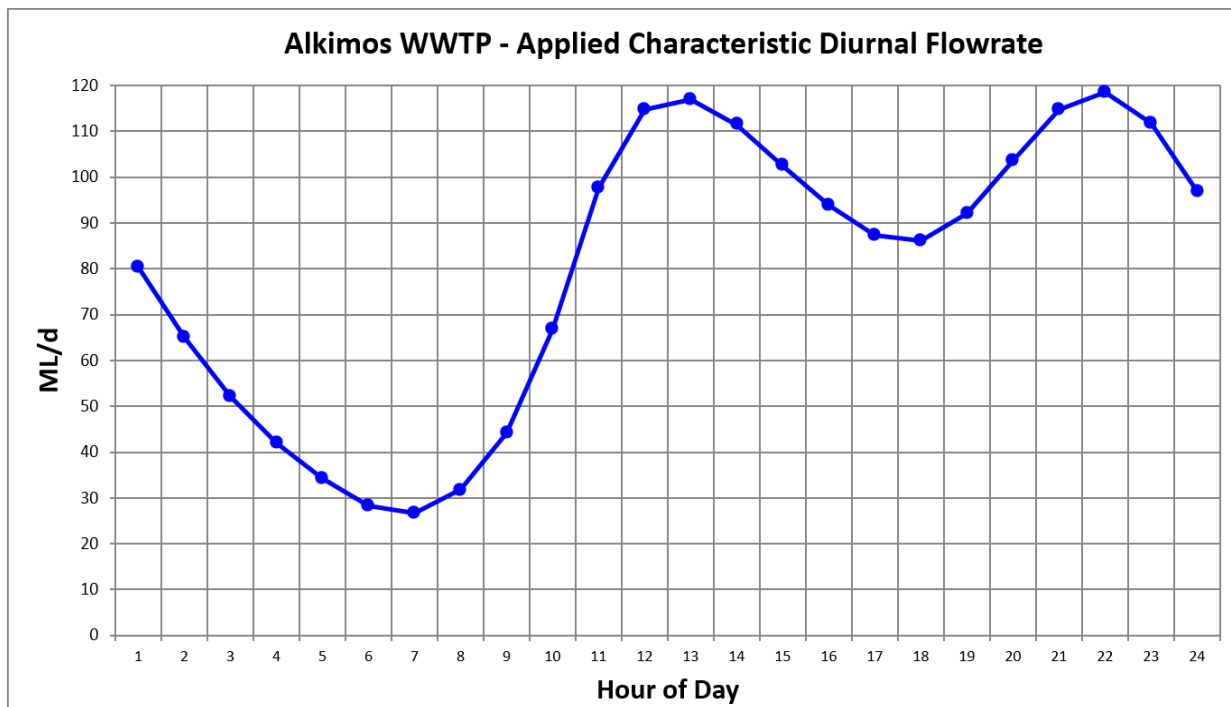


Figure 3-2 Diurnal variation in WWTP discharge flowrate as applied in scenario testing, extrapolated based on 11 months of observed operational flows at existing Alkimos WWTP facility.

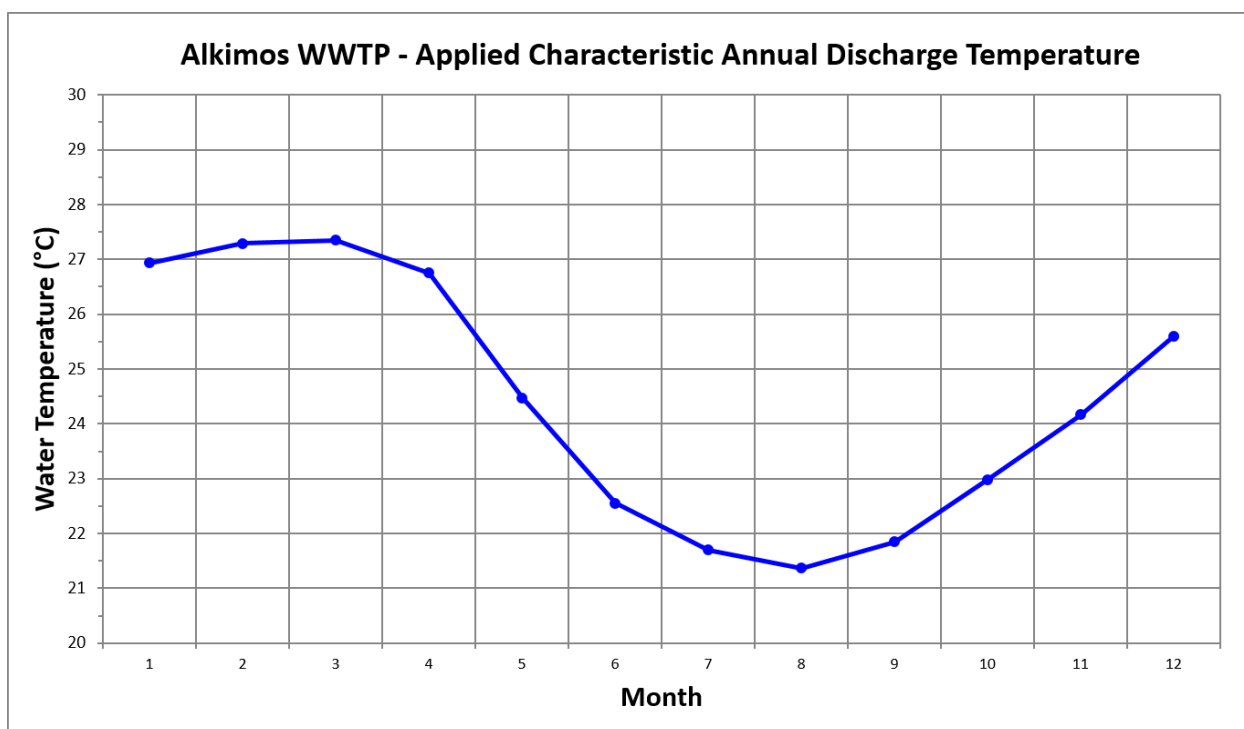


Figure 3-3 Annual variation in WWTP discharge temperature as applied scenario testing, based upon measured discharge temperatures from the existing Alkimos WWTP facility.

3.3 Development Overview - ASDP

The ASDP development option described in the present report consist of a reverse osmosis plant capable of generating in excess of 300 ML/d of potable water, along with 337 ML/d (3.90 m³/s) of associated reject brine. Unlike the WWTP, these values are taken as constants over the 12 month simulation.

Two candidate intake locations as well as two candidate outfall locations have been identified for the proposed Alkimos ASDP facility, as indicated in Figure 3-1. Each of the candidate intake locations would consist of two adjacent screened riser structures with intakes at a distance of 3 to 5 m above the seabed. For reasons of constructability as well as cost, the two candidate outfall locations consider different diffuser arrangements. A ‘traditional’ linear diffuser is preferable for the shallow Outfall A option, while two rosettes are preferred for the deeper Outfall B option (Water Corporation, 2018).

Based in part on the results of the initial model screening assessment (documentation pending in DHI, 2019), the preferred solution has been identified as the combination of Intake A / Outfall B. Intake A is located in 12.7 m of water depth at MSL, while Outfall B is in approximately 18.4 m water depth at MSL. However, it is important to note that Outfall B is in practice located on a slope such that the water depth at the two rosettes differs by approximately 0.8 m. Equally important to the character of the response of the brine wastefield, the diluted discharge retains excess salinity and excess density at the end of the near field, and will descend sharply downslope towards the deeper portion of the channel. As a result of the differing water depth of the two rosettes, and the lack of excess water depth above the ports, several options of rosette design were investigated in DHI (2018). These options incorporate partial burial of the rosette superstructure, as well as reductions in vertical discharge angles and altered port geometries. Consequently, some entries in Table 3-2 are shown as ranges.

Table 3-2 Particulars for the preferred candidate Alkimos ASDP rosette outfall as simulated.

Parameter	Value
Rosette Midpoint Coordinates	(370508, 6499408) and (370556, 6499438)
Separation between rosettes	50m
Water depth at rosettes	-18.8 and -18.0m (MSL)
Number of Ports	4 ports x 2 rosettes = 8
Port Spacing	Equidistant (90°)
Port Diameter	0.336 to 0.351m
Port Elevations above Seabed	1.75 to 3.25m
Vertical discharge angle	45 to 60°
Mean Daily Flow Rate	337 ML/day (3.90 m ³ /s)
Port exit velocity	5.04 – 5.5 m/s
Discharge Salinity	$S_{out} = 1.925 \times S_{in}$
Discharge Temperature	$\Delta T = 4^{\circ}C$ ($T_{out} = T_{in} + 4^{\circ}C$)
Discharge DO	100% saturation
Bacterial load (Total TTC)	0
Bacterial load (Enterococci spp.)	0

*Drawings show slightly larger D=0.106m for offshore 60 ports **with diurnal variation (Figure 3-2).

The ASDP brine reject stream has been defined by Water Corporation (2018) as imparting a fixed $\Delta T = 4^{\circ}\text{C}$ above the intake seawater. The discharge salinity was similarly specified as being a factor of 1.925 times that of the intake seawater. The ASDP discharge carries no bacterial load, and the DO of the discharge is assumed to be 100% saturated.

Given the primacy of the ASDP discharge salinity in the context of the present impact assessment, and the uncalibrated nature of the ambient salinity in the Local Hydrodynamic Model, some conservatism has been applied in the calculation of the ASDP discharge salinity. In order to ensure that the time-varying ASDP excess salinity specified in the model is never underestimated, the ASDP plant discharge ($S_{\text{out}} = 1.925 \times S_{\text{in}}$) has been calculated using the sine curve shown in Figure 3-4 as S_{in} . Using this approach, the reference intake salinity ranges from $S_{\text{in}} = 36.0$ to 37.0 ppt, with corresponding $S_{\text{out}} = 69.3$ to 71.2 ppt.

The black dotted background salinity curve shown in Figure 3-4 was used solely as a reference intake salinity for the a priori calculation of excess salinity at the outfall. This reference curve was chosen for the sake of conservatism a) as salinity in the model is effectively uncalibrated and b) to be able to incorporate situations where ambient salinity may rise above the levels indicated by the sparse survey data, and/or to be able to incorporate a degree of recirculation beyond that anticipated. For perspective, a 0.5 ppt increase in ambient salinity results in an increase in discharge salinity of $0.5 \times (1.925 - 1) = 0.4625$ ppt, which leads to an increase in ASDP plume salinity of just 0.015 ppt after the design dilution of 1:30. This increase of ~1.5% in plume excess salinity will not materially alter the impact assessment, and largely de-risks variability in intake salinity as a factor affecting permitting compliance.

For reference, the modelling performed in support of the original WWTP permitting (WP, 2005) applied uniform background salinity and temperature values as shown in Table 3-3.

The target dilution rate for the ASDP is based on meeting the LEPA criterion of median salinity not exceeding 1.3 ppt above background. For a conservatively high ambient condition of 37 ppt and a discharge salinity of 71.2 ppt, a dilution of 26.3 would be required. A dilution of 30 would give a value of 1.1 ppt above ambient, and allows some degree of conservatism. This dilution has been achieved for both linear and rosette diffusers (Marti et al 2011, Antenucci et al 2015, Miller and Smith 2017).

The conceptual design and near-field behaviour of the Outfall B rosettes is described in detail in DHI (2018b). The conceptual design work performed in DHI (2018b) confirmed that a dilution target of 1:30 is achievable for the ASDP application with the proposed two rosette arrangement.

The present work carries forward this 1:30 near-field dilution as an input to the far-field modelling assessment.

Table 3-3 Representative background salinity and temperature conditions as applied for previous modelling of the Alkimos WWTP in WP (2005).

Water Property	Summer	Autumn
Temperature ($^{\circ}\text{C}$)	23.0	19.0
Salinity (ppt)	36.5	35.3

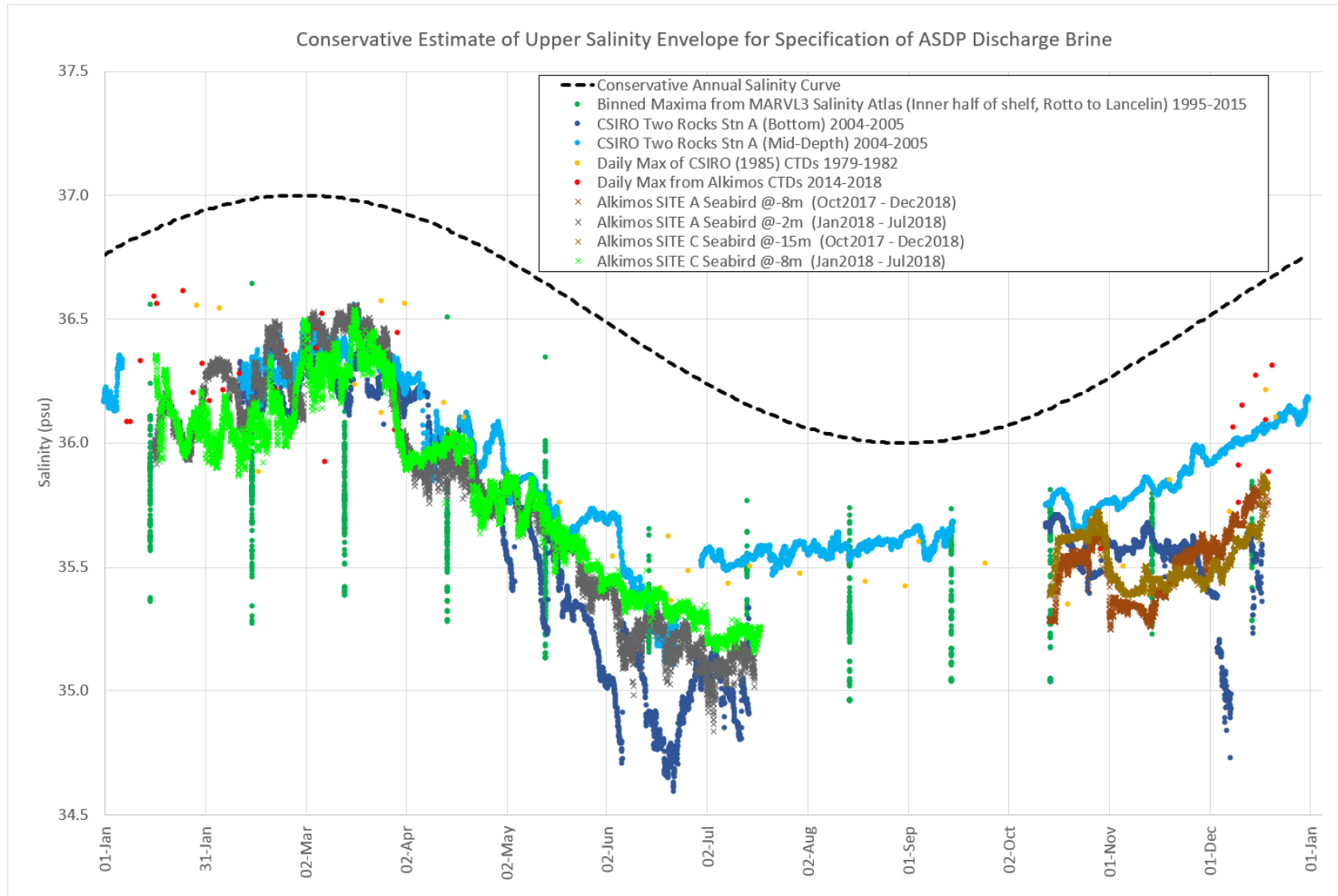


Figure 3-4 Assembly of ambient salinity measurements from multiple sources plotted onto a common generic 12 month time axis, superimposed by the sine curve used as a conservative estimate of the upper salinity envelope for the calculation of ASDP discharge salinity.

3.4 Near-field Dilution and Far-field Coupling

3.4.1 General

Near-field mixing is generally considered to be that controlled primarily by the engineering design of the diffuser, whereas far-field mixing is that due to environmental processes. Near-field mixing occurs at scales of metres, typically smaller than can be practically be resolved in a far-field model. In order to simulate the effects of outfalls on the far-field, coupling of the near-field and far-field models needs to occur.

Several options are available for this coupling

1. Fundamental scaling – Based on fundamental scaling of the fluid mechanics and verified in the laboratory and field, this method calculates near-field dilution based on discharge and ambient parameters. The discharge is then placed directly into the numerical grid using dynamic coupling to MIKE3 using moving sources in space and time with the far-field model grid size selected to ensure the resulting numerical dilution matches the calculated near-field dilution (eg Roberts et al 1997, and other more recent work).
2. Integral models – As above, but using models such as CORMIX or Visual PLUMES to compute the near-field dilution.
3. CFD - Use of Computational Fluid Dynamics (CFD) model to compute nearfield dilution, with dynamic coupling to MIKE3 using moving sources in space and time.

As discussed in previous sections, two outfall locations were under consideration for this work, one located on the reef complex, and another at a deeper site located within the lagoon (Water Corporation, 2018). The concept design for the shallow diffuser is for a linear multiport diffuser, whereas the concept design for the (preferred) deeper diffuser is for a rosette type. Some details of these diffusers remain to be determined at later stages of the design process.

Given the concept stage of the diffuser designs and the use of the scenarios herein to assist site selection, the first method above was used for coupling. For the dense ASDP discharge, this allows for direct inclusion of the extensive recent work completed in the laboratory on multiport brine diffusers (Abessi and Roberts 2014, Abessi et al 2016, Abessi and Roberts 2017), and the field validation of this work to Water Corporation desalination diffusers (Antenucci et al 2015).

The approach taken simplifies the coupling of the near-field and far-field models, whilst still retaining sufficient accuracy for this level of assessment. It also allows for sensitivity analysis, if required, of lower dilution rates if the engineering design process is not able to meet the above targets.

3.4.2 WWTP Near-field Characterisation

The near-field character of the WWTP discharge has been quantified using semi-empirical relationships generated by Philip Roberts and various graduate students. This work has been widely published and accepted in the literature, see Roberts et al (1989a, 1989b, 1989c), Tian et al (2004a, 2004b, 2006) and Daviero and Roberts (2006) – referenced in the following broadly hereafter as the “Roberts wastewater relationships”. Key aspects of the application of this methodology to the Alkimos WWTP is summarised here.

The above methodology provides semi-empirical relationships for the estimation of basic characterisation of wastefield geometry as well as the achieved dilution at the end of the

near field for buoyant near-bottom discharges emanating from a linear diffuser. As such they are appropriate for assessment of the WWTP discharge but a separate set of guidelines are required for the (dense) ASDP brine discharge.

The above Roberts wastewater relationships provide estimates of plume character as a function of depth, ambient current, ambient density and stratification, effluent density, and diffuser particulars.

Aside from the diffuser particulars, all other inputs to the formulation are in practice time-varying. The following methodology is thus applied in the specification of sources in the far-field Local Hydrodynamic Model:

- 1) The Local Hydrodynamic Model is simulated for the full production year, where both the WWTP and ASDP sources are omitted. The output of this simulation provides ambient flow, salinity and temperature information as input to the WWTP near-field calculation using the relations cited above. This information is used both to define the input ambient conditions for the Roberts calculations, as well as providing the ambient salinity and temperature to be applied in pre-dilution water at the source points.
- 2) Using the above Roberts wastewater relationships, the WWTP near field character is calculated over the entire simulation year at a timestep of 30 min. The output of these calculations yields an estimate of the upper and lower bounds of the wastefield, the downstream distance to the end of the near field, as well as the achieved dilution at the end of the near field. This information is sufficient to define the time-variable input to a network of sources within the far-field model.
- 3) The locations of the far-field source points are fixed in planform, but are variable over the vertical. As such, the far-field model takes on the vertical distribution of the WWTP that is achieved at the end of the near field region. The effluent discharge is distributed between the active source points with a scaling based upon the individual cell volumes. As the mesh has been constructed such that all source points are equal in planform surface area, the effluent flow in each source point is effectively scaled by the cell thickness. Effluent mass is conserved in this process.
- 4) In order to ensure that the far-field model reflects the target near-field dilution within the range of interest, pre-dilution water is added to the active source cells up to a maximum dilution of 1:250, utilising the time-varying ambient salinity and temperature from step 1) above. The pre-dilution water is introduced into the model, and is not withdrawn from sinks elsewhere.

The source network applied for the WWTP outfall is shown in Figure 3-5, where uniform equilateral triangles have been imposed in the immediate vicinity of the outfall in order to maintain consistency in mesh element volume. A total of 36 lateral sources are active. Given the 13 vertical layers, the total number of active sources in three dimensions varies from 36 (when the plume is inserted into only one layer) to $13 \times 36 = 468$ when the near-field behaviour results in a fully mixed water column.

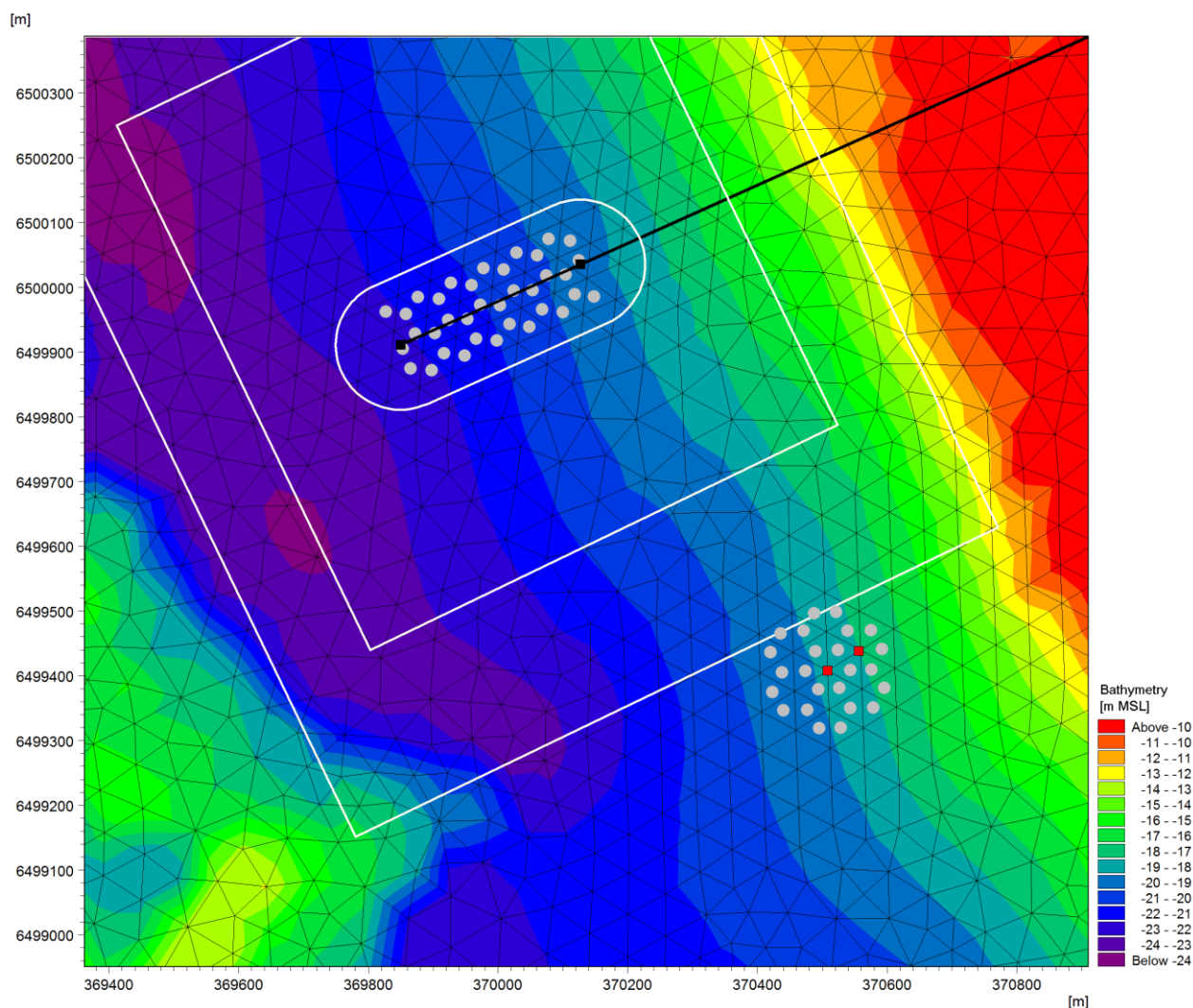


Figure 3-5 Network of lateral sources applied to describe the WWTP linear diffuser (upper left, where diffuser endpoints are indicated with black squares) and ASDP rosette diffusers (lower right, where red squares denote rosette locations).

3.4.3 ASDP Near-field Characterisation

The near-field characterisation of the ASDP discharge and subsequent implementation into the far-field model is also based upon semi-empirical relationships, but ones specific to dense brine outfalls (DHI, 2018). The details of the near-/far-field coupling is less complex for the ASDP as the dense plume is far less sensitive to the ambient current or water column stratification for typical currents and stratification at this site. Accordingly, both the source arrangement in space as well as the source discharge rate are static. The salinity and temperature of the sources do vary for both the effluent (being itself a function of the intake water) as well as predilution water which again originates from the 12 month pre-development simulation where outfalls are omitted.

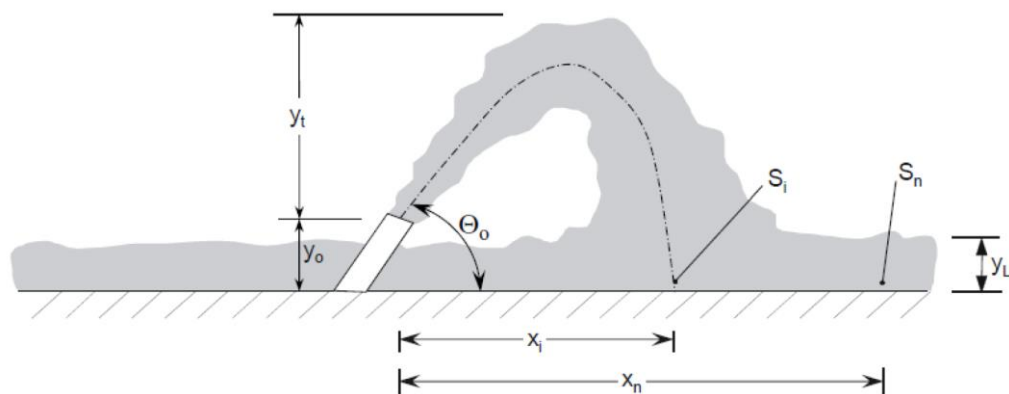


Figure 3-6 Definition sketch for near-field behaviour of a dense discharge from a single port diffuser (after Roberts, 1997).

As discussed in Section 3.3, it is assumed here that engineering design of ASDP diffuser will be sufficient to ensure that target dilution of 30 is met at the end of the near-field region. This may involve some degree of subsequent tuning of port diameter, port orientation, port pressure head, duckbill valves, port capping or other parameters during detailed design. The present coupling approach makes the conservative assumption that ambient currents do not influence the near-field dilution.

The source network applied for the ASDP outfall is shown in Figure 3-5, where uniform equilateral triangles have again been imposed in the immediate vicinity of the outfall. A total of 24 lateral sources are active, which are distributed over the bottom four layers of the model, resulting in a total of 96 active source points. The lateral source arrangement is skewed slightly toward the offshore rosette, in expectation that the sloping bed will have some effect even within the near field and limit the upslope extent of the wastefield. The distribution of effluent and pre-dilution (at a constant rate of 1:30) is again distributed according to cell volume. ASDP effluent mass is conserved.

3.5 Dissolved oxygen

A key concern associated with the discharge of brine into the environment is the potential impact on dissolved oxygen. To determine the impacts of the proposed ASDP plant on dissolved oxygen, an ECO Lab model was coupled with the MIKE3 models to determine how dissolved oxygen behaves under the various scenarios considered.

Dissolved oxygen processes simulated in the ECO Lab model were as follows:

- Boundary fluxes from the regional ocean model
- Atmospheric exchange
- Sediment oxygen demand

Boundary fluxes from the regional ocean model were set to saturation based on water temperature. Atmospheric exchange of dissolved oxygen was simulated as a function of water column dissolved oxygen, wind speed, water depth and ambient flow velocity (DHI 2017).

Sediment oxygen demand in Cockburn Sound has previously used rates of 0.46 g/m²/d in modelling impacts of the Perth Seawater Desalination Plant (CWR 2006). Recent measurements in Marmion Lagoon during winter and summer indicate mean values of 0.19 and 0.36 g/m²/d respectively, with standard deviations of 0.07 and 0.14 g/m²/d

respectively (BMT 2018). These results are considered to be more reflective of conditions at Alkimos than the protected waters of Cockburn Sound.

ECO Lab uses a Michaelis-Menton equation to describe the sediment oxygen demand as a function of overlying dissolved oxygen concentration and water temperature. Fitting the above data based on water temperatures of 17 and 22°C for winter and summer respectively resulted in the following parameters being used:

- Reference sediment oxygen demand (20°C, saturation) = 0.28 g/m²/d
- Arrhenius temperature multiplier = 1.14
- Half saturation constant = 0.1 mg/L

3.6 Fecal Indicator Bacteria

The WWTP discharge is configured to release two fecal indicator bacteria (FIB) of interest – Total Thermotolerant Coliforms (TTC) and Enterococci spp. Prior modelling of the WWTP discharge (Worley Parsons 2005) used a constant first-order decay rate (equivalent to a dark decay rate) of 0.03838 hr⁻¹ (0.92 day⁻¹) for enterococci and a variable die-off rate for TTC as a function of the day ranging between 0.06 and 1.0 hr⁻¹ (1.44 – 24 day⁻¹), with the lower value representing the dark decay rate and the daily average value 9.1 day⁻¹.

Review of recent literature indicates a wide range of dark decay rates for the FIB of interest that encompass these values (Hipsey et al 2008, Marracini et al 2016). Visible and UV-B light are known to increase decay rates (Davies-Colley et al 1994, Sinton et al 2002). Unexplained variation in inactivation kinetics is commonly found (Davies-Colley et al 1994, Sinton et al 1994), and the relative importance of the various mechanisms for sunlight inactivation are also still under investigation (Maracini et al 2016b). There is thus some uncertainty in the application of these rates.

We utilise the solar radiation inactivation equation following Hipsey et al (2008), where the decay rate due to light is

$$k_l = \sum_{b=1}^N \varphi k_b f_b I_z \left(\frac{1 - \exp(-\eta_b \Delta z)}{\eta_b \Delta z} \right)$$

where N is the number of discrete solar bandwidths under consideration, b is the bandwidth class, φ is a constant to convert units from seconds to days and J to MJ (=8.64e-2), k_b is the base decay rate in seawater for light band b , f_b is the fraction of incident light in light band b , I_z is the light available at depth z , η_b is the light attenuation coefficient for light band b , and Δz is the layer thickness. Note that

$$I_z = I_0 \exp(-\eta_b z)$$

where I_0 is the incident light on the water surface (W/m²).

Mean daily UV-B fluxes in Perth vary seasonally between 0.75 – 1.75 W/m² (Lubin et al 1998), whereas mean daily peak radiation varies seasonally between approximately 800 and 1200 W/m² (BOM 2018) – UV-B thus accounts for less than 0.2% of the incoming solar radiation. UV-A is generally considered to be 5% of UV-B light, so is an even smaller component. Decay coefficients for UV light are similar to those for visible light (Sinton et al 1994), indicating that visible light is by far the most significant component. We thus apply

$$k_l = \varphi k_{VIS} I_z \left(\frac{1 - \exp(-\eta_{VIS} \Delta z)}{\eta_{VIS} \Delta z} \right)$$

Values for k_{VIS} were derived from Sinton et al (1994), who conduct experiments using effluent from an activated sludge plant diluted in seawater, with k_{VIS} (TTC) = 1.02 m²/MJ and k_{VIS} (Ent) = 0.49 m²/MJ. Units of k_i are day⁻¹.

Dark decay rates used those previously applied, namely 0.92 day⁻¹ for Enterococci and 1.44 day⁻¹ for TTC (Worley Parsons 2005).

4 Results and Discussion

4.1 General

Result graphics are provided in the following sections, as well as in Appendices B through D.

4.2 ASDP Wastefield

The brine discharge, following dilution within the near field down to an excess salinity of approximately 1.1 ppt above ambient, is seen to descend perpendicularly downslope to the deep portion of the channel between the outer and second reef lines where the existing WWTP diffuser is located. This behaviour is a near-permanent feature, and is only minimally affected by the behaviour of the water column above it. The descending brine wastefield then bifurcates as it approaches the barrier of the outer reefline and spreads at reduced velocity in both shore-parallel directions and forms a semi-permanent, kilometre-scale near-bed stratified feature within the channel. The brine layer shows variability from month to month depending on hydrographic conditions, but does not (within the year simulated) demonstrate major changes in dimensions by season.

Appendix B presents mapping of modelled ASDP excess salinity fields, with each figure incorporating panes of the median, 95th percentile and maximum excess salinity fields. Figure B-1 provides annual statistics of the dilution field. Figures B-2 through B-13 provide similar results by month in the sequence of the 12 month simulation, specifically April 2017 through March 2018.

In all cases these fields are calculated by first collapsing the 3D ASDP tracer output field to a 2D field containing the maximum concentration over the water column at each timestep. As the dense ASDP plume arranges itself such that the highest excess salinity is almost always in the bottom layer, this post-processing results in mapping which is virtually identical to post-processing the bottom layer alone. The vertical maximum is applied for consistency with the processing of the WWTP wastefield, for which the location of the highest concentration over the water column is more variable.

The ASDP tracer concentration (a value between 0 and 1) is then multiplied by a reference excess salinity of $37 \times (1.925 - 1) = 34.225$ ppt. In this calculation, 37 ppt is the annual maximum of the ambient (intake) salinity using the conservative curve (Figure 3-4) applied for the calculation of the ASDP discharge brine and the factor 1.925 is the concentration factor for discharged brine relative to intake salinity.

Figure 4-1 shows the 95th percentile excess salinity from the model, as calculated over the full 12 month simulation, as a cross-shore vertical section of the model which passes through the two ASDP rosettes (the positions of which are indicated by the vertical black lines). A similar plot is shown in Figure 4-3, but where the vertical section is aligned along the feeder pipe of the WWTP outfall, with the vertical black lines indicating the locations of the first and last diffuser ports of the WWTP outfall. The negatively buoyant character of the plume is clearly apparent, as is its immediate descent from the diffuser. White shaded areas of the water column indicate ASDP dilution of greater than 1:100.

4.3 WWTP Wastefield

Appendix C presents mapping of modelled WWTP-derived faecal indicator bacteria concentrations, with specific reference to the delineation of zones around the facility for safe consumption of seafood and recreation. Their specific definitions, per Water Corporation (2018) with subsequent clarification from BMT (2018):

- Consumption of seafood (Zone S2): median thermotolerant faecal coliform bacterial concentration not to exceed 14 CFU / 100mL. This is to be assessed within 50cm of the bed, and so is calculated from the bottom layer of the model, with emphasis on the summer months of December to March.
- Primary or secondary recreational contact (Zone S3): maximum pooled Enterococci spp. must not exceed the NHMRC 'category A' guidance value of 40 Enterococci spp. MPN / 100mL. This is to be assessed within 50cm of the surface, and so is calculated from the top layer of the model, with emphasis on the summer months of December to March.

Figure C-1 provides mapping of the seafood and recreational criteria for the summer months of December to March. Figures C-2 through C-13 provide similar results by month in the sequence of the 12 month simulation, specifically April 2017 through March 2018.

Figure 4-2 shows the 5th percentile dilution (95th percentile tracer concentration) from the WWTP outfall, as calculated over the full 12 month simulation, as a cross-shore vertical section of the model which passes through the two ASDP rosettes (the positions of which are indicated by the vertical black lines). The far-field character of the WWTP plume, which was often but not always surface attached, is clearly visible. White shaded areas of the water column indicate WWTP dilution of greater than 1:1000.

A similar plot is shown in Figure 4-4, but where the vertical section is aligned along the feeder pipe of the WWTP outfall, with the vertical black lines indicating the locations of the first and last diffuser ports of the WWTP outfall. The section shows a strong WWTP signature as it bisects the mixing zone. While the plume is positively buoyant, the image illustrates that the near-field behaviour of the plume may result in surface attachment, mixing over the full water column, or insertion within water column during periods where a moderate water column density gradient prevails. White shaded areas of the water column indicate WWTP dilution of greater than 1:1000.

It is clear from Figure 4-1 through Figure 4-4 that far-field interactions between the WWTP and ASDP wastefields do occur but are limited, with the two plumes following the expected behaviour of residing primarily in the upper and lower portions of the water column, respectively.

Plume interactions also occur within the near-field regions of the two outfalls, where the respective near-field plume will on occasion (depending upon prevailing ambient flow conditions) interact with the far-field plume from the other. Such effects are not captured in the present assessment.

4.4 ASDP Seawater Intake

The performance requirements at the ADSP seawater intake have been established in Water Corporation (2018) as follows:

The seawater intake shall be located such that recirculation risks due to the brine and treated wastewater discharges are managed to the following assumed limits at the depth

in the water column where the intake screens will be located (nominally 3 to 5m above the seabed):

- TTC < 20 / 100mL for 95% of the time, calculated over a period of no more than one week, and not to exceed 2,000 / 100mL at any time
- Enterococci spp. < 4 MPN / 100mL for 95% of the time, calculated over a period of no more than one week, and not to exceed 400 / 100mL at any time
- TDS < 0.2 PPT above ambient TDS for 95% of the time, calculated over a period of no more than one week, and not to exceed +0.4 PPT at any time

Results were extracted from the model layers intersecting with the window of +3 to +5m ASB and interrogated to generate the above statistics. The results for the above constituents are provided as time series over the simulation year in Figure 4-5 and Figure 4-6, and as percentiles of instantaneous values over the simulation year in Figure 4-7 and Figure 4-8.

It is clear that both diluted ASDP brine and WWTP bacteria occur at the ASDP intakes in a limited and highly episodic manner. An increase in events is seen during the summer months. An interrogation of the results shows that the mechanisms causing dilute levels of brine and bacteria to be present at the intake are complex, and tend to occur during specific combinations of environmental forcing. Both brine and bacterial intake events are correlated with flow reversals in the ambient longshore currents, and in particular when such events occur in combination with easterly winds. The effects of the latter are the primary explanation for the increase in events seen in summer. Bacterial events occur less frequently, due in part to decay, but primarily due to the fact that much of the time the WWTP discharge is located too high in the water column to affect the intakes. The largest bacterial events thus occur due a more complex combination of flow reversal, easterly winds, and ambient flow/water column character which is conducive to distributing the WWTP effluent lower in the water column.

Figure 4-7 shows that the median excess salinity concentration at the ASDP intakes is 0.002 ppt, with a maximum value of 0.16 ppt. Given the low concentration and brief duration of such events, recirculation is not expected to be a concern for the desalination facility with the proposed intake / outfall arrangement.

Statistics are formally tabulated against the above performance guidelines in Table 4-1. At the ASDP intakes, water quality performance criteria relating to the ASDP and WWTP discharges are met throughout the 12-month simulation. Concentrations of fecal indicator bacteria (FIB) at the ASDP intakes were assessed against 95% concentration criteria for both Thermotolerant Coliforms (TTC) and Enterococci spp., and found to be within acceptable limits. Similarly, ASDP tracer concentrations at the ASDP intakes were also within acceptable limits, again indicating that recirculation of the desalination facility is not a significant concern.

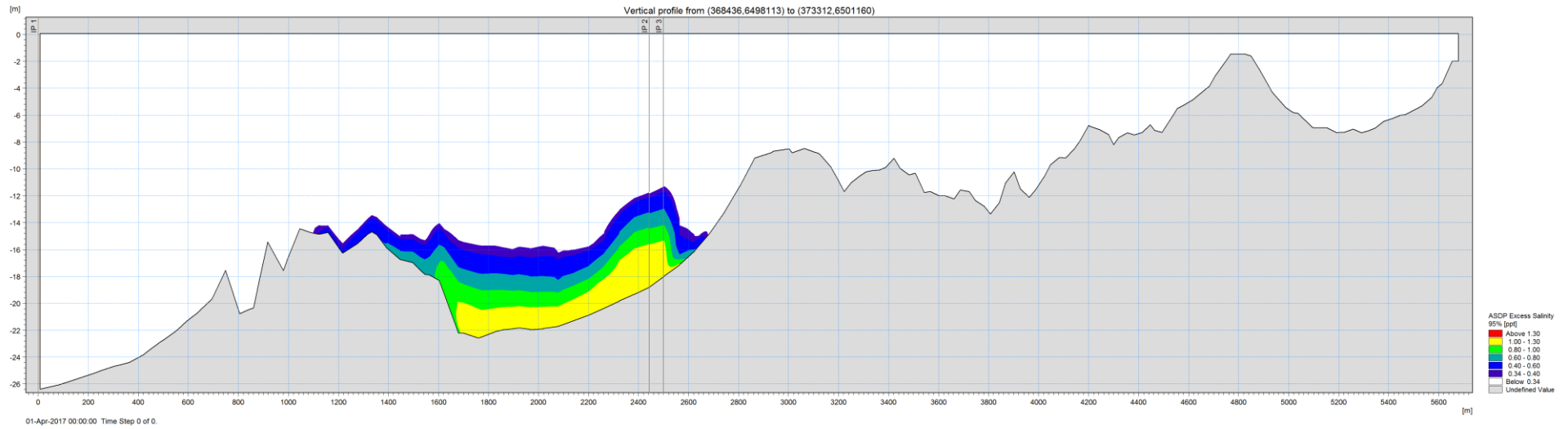


Figure 4-1 Vertical cross-shore section through ASDP rosettes – annual 95th percentile excess salinity.

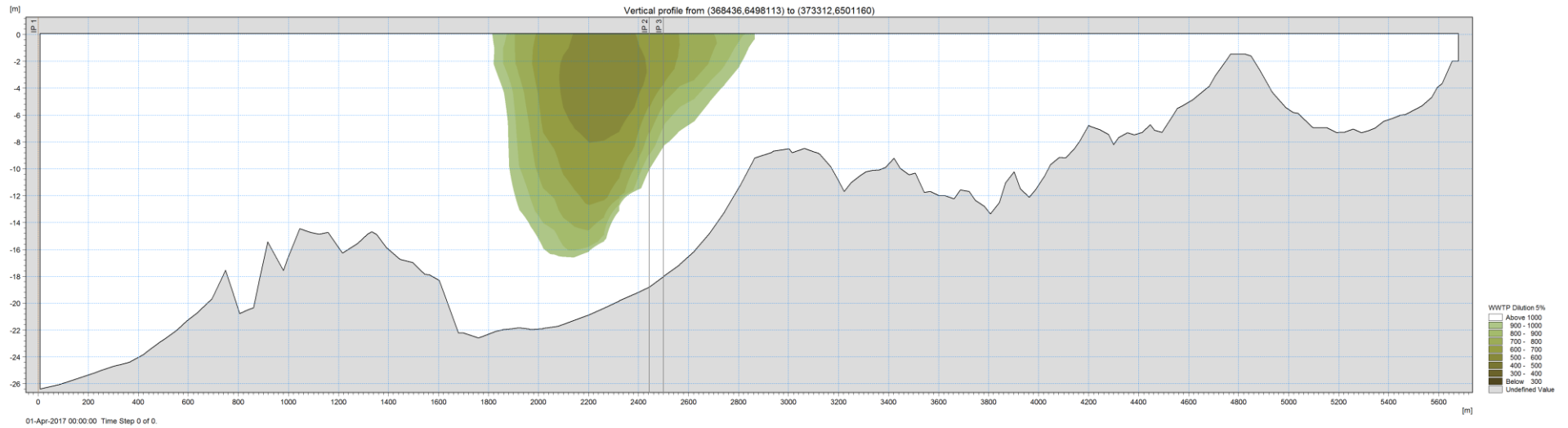


Figure 4-2 Vertical cross-shore section through ASDP rosettes – annual 95th percentile WWTP tracer concentration (= 5th percentile dilution).

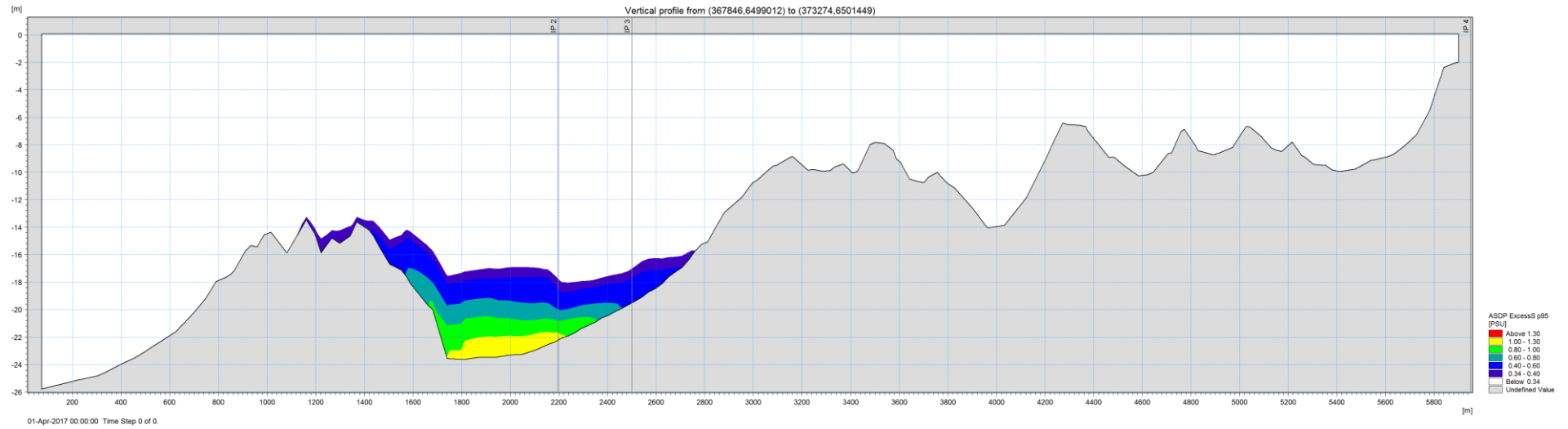


Figure 4-3 Vertical cross-shore section through WWTP diffuser line – annual 95th percentile excess salinity.

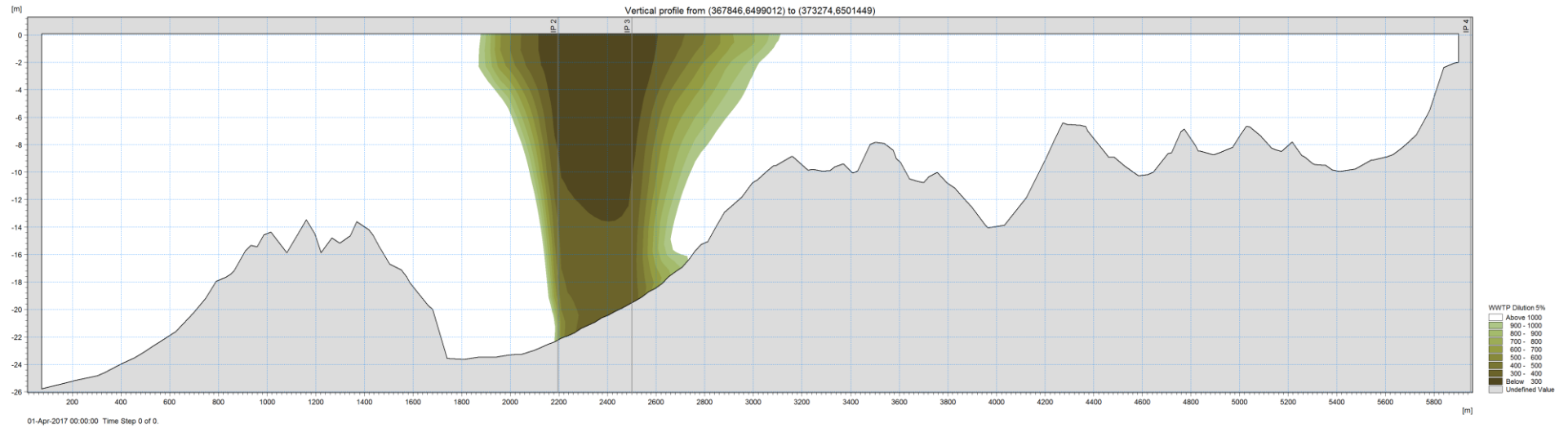


Figure 4-4 Vertical cross-shore section through WWTP diffuser line – annual 95th percentile WWTP tracer concentration (= 5th percentile dilution).

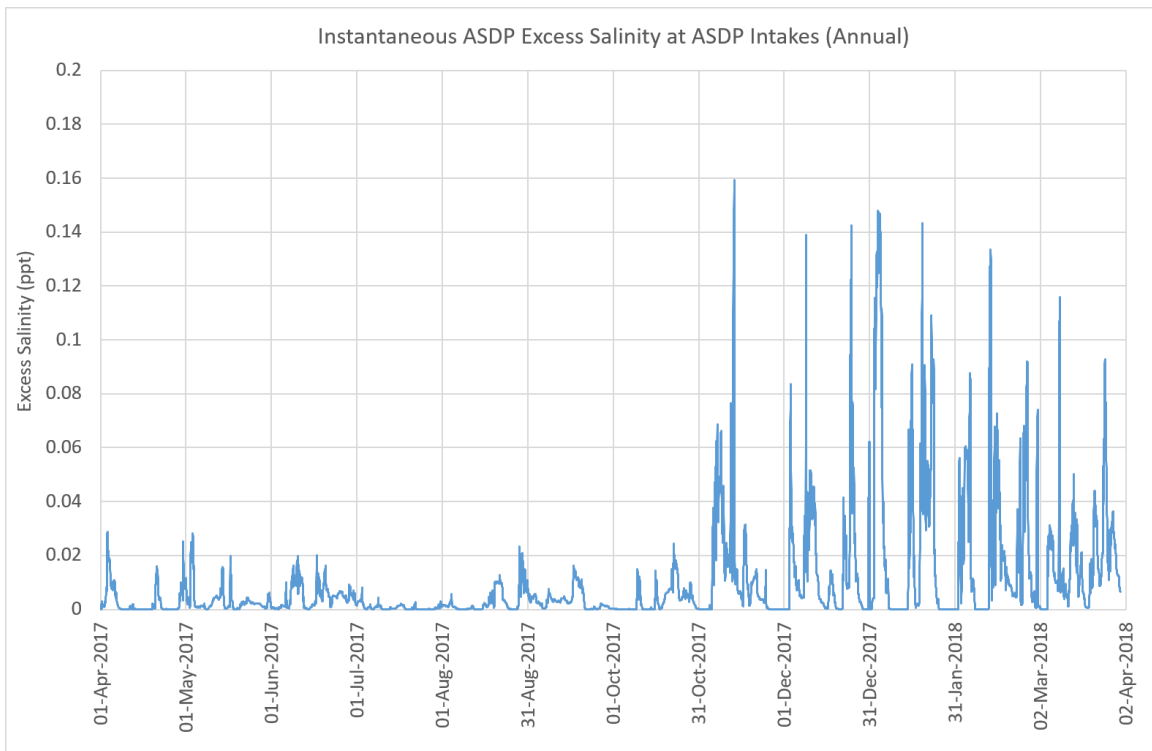


Figure 4-5 Annual time series plot of instantaneous excess salinity at the ASDP intake location.

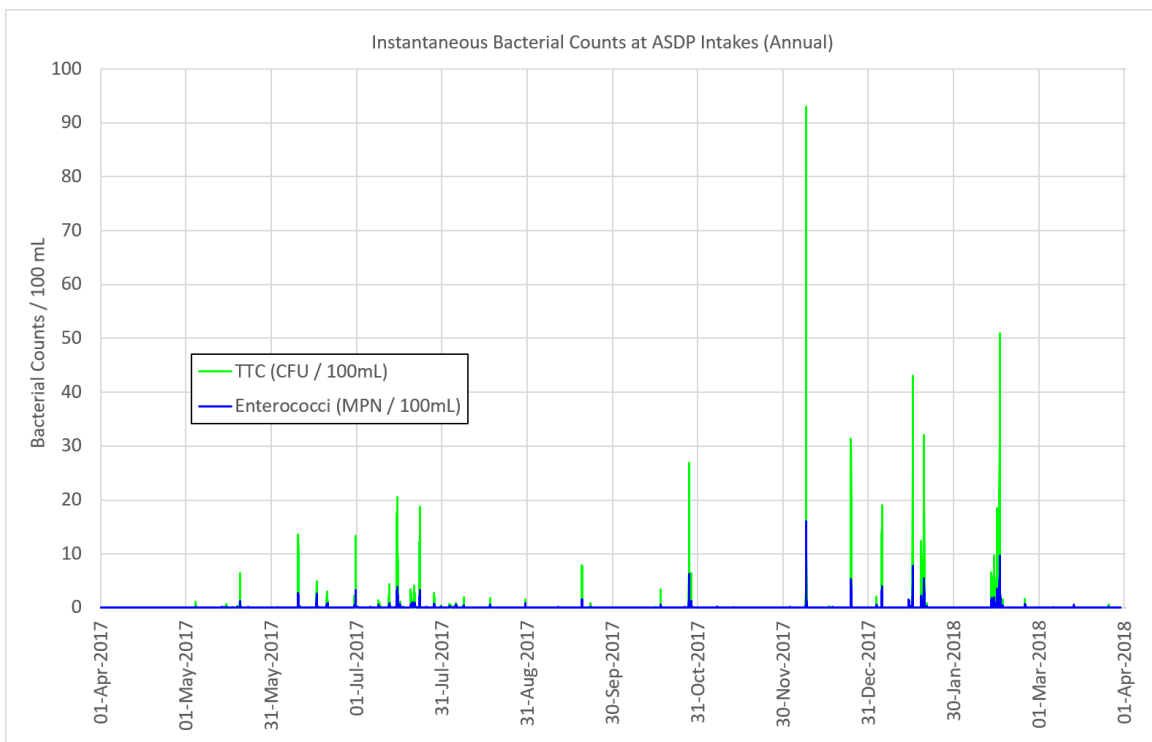


Figure 4-6 Annual time series plot of instantaneous FIB bacterial counts at the ASDP intake location.

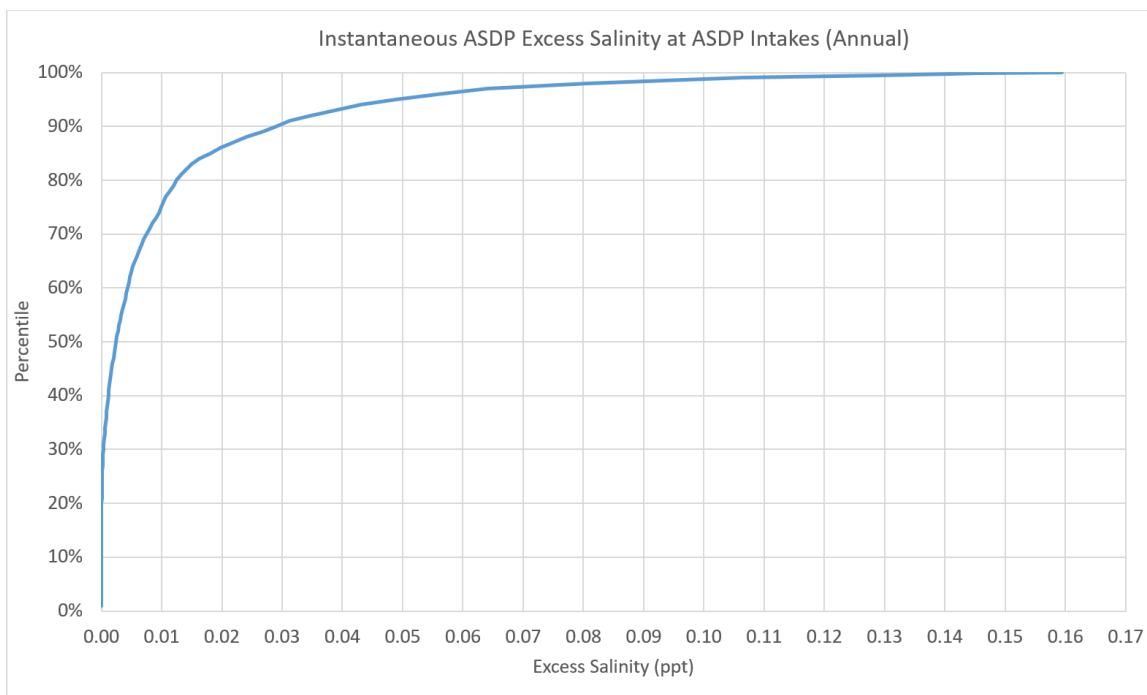


Figure 4-7 Annual percentile plot of instantaneous excess salinity at the ASDP intake location.

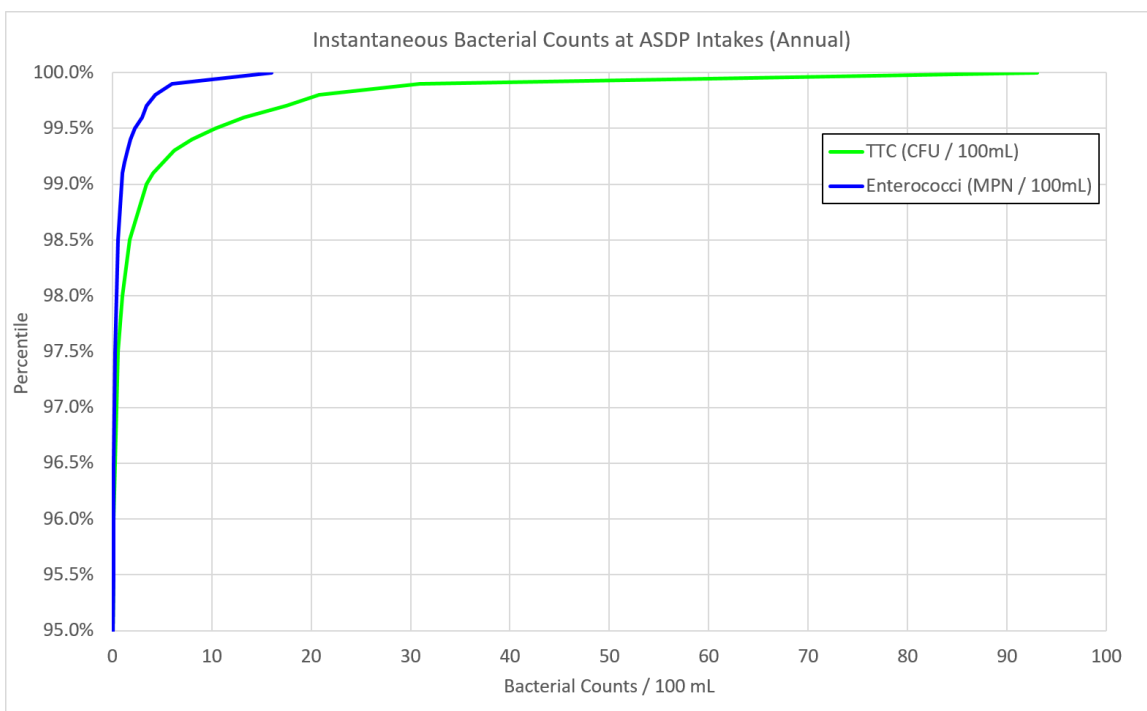


Figure 4-8 Annual percentile plot of instantaneous FIB bacterial counts at the ASDP intake location. Note that the focussing of the y-axis on 95th percentile and above to facilitate viewing.

Table 4-1 Water quality performance statistics at the ASDP intake. Results are colour coded with green comfortably within modelled criteria, yellow also within the criteria modelled however is encroaching towards the criteria, and red signals exceedance of the criteria (of which there are none).

BACTERIAL CONCENTRATIONS AND ASDP EXCESS SALINITY AT ASDP INTAKES

Criteria		Apr 2017	May 2017	Jun 2017	Jul 2017	Aug 2017	Sep 2017	Oct 2017	Nov 2017	Dec 2017	Jan 2017	Feb 2017	Mar 2017	FULL YEAR
95% TTC	< 20 CFU/100mL	0.0	0.6	1.0	10.0	0.5	0.3	2.0	0.2	0.2	10.8	8.9	0.0	10.8
Max TTC	< 2000 CFU/100mL	0.0	6.4	13.6	20.6	1.9	8.0	26.9	0.2	93.0	43.0	50.9	0.5	93.0
95% Enterococci	< 4 MPN/100mL	0.0	0.2	0.4	2.2	0.2	0.1	0.5	0.1	0.2	2.2	2.4	0.1	2.4
Max Enterococci	< 400 MPN/100mL	0.0	1.3	2.8	3.8	0.9	1.6	6.3	0.2	16.0	7.8	9.7	0.5	16.0
95% ASDP Excess Salinity	< 0.2 ppt	0.02	0.02	0.02	0.01	0.02	0.02	0.02	0.12	0.14	0.14	0.12	0.09	0.14
Max ASDP Excess Salinity	< 0.4 ppt	0.03	0.03	0.02	0.01	0.02	0.02	0.02	0.16	0.14	0.15	0.13	0.12	0.16

Exceeds Guideline
> Half Guideline
< Half Guideline

4.5 Dissolved Oxygen Saturation

Appendix D presents mapping of modelled fields of dissolved oxygen (DO) saturation. The anthropogenic aspect of this potential impact lies primarily with the additional near-bed residence time associated with stratification induced by the diluted brine wastefield of the ASDP. In terms of initial oxygen deficit, the WWTP discharge is far more significant than the ASDP. However, the initial dilution of the WWTP plume is far higher, its exposure to the seabed is far lower, and its mobility at the surface is far greater than is the ASDP discharge.

The result fields presented in Appendix D are calculated from the bottom layer of the 3D model. The bottom layer is then assessed in terms of the non-exceedance of 90% DO saturation, evaluated as a running median over a 7 day window.

Figure D-1 provides a map of the exceedance of this criterion over the full annual simulation. These exceedances are seen to all occur within the three months of April, May and June 2017, the results of which are shown in Figures D-2, D-3 and D-4, respectively. The remaining months are blank fields and omitted for brevity.

It should be noted that the violations of the median 90% DO saturation criterion as plotted are only slightly below this threshold. The minimum 7-day median DO saturation percentage over the year is 88%.

Sensitivity tests have shown that exceedances of the criterion are extremely sensitive to the vertical dispersion. Even small departures from the conservatively small dispersion applied in the present assessment results in the disappearance of all exceedances shown in Appendix D. For this reason, it is considered highly unlikely that sediment oxygen demand in combination with the additional residence time imposed by the ASDP plume would in practice result in exceedances of the specified DO criterion within the area of interest.

DO impacts associated with biological and chemical oxygen demand have not been considered in the present work.

5 References

- BMT (2018): email communication between BMT and Water Corporation, 09 Nov 2018.
- BoM (2018a): Surface wind records from Rottnest Island, Swanbourne, Ocean Reef and Hillarys, acquired from BoM by DHI under license.
- BoM (2018b): “Australian Baseline Sea Level Monitoring Project Hourly Sea Level [ABSLMP] and Meteorological Data”. <http://www.bom.gov.au/oceanography/projects/abslmp/data/index.shtml> [last access May 2018], Australian Bureau of Meteorology.
- CSIRO (2006): “Two-Rocks Moorings Data Report”, CSIRO Marine and Atmospheric Research Paper 005, Jan 2006.
- Daviero, G. J., and Roberts, P. J. W. (2006): “Marine wastewater discharges from multiport diffusers. III: Stratified stationary water.” *J. Hydraul. Eng.*, 132 (4), 404–410.
- Davies-Colley, R.J., R.G. Bell and A.M. Donnison (1994): “Sunlight inactivation of Enterococci and fecal coliforms in sewage effluent diluted in seawater”. *Applied and Environmental Microbiology*. 2049-2058.
- DHI (2017): “Water Quality, MIKE ECO Lab WQ Templates, Scientific Description” DHI Water & Environment, 2017.
- DHI (2018a): “Alkimos Hydrodynamic Modelling, Calibration Report”, Draft Report prepared for Water Corporation by DHI Water & Environment Pty. Ltd., Rev. B, 12 Oct 2018.
- DHI (2018b): “Alkimos Seawater Desalination Plant, Brine Outfall Concept Design”, Report prepared for Water Corporation by DHI Water & Environment Pty. Ltd., Rev. 3.0, 11 Dec 2018.
- DHI (2019): “Alkimos Hydrodynamic Modelling, Scenario Screening Report”, Draft Report under preparation for Water Corporation by DHI Water & Environment Pty. Ltd.
- Doneker, R.L. and G.H. Jirka (2017): “CORMIX User Manual, A Hydrodynamic Mixing Zone Model and Decision Support System for Pollutant Discharges into Surface Waters”.
- DoT (2016): 5m gridded LIDAR data from 2016 survey, WA Dept of Transport. (Provided to DHI by DoT on 07 Jun 2018).
- DoT (2009): 5m gridded LIDAR data from 2009 survey, WA Dept of Transport. (Provided to DHI by BMT 26 Sep 2017).
- Frick, W.E., P.J.W. Roberts, L.R. Davis, J. Keyes, D.J. Baumgartner and K.P. George (2003): “Dilution Models for Effluent Discharges, 4th Edition (Visual Plumes)”, USEPA publication EPA/600/R-03/025, March 2003.
- Fugro (2005): “Alkimos Current & Wave Measurement Study, 30 April 2005 to 26 June 2005”, Report prepared for Water Corporation, Fugro GEOS Ref. C10658/3710/R1, September 2005.

- Gallop, S.L., F. Verspecht and C.B. Pattiaratchi (2012). "Sea breezes drive currents on the inner continental shelf off southwest Western Australia". *Ocean Dynamics*. 62: 569-583.
- Hipsey, M.R., Antenucci, J.P. and J.D. Brookes (2008): "A generic, process-based model of microbial pollution in aquatic systems". *Water Resources Research*. 44, W07408, doi:10.1029/2007WR006395.
- HYCOM (2016): Data from HYCOM+NCODA Global 1/12° Analysis (GLBa0.08), www.hycom.org, HYCOM Consortium.
- Jeppesen (2014): C-MAP Global Chart Database.
- Jones, O., J.A. Zyserman and Y. Wu (2014): "Influence of apparent roughness on pipeline design conditions under combined waves and current", Proceedings of the ASME 2014 33rd International Conference on Ocean, Offshore and Arctic Engineering,
- Lubin, D. E.H. Jense and H.P. Gies (1998): "Global surface ultraviolet radiation climatology from TOMS and ERBE data". *Journal of Geophysical Research*. 103. D20. 26061-26091.
- Maraccini, P.A., M.C.M. Mattioli, L.M. Sassoubre, Y.Cai, J.F. Griffith, J.S. Ervin, L.C. Van De Werfhorst and A.B. Boehm (2016): "Solar inactivation of Enterococci and Escherichia coli in natural waters: effects of water absorbance and depth". *Environmental Science and Technology*. 50: 5068-5076.
- Maraccini, P.A., J. Wenk and A.B. Boehm (2016): "Photoinactivation of eight health-relevant bacterial species: determining the importance of the exogenous indirect mechanism". *Environmental Science and Technology*. 50:5050-5059.
- Mihanovic, H., C. Pattiaratchi and F. Verspecht (2016). "Diurnal sea breezes force near-inertial waves along Rottnest Continental Shelf, Southwestern Australia". *Journal of Physical Oceanography*. 46: 3487-3508.
- MixZon (2015): "CORMIX User Manual - A Hydrodynamic Mixing Zone Model and Decision Support System for Pollutant Discharges into Surface Waters", MixZon Inc.
- Oceanica (2006): "Alkimos BPPH Loss Assessment", Memo prepared for Water Corporation, 12 Oct 2006.
- Roberts, P. J. W., Snyder, W. H., and Baumgartner, D. J. (1989a): "Ocean outfalls. I: Submerged wastefield formation." *J. Hydraul. Eng.*, 115 (1), 1–25.
- Roberts, P. J. W., Snyder, W. H., and Baumgartner, D. J. (1989b): "Ocean outfalls. II: Spatial evolution of submerged wastefield." *J. Hydraul. Eng.*, 115 (1), 26–48.
- Roberts, P. J. W., Snyder, W. H., and Baumgartner, D. J. (1989c): "Ocean outfalls. III: Effect of diffuser design on submerged wastefield." *J. Hydraul. Eng.*, 115 (1), 49–70.
- RPS APASA (2016): "Ocean Reef Marina Development, Phase 2: Water Quality Modelling", Report prepared for MP Rogers, Rev. 5, 01 Aug 2016.
- Saha, S., et al. (2011, updated monthly): "NCEP Climate Forecast System Version 2 (CFSv2) Selected Hourly Time-Series Products". Research Data Archive at the National Center for Atmospheric Research, Computational and Information Systems Laboratory. <http://dx.doi.org/10.5065/D6N877VB>.

- Sinton, L.W., R.J. Davies-Colley and R.G. Bell (1994): "Inactivation of enterococci and fecal coliforms from sewage and meatworks effluents in seawater chambers". *Applied and Environmental Microbiology* 60: 2040-2048.
- Sinton, L.W., C.H. Hall, P.A. Lynch and R. Davies-Colley (2002): "Sunlight inactivation of fecal indicator bacteria and bacteriophages from waste stabilization pond effluent in fresh and saline waters". *Applied and Environmental Microbiology*. 1122-1131.
- Soulsby, R.L. (1997): *Dynamics of Marine Sands: a Manual for Practical Applications*, Thomas Telford Publications, London.
- Tian, X., Roberts, P. J. W., and Daviero, G. J. (2004a): "Marine waste-water discharges from multiport diffusers. I: Unstratified stationary water." *J. Hydraul. Eng.*, 130 (12), 1137–1146.
- Tian, X., Roberts, P. J. W., and Daviero, G. J. (2004b): "Marine waste-water discharges from multiport diffusers. II: Unstratified flowing water." *J. Hydraul. Eng.*, 130 (12), 1147–1155.
- Tian, X., Roberts, P. J. W., and Daviero, G. J. (2006): "Marine waste-water discharges from multiport diffusers. IV: Stratified flowing water." *J. Hydraul. Eng.*, 132 (4), 411–419.
- UNESCO (2014): The GEBCO_2014 SID Grid, version 20141103, <http://www.gebco.net>.
- Water Corporation (2016b): "Alkimos Wastewater Treatment Plant - Site B, City of Wanneroo, Ministerial Statement 755 2015/16 Performance and Compliance Report".
- Water Corporation (2016a): "Alkimos Wastewater Treatment Plant - Marine Treated Wastewater Discharge Monitoring and Management Plan", May 2016.
- Water Corporation (2017): "Alkimos Wastewater Treatment Plant - Site B, City of Wanneroo, Ministerial Statement 755 2016/17 Performance and Compliance Report".
- Water Corporation (2018): "Alkimos SDP – Marine Modelling Guidance to Modelling Consultant, Technical Advice (Version 4)", Doc# 19411717v4, July 2018.
- WP (2005): "Alkimos Wastewater Treatment Plant, Hydrodynamic Modelling of Outlet Discharge", Report prepared for Water Corporation, Worley Parsons ref. 302/08986/a04, 25 Oct 2005.
- WP (2008): "Alkimos Outfall Dredge Management Plan, Hydrodynamic and Sediment Transport Modelling of Dredge Plume", Report prepared for Alkimos Alliance, Worley Parsons ref. 301012-00064/0, 28 Jun 2008.

APPENDIX A
Scenario Screening Design Periods

A Scenario Screening Design Periods

The appendix provides a review of climatological forcing relevant to the Alkimos site. While performed in the context of the identification of seasonally representative 30 day design periods for use in the scenario screening process, it is also of general relevance for site characterisation.

This work was performed in early June 2018, after which time a number of key datasets (most notably the latter portions of the Gardline AWAC deployments) were provided to DHI, and it has not been revisited. The work can be updated in a subsequent submittal of this report if required.

Alkimos Desalination Outfall Modelling

Discussion Regarding Design Periods

Via email

01 June 2018



Simulation Periods for Production -- Context

- Previous simulations performed by WP (2005) considered two design periods of 3 months, intended as representative of summer (Dec 2004 – Feb 2005) and autumn (Mar – May 2005). Also focuses on April, which is considered critical due to annual wind speed minimum.
- Much more data available post-2005 to characterize site. Present work also includes wave effects, which was not considered in choice of 2005 sim periods
- Simulations within calibrated model are heavy; in order to ensure that model is a practical tool this must be managed. Long continuous simulations are undesirable as shorter ones can be run in parallel for quicker response time.
- Approach must capture conditions in a manner sufficient to support Water Corporation decisionmaking
- Approach must be defensible to regulators

Simulation Periods for Production – Decision Points and Strategy

- Maintain identical 2005 simulation periods for consistency or redefine
- Maintain strategy of 2 x 3 month blocks per WP(2005) or redefine
- Base on wind climate alone per 2005 or consider additional environmental contributions (direct estimates of residual flows, waves)

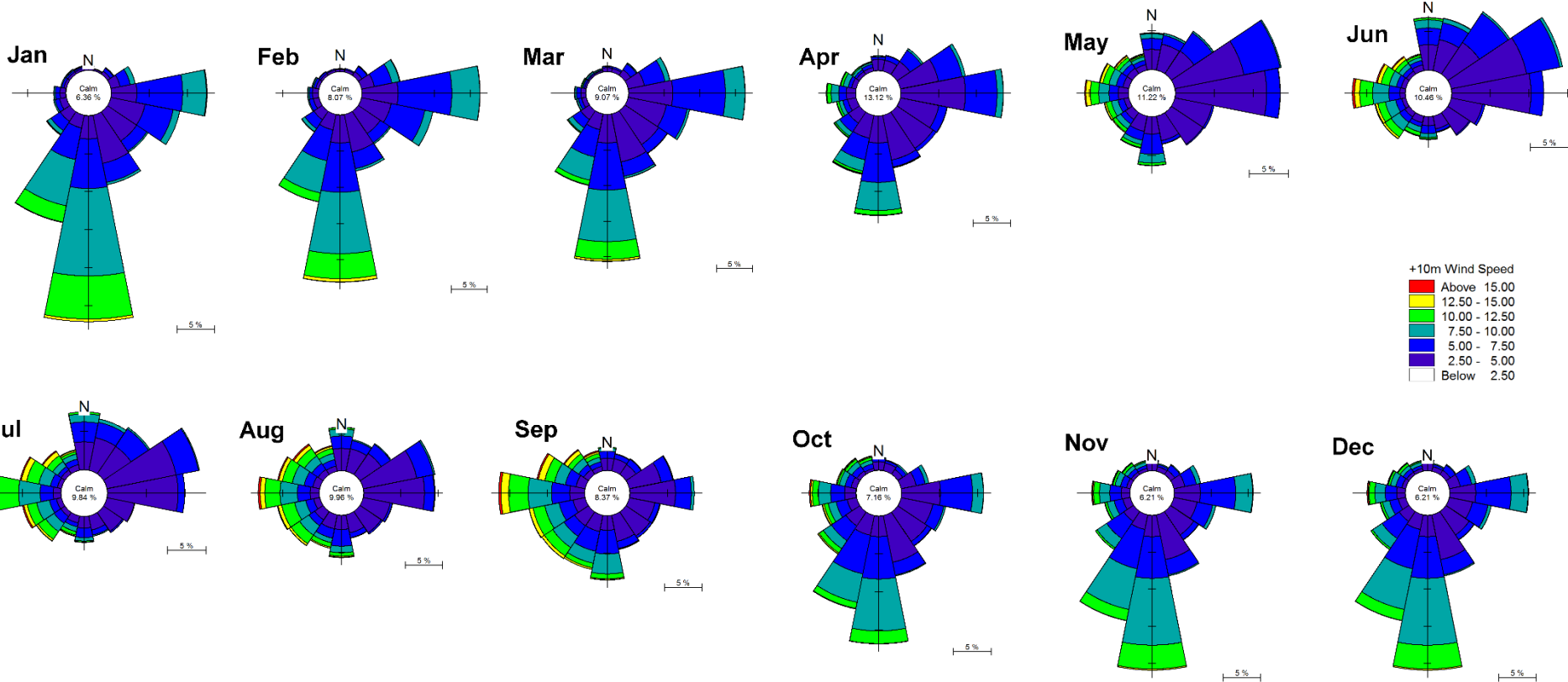
Simulation Periods for Production – Climate Characterization

Characterize long term climate of site using the following resources:

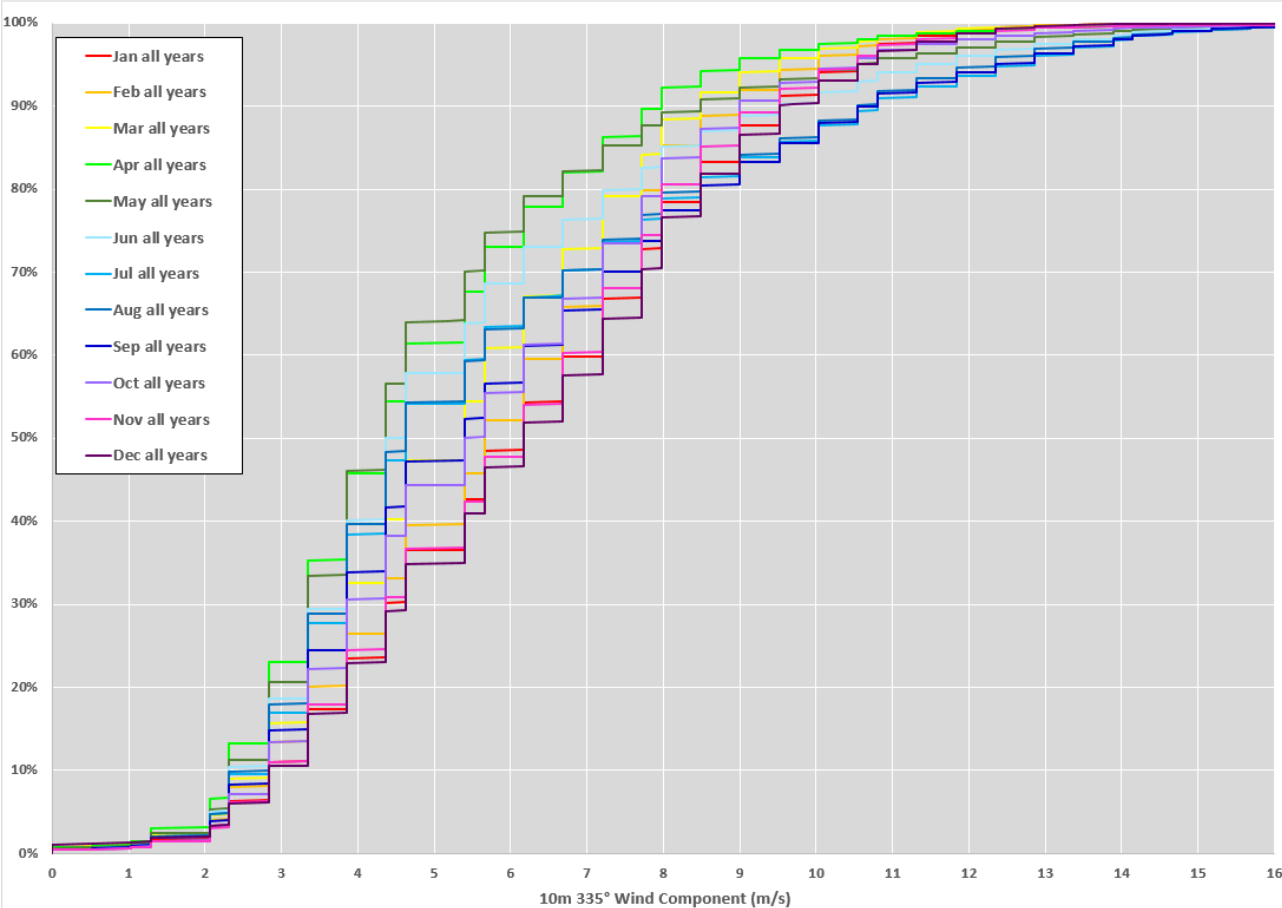
- Wind: 18 years of measured wind speed at Ocean Reef BoM station, also shore-parallel component of measured wind speed (both corrected to +10m values)
- Waves: 12 years of measured wave conditions from Rottnest DoT buoy (noting this measured Hs scales roughly linearly to Gardline D station), so an acceptable analog
- Residual currents: 6 years of hindcast flows from DHI's 3D hydrodynamic model of SW Australia, supported by shorter measurements at Two Rocks and Gardline D

Wind Climate

(Ocean Reef BoM Station Shown; all of given month 2000-2018)

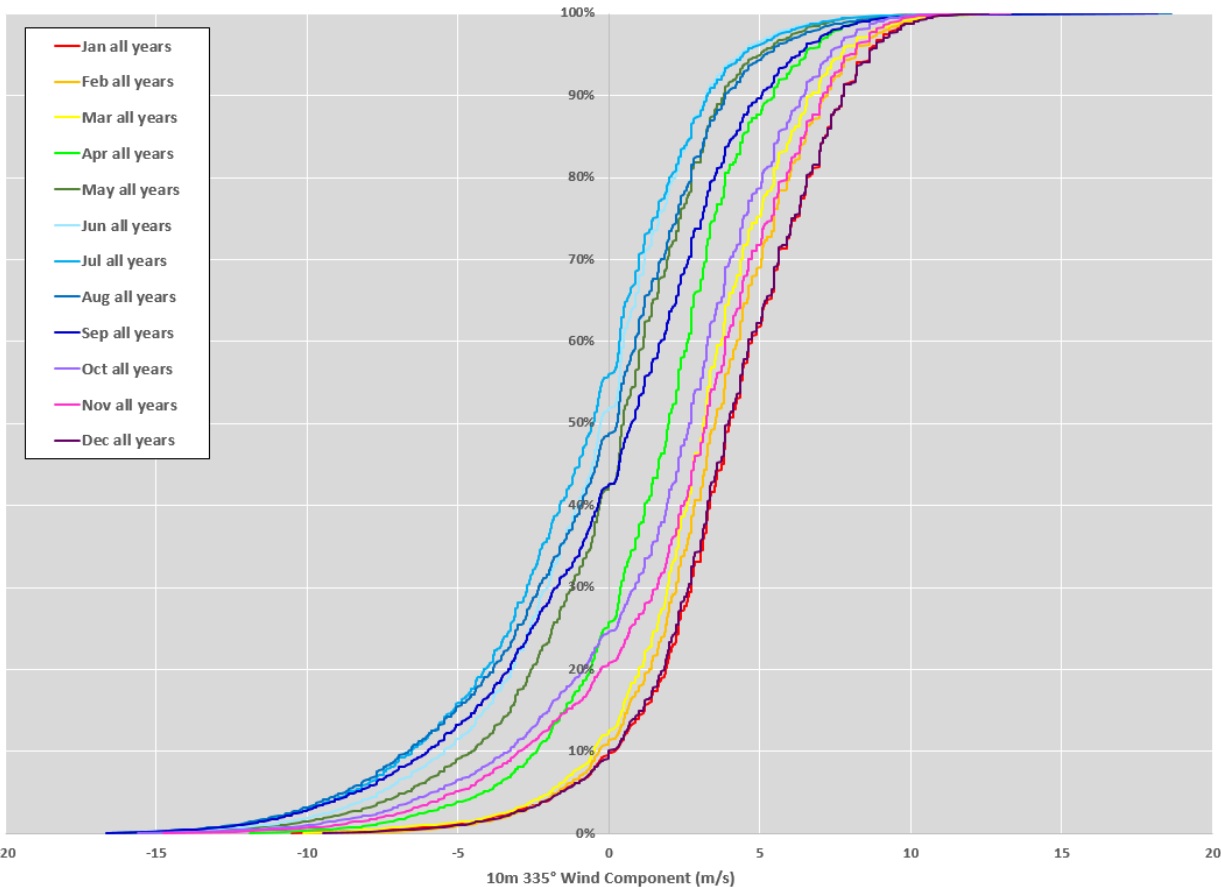


Wind Climate – Monthly Percentiles 2000-present (Ocean Reef BoM Station Wind Speed)



- Stepped as original data provided in integer values of km/hr
- Weakest median winds typically in Apr/May, strongest in Jan
- Strongest (>90th percentile) winds in winter.

Wind Climate – Monthly Percentiles 2000-present (Ocean Reef BoM Station 335° projected component)

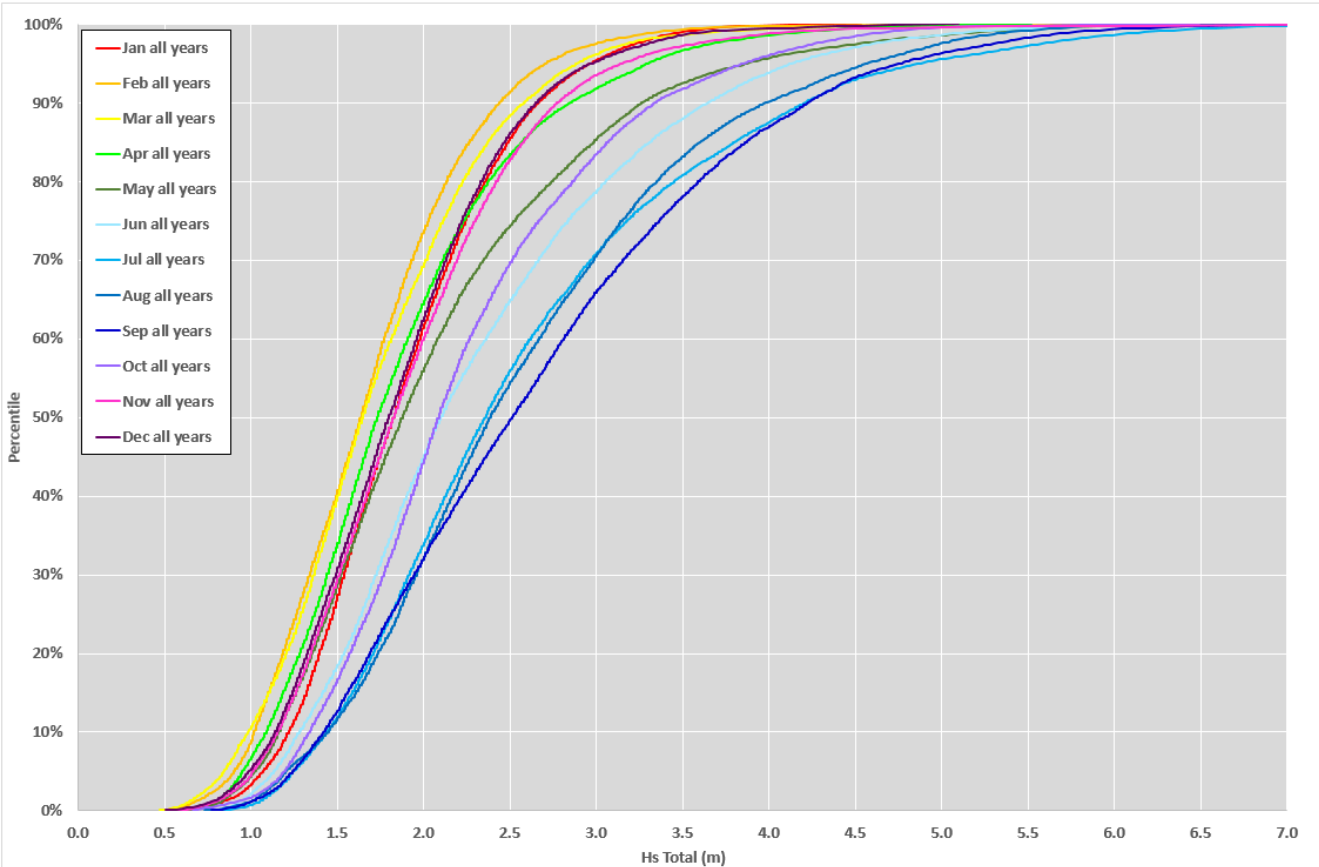


NOTE DIRECTIONAL CONVENTION APPLIED IN THIS FIGURE IS BLOWING TOWARD

- Apr and Jun are transitional months
- Dec-Mar cluster very well (also in wind roses prev slide) with mean residual directed toward north
- Jun-Aug cluster very well (also in wind roses prev slide) with mean residual near zero
- Seasonal character aligns very well with observed residual current behaviour, noting prevailing southward oceanic drift

Wave Climate

(Rottnest Significant Wave Height, 2005-present)



- Mar, May and to some degree Jun are transitional months
- Jul-Sep cluster well with high wave energy
- Dec-Apr cluster well with moderate wave energy

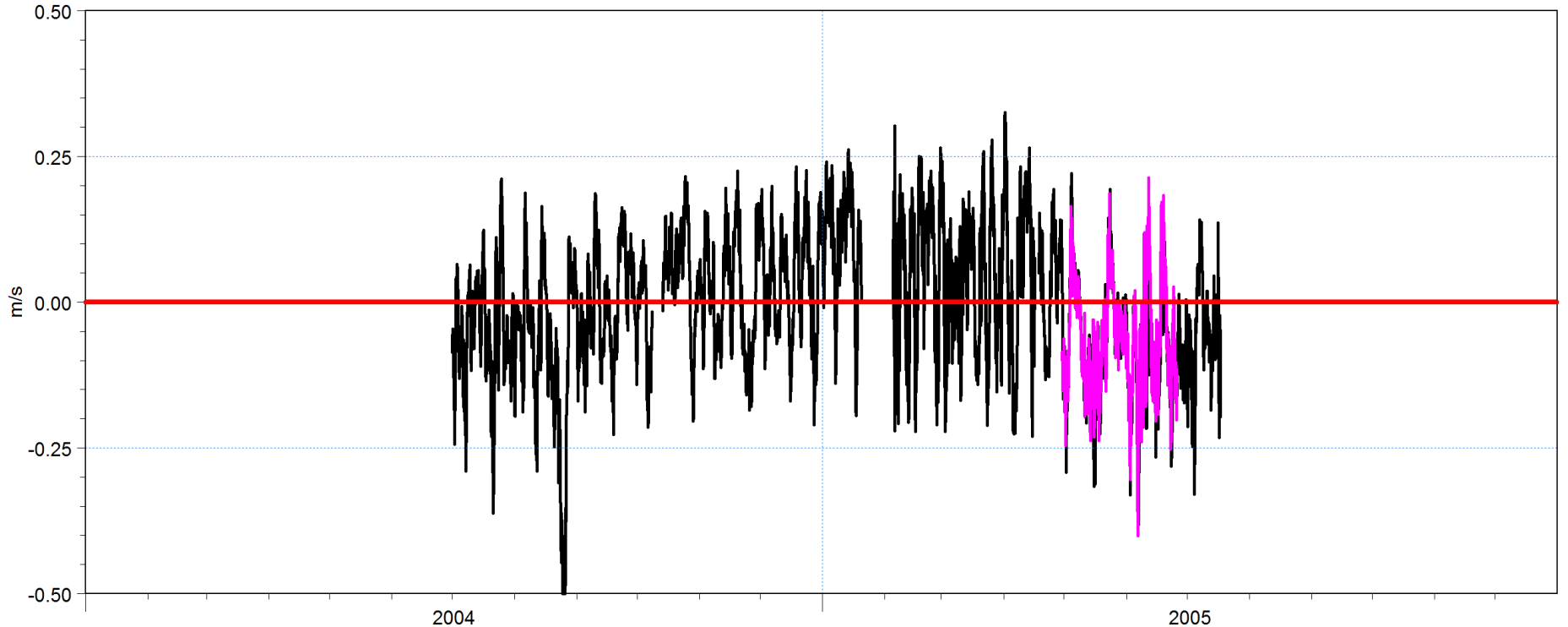
Residual Current Climate – Two Rocks Mooring A



Residual Current Climate

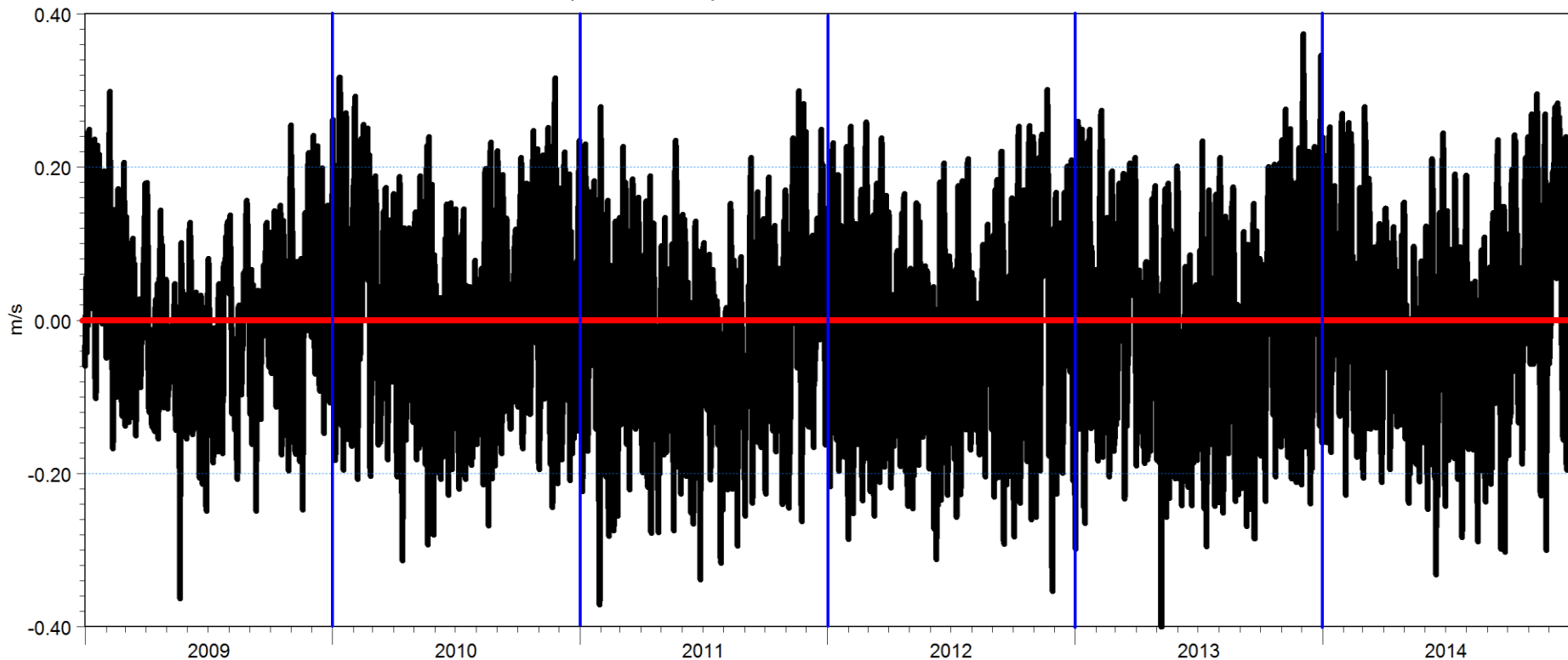
(Fugro B station plotted with Two Rocks Station A, 2004-2005)

Two Rocks A Projected Dep-Int Current (m/s) @ 331° [m/s] — (both measured)
Fugro B Projected Dep-Int Current (m/s) @ 335° [m/s] — (both measured)



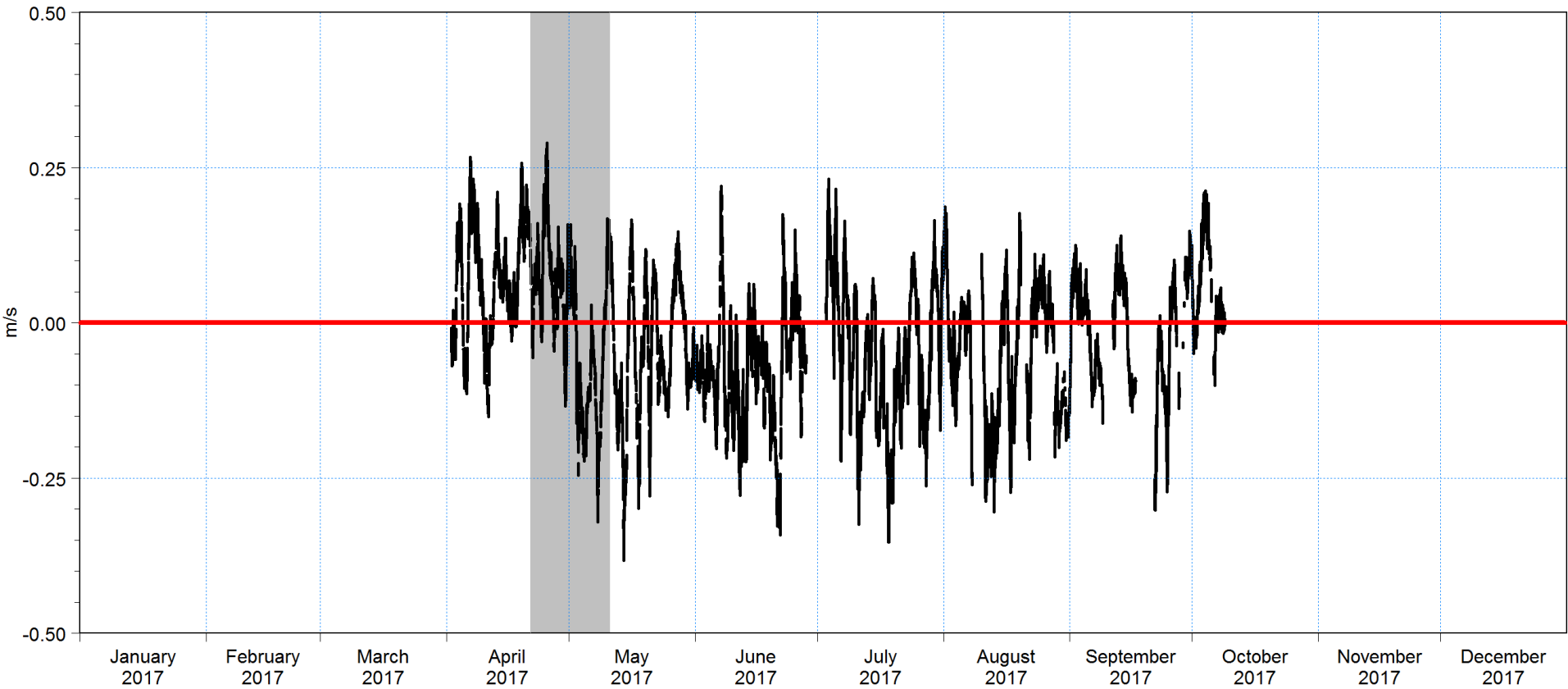
Residual Current Climate (2009-2014 inclusive) (DHI 3D Hindcast; Coarse; Extraction @ Gardline D Location)

AMSA 3D MODEL @ Gardline D, projected 335° [m] — (hindcast)

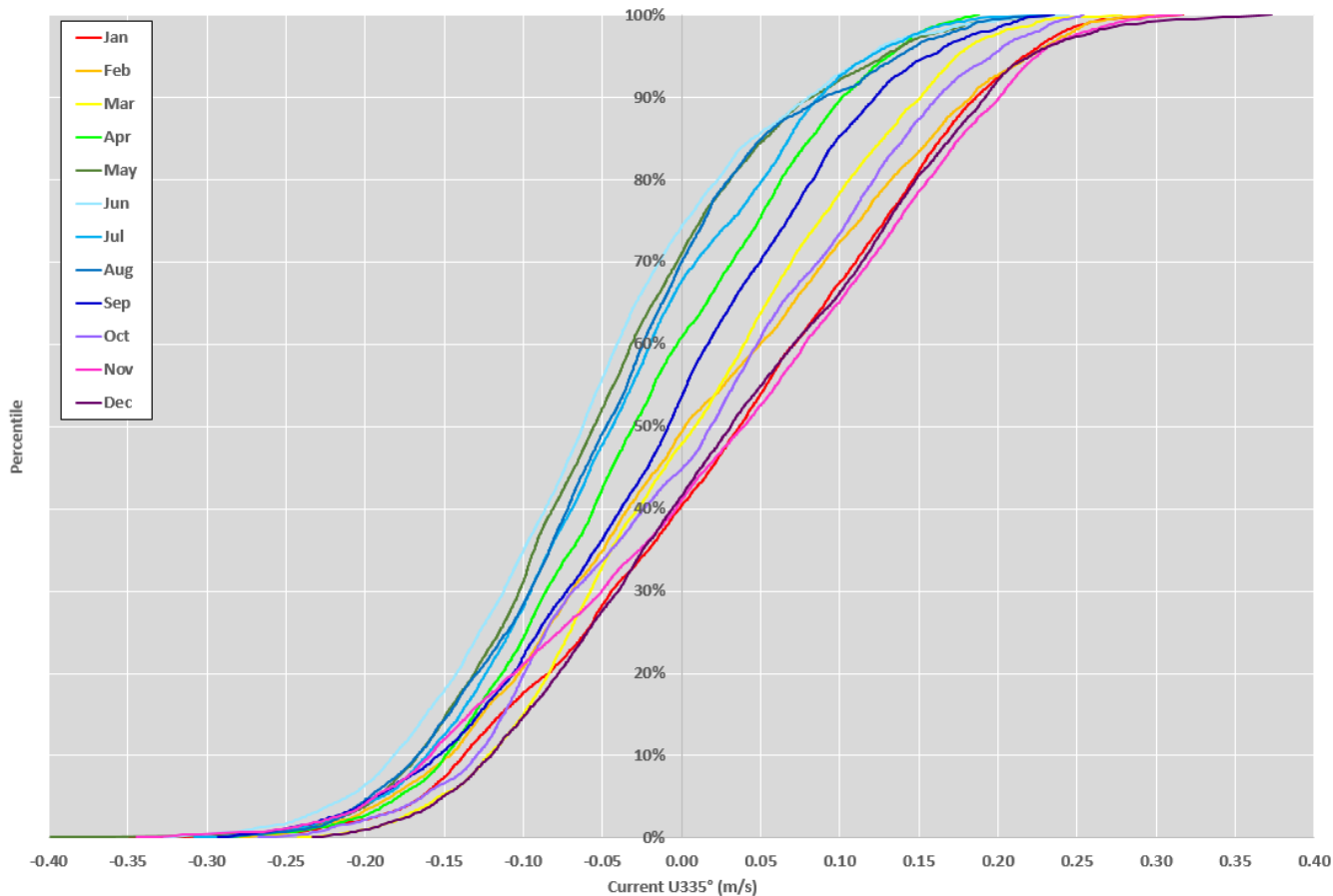


Residual Current Climate (Gardline D, deployments 1 and 2)

Gardline D projected 335° [m/s] — (measured)

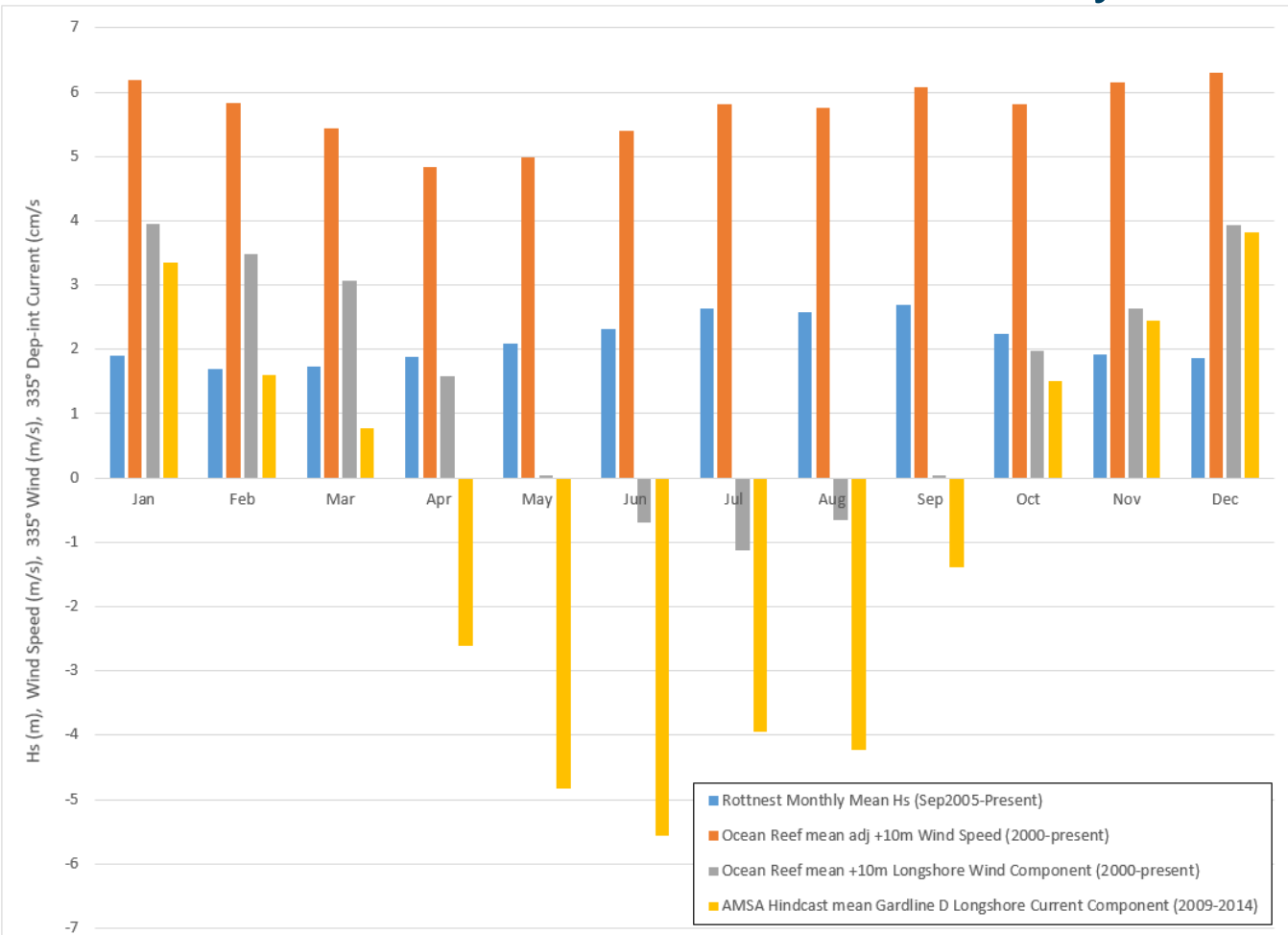


Residual Current Climate – Monthly Percentiles 2009-2014 (335° projected component extracted at Gardline D location)



- Again Apr and Jun are transitional months, also Mar to some degree
- Nov-Jan cluster very well with prevailing northward residual flow
- Jun-Aug cluster very well with prevailing southward residual flow
- Clear that northward orientation in existing WWTP regulatory boundary is a result of applied 2005 simulation periods, which are either dominantly northward which generates a northward extended plume footprint or a mix of N/S which generate a much smaller median field. No dominantly southward condition was simulated.

Climate Characterization -- Summary



Reasonable to target periods representative of winter (roughly Jun-Aug) and Summer (roughly Dec-Feb), and possibly a shorter period targeting weak April winds

Simulation Periods for Production – Decision Points and Strategy

- Establish new design periods, as there is far more data to justify such decisions that was available in 2005, and waves are now also a contributor. For maximum transparency, target recent year over which Gardline instruments were in place.
- Prefer series of shorter simulation periods vs. full year, due to limitations imposed by a single long block of CPU time which would limit turn-around time for testing.
- We propose short simulations for efficiency of design screening, with a full continuous 12 month simulation for the final preferred design. The latter is considered overkill, but is likely to be useful for regulator engagement.
- Given inherent variability of shorter term records in relation to long-term statistics, seek records on the order of 1 month (long enough to provide a distribution of events but short enough to allow for computational efficiency throughout the design screening stage).

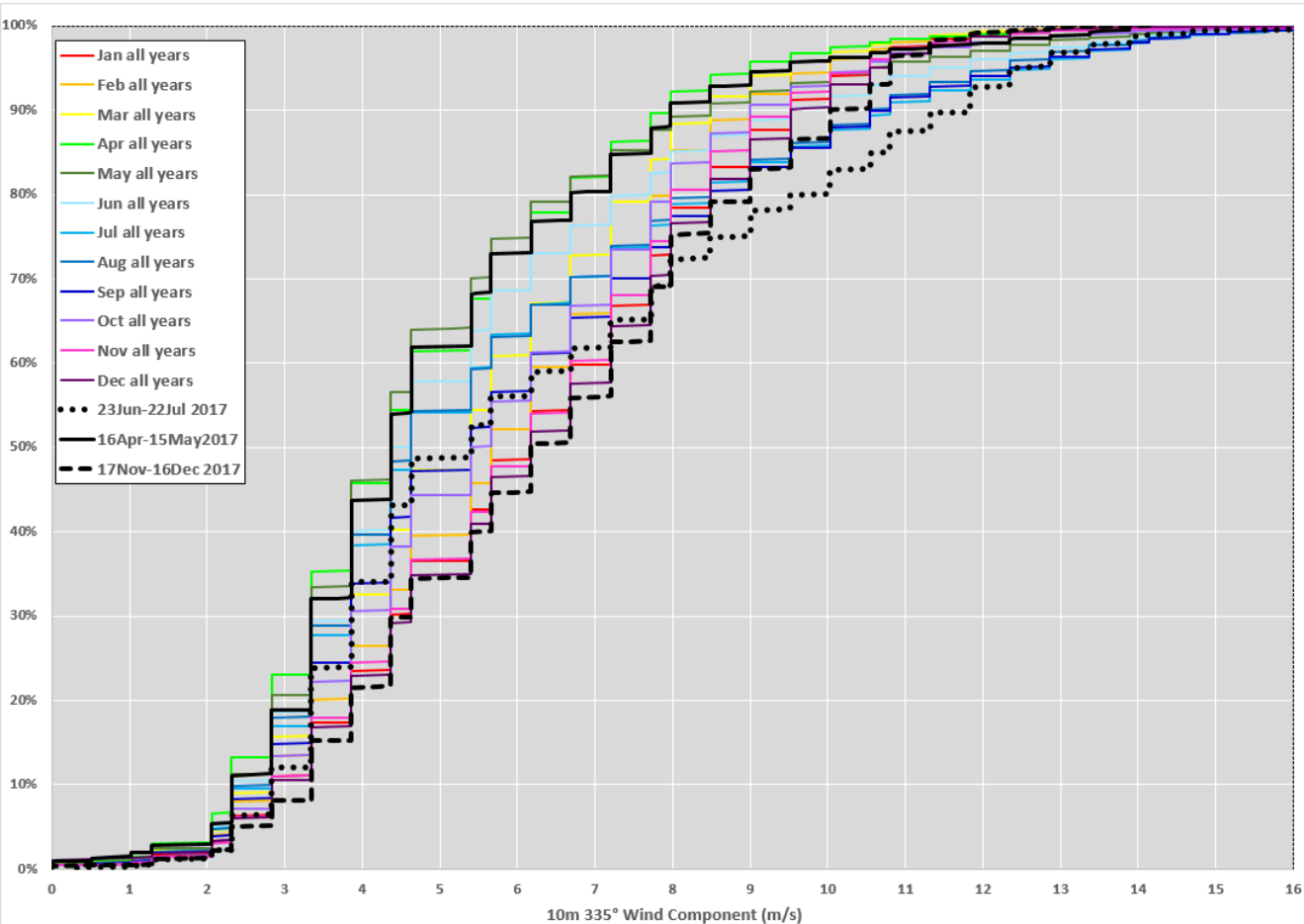
Proposed Simulation Periods for Production

For screening each of the following are proposed as 30 days' production subsequent to model spin-up:

- Winter: 23 Jun – 22 Jul 2017
- Summer: 17 Nov – 16 Dec 2017
- Transitional: 16 Apr – 15 May 2017

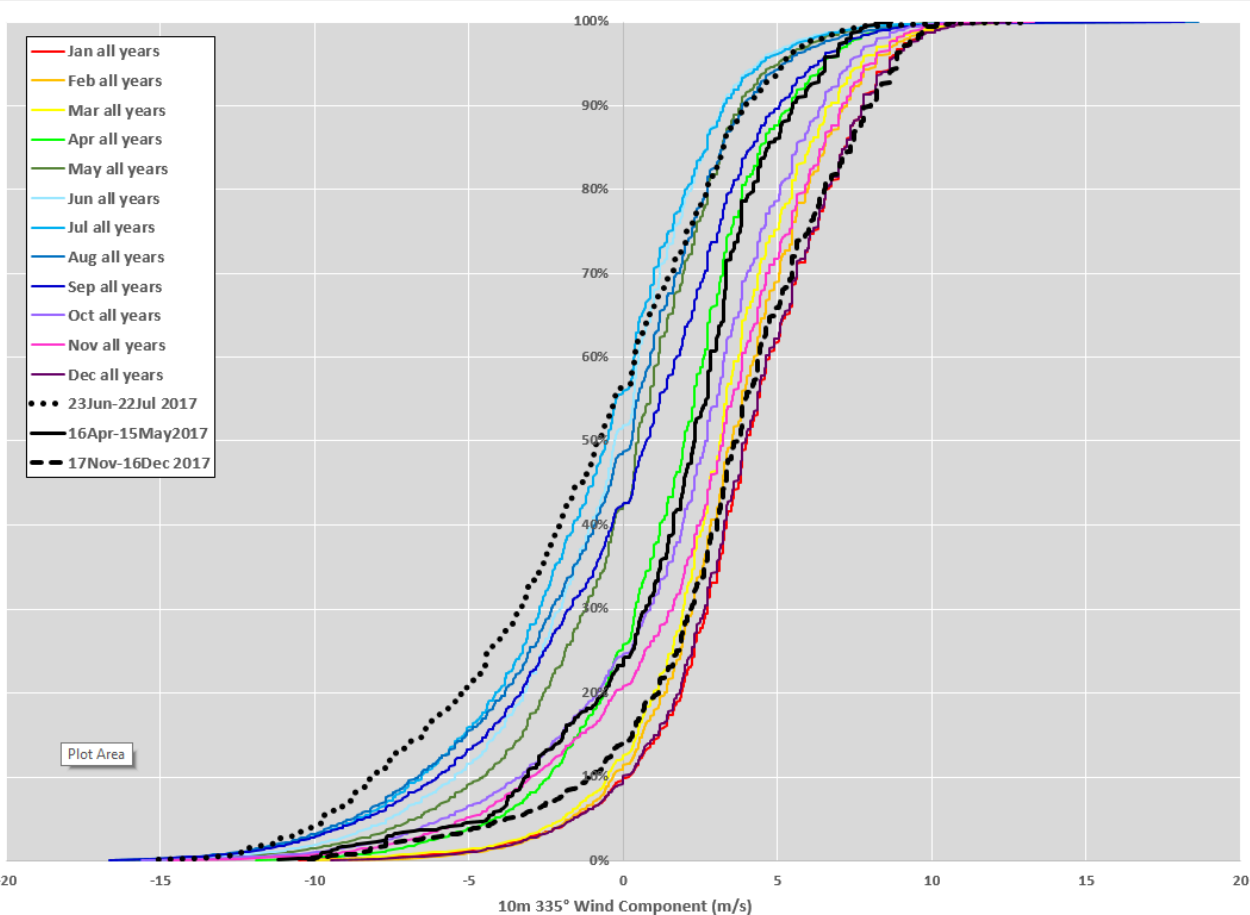
... with the final preferred solution then being simulated for a full calendar year

Proposed Simulation Periods for Production - Windspeeds



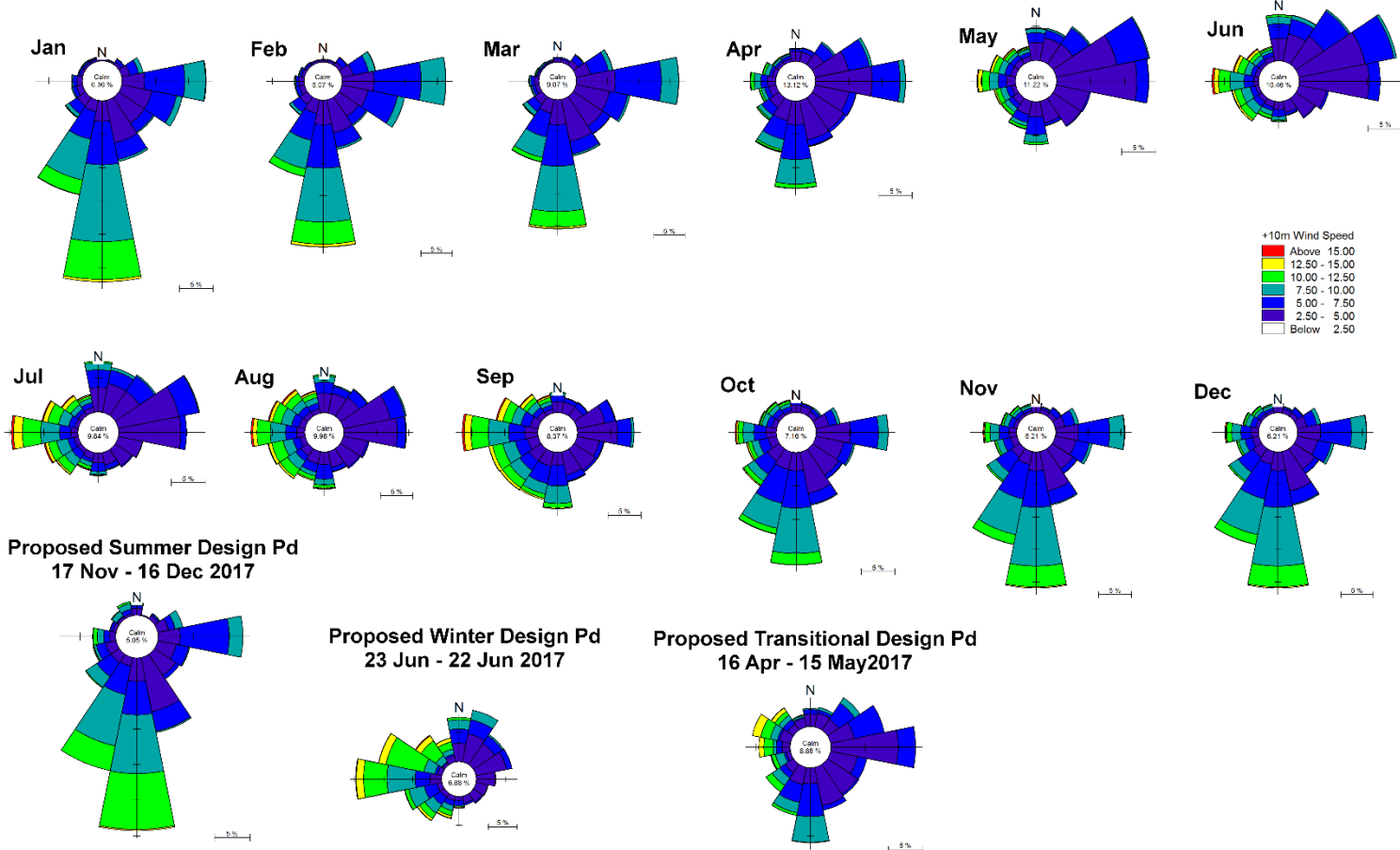
- 23Jun-22Jul aligns reasonably well with long-term Winter months, though higher percentiles are slightly higher than typical
- 17Nov-16Dec aligns well with long-term Summer months
- 16 Apr-15 May period exhibits weak wind speeds expected of autumn transitional period

Proposed Simulation Periods for Production – 335° Winds



- 23Jun-22Jul aligns well with long-term Winter months. There is a slight over-representation of winds directed southward.
- 17Nov-16Dec aligns very well with long-term Summer months
- 16Apr-15May also sits very well as a transitional period (aligning with Apr and Oct)

Proposed Simulation Periods for Production – Wind Roses

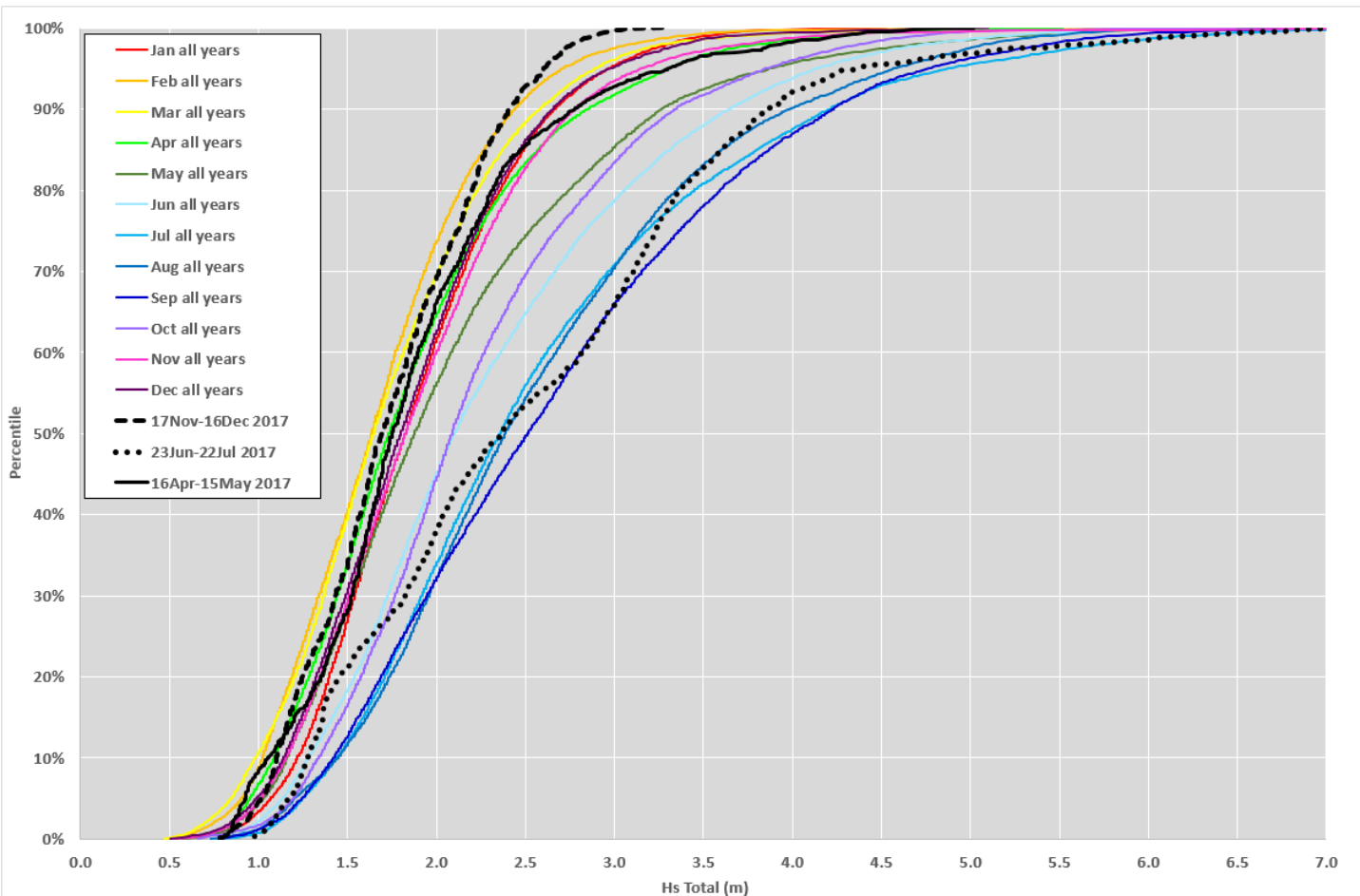


- 23Jun-22Jul aligns reasonably well with long-term Winter months, though per previous slide there is a slight over-representation of winds blowing from northern sectors (from window of WNW through NNW)
- 17Nov-16Dec aligns very well with long-term Summer months
- 16 Apr-15 May period aligns very well with Apr/May transition

Proposed Simulation Periods for Production – Residual Currents

- Slide 11 shows that 23Jun-22Jul Winter period features dominantly southerly residual flow, with numerous reversals especially in late Jun / early Jul. This aligns with expectations.
- For the 17Nov-16Dec Summer period, DHI does not have AWAC data from this deployment. However, the wind statistics suggest that the residual flow should be dominantly northward as desired for a Summer design period.
- For the 16Apr-15May Transitional period, residuals are a roughly even split with the end of Apr dominantly northward and May being southward.

Proposed Simulation Periods for Production - Waves



- 23Jun-22Jul aligns well with long-term Winter months
- 17Nov-16Dec aligns well with long-term Summer months, though the strongest waves > 90th percentile are somewhat weaker than is typical.
- 16Apr-15Apr period aligns well with a typical Apr, and is somewhat low for a typical May.

APPENDIX B

ASDP Excess Salinity Fields

B ASDP Excess Salinity Fields

This appendix presents mapping of modelled ASDP excess salinity fields, with each figure incorporating panes of the median, 95th percentile and maximum excess salinity fields.

In all cases these fields are calculated by first collapsing the 3D ASDP tracer output field to a 2D field containing the maximum concentration over the water column at each timestep. The tracer concentration is a value between 0 and 1.

In the present appendix this factor is then multiplied by a reference excess salinity of $37 \times (1.925 - 1) = 34.225$ psu. In this calculation, 37 psu is the annual maximum of the ambient (intake) salinity using the conservative curve applied for the calculation of the ASDP discharge brine. The ratio of brine concentration by the ASDP facility has been provided by Water Corporation as 1.925 relative to intake salinity (Water Corporation, 2018).

Figure B-1 provides annual statistics of the annual excess salinity field. Figures B-2 through B-13 provide similar results by month in the sequence of the 12 month simulation, specifically April 2017 through March 2018.

All plots include overlays indicating the preferred ASDP intake and outfall locations.

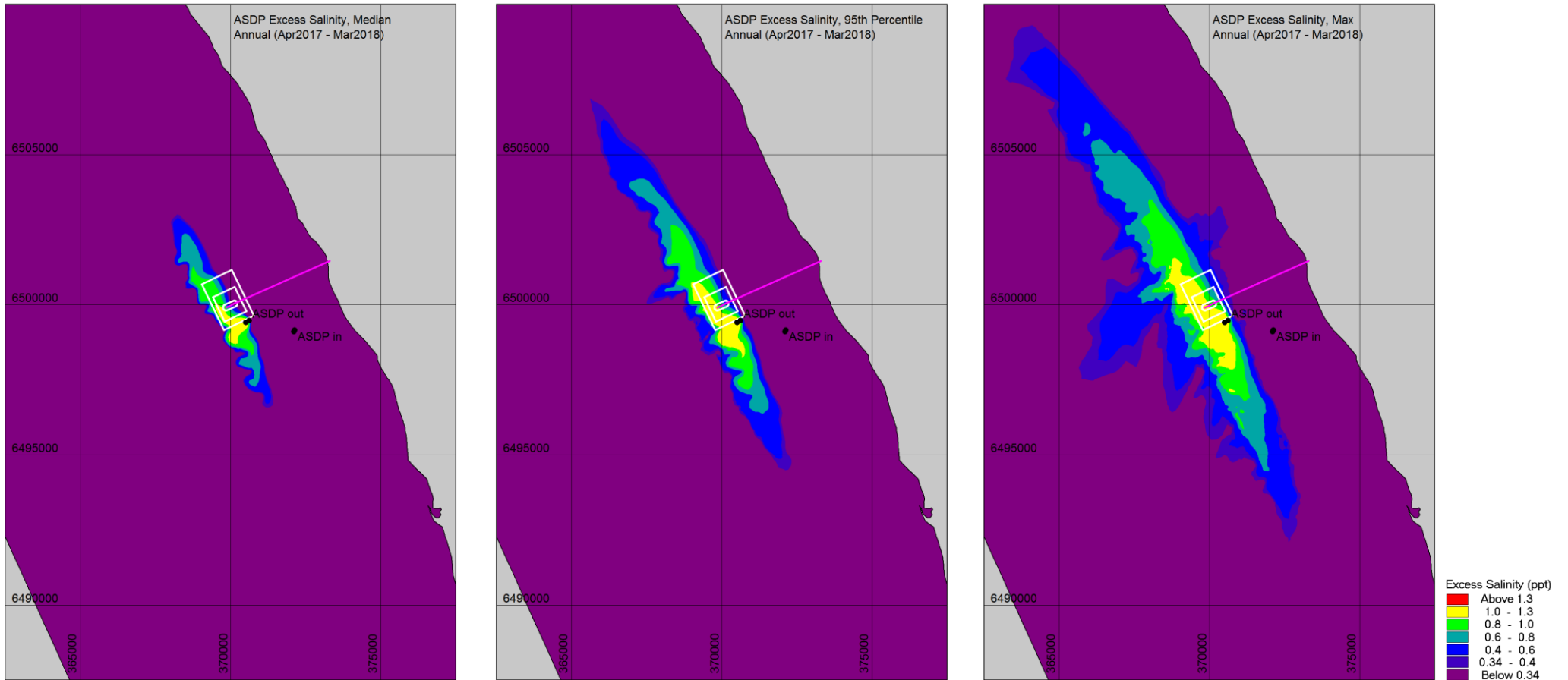


Figure B-1 Median, 95th percentile and maximum ASDP excess salinity. Annual statistics (April 2017 – March 2018). Processed by first collapsing the 3D ASDP tracer output field to a 2D field containing the max concentration over the water column at each timestep.

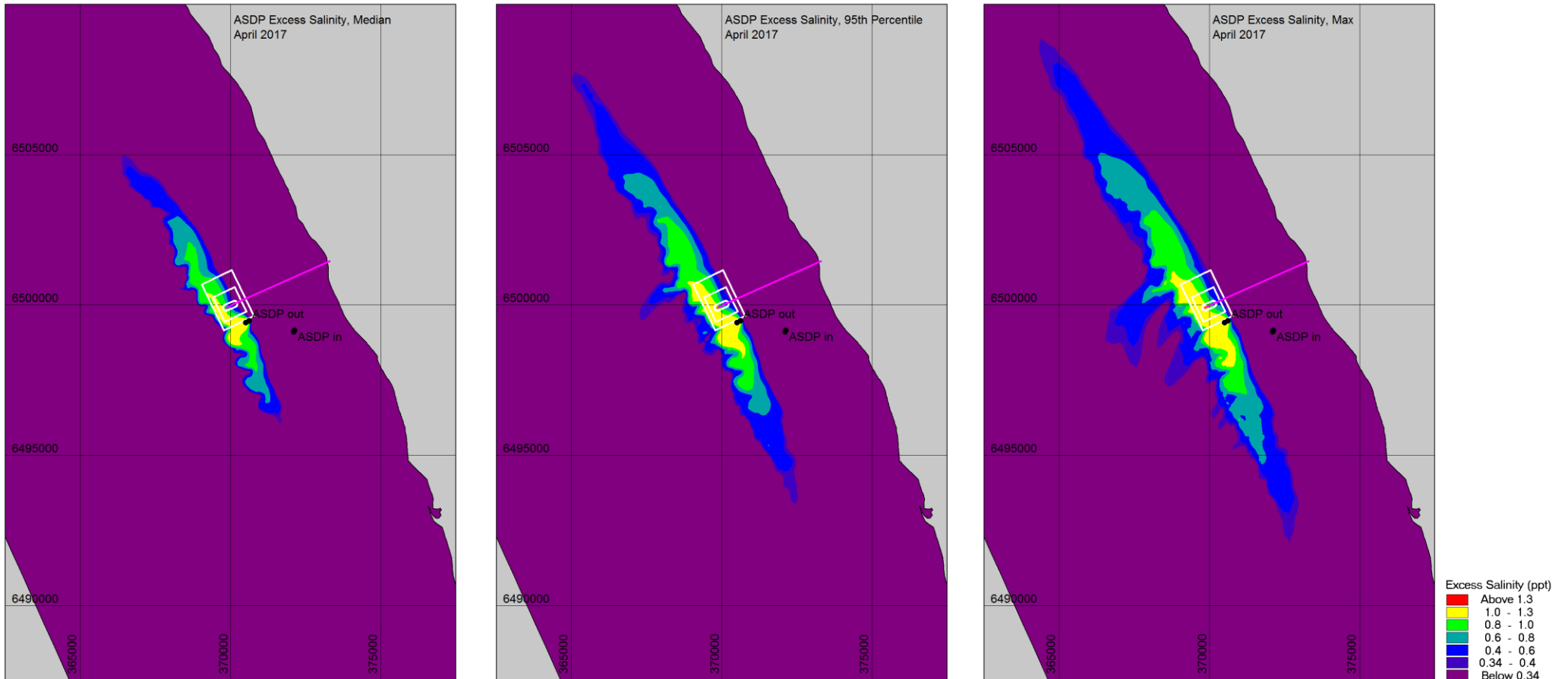


Figure B-2 Median, 95th percentile and maximum ASDP excess salinity. Monthly statistics (**April 2017**). Processed by first collapsing the 3D ASDP tracer output field to a 2D field containing the max concentration over the water column at each timestep.

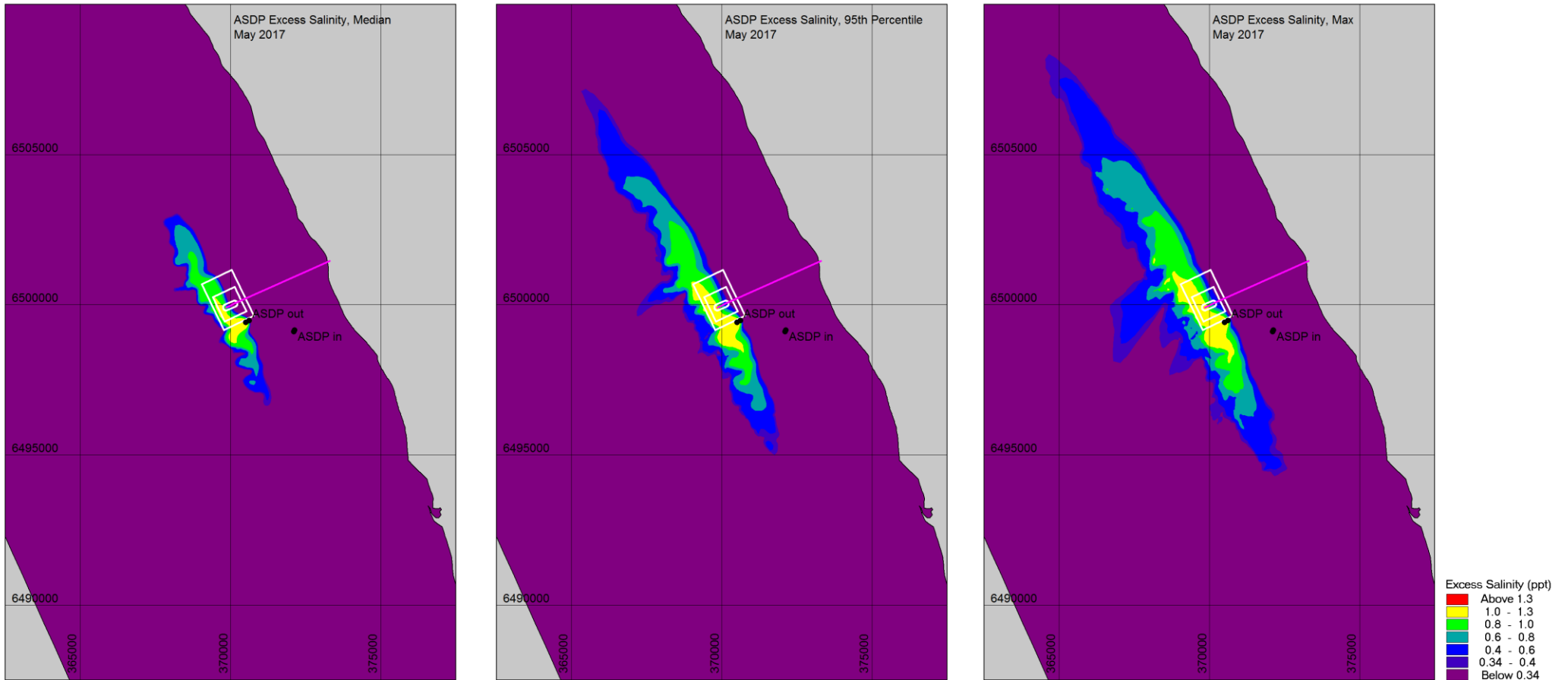


Figure B-3 Median, 95th percentile and maximum ASDP excess salinity. Monthly statistics (**May 2017**). Processed by first collapsing the 3D ASDP tracer output field to a 2D field containing the max concentration over the water column at each timestep.

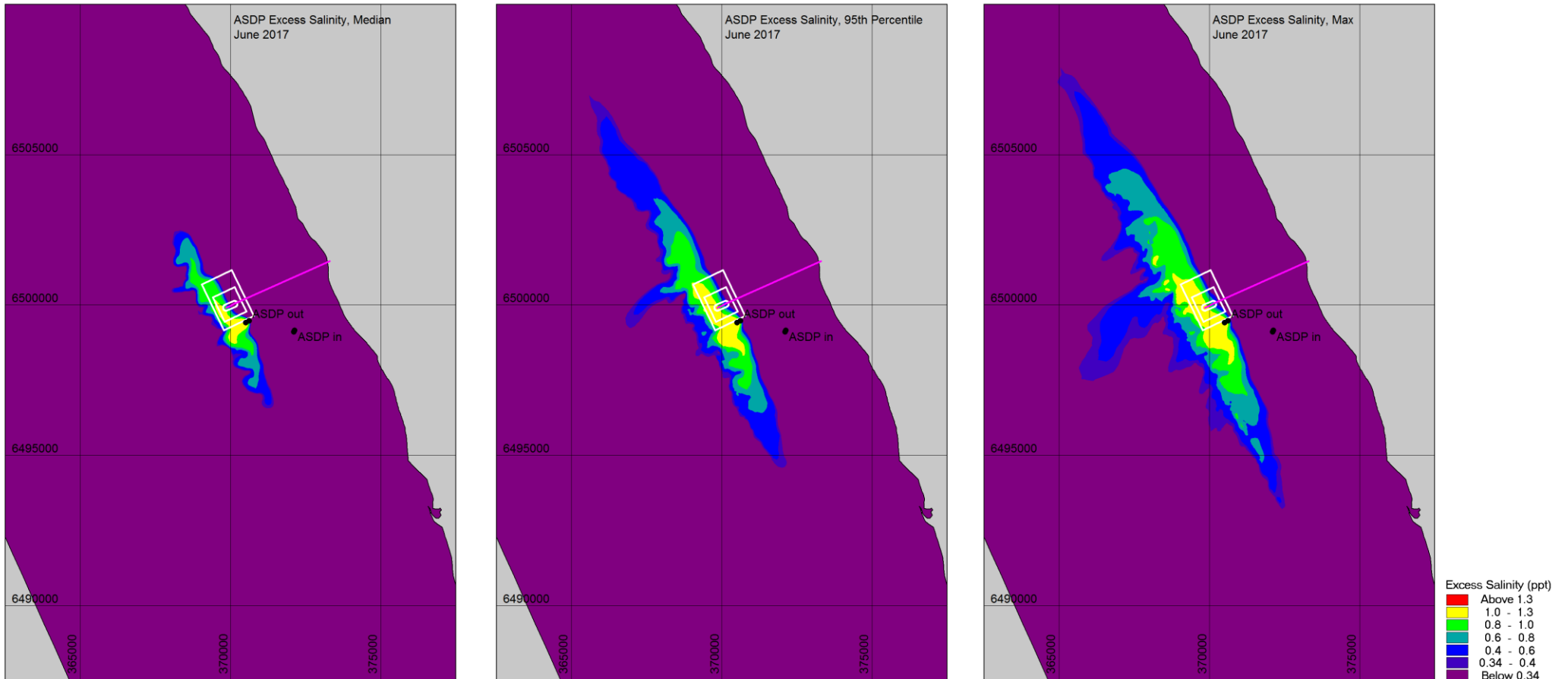


Figure B-4 Median, 95th percentile and maximum ASDP excess salinity. Monthly statistics (**June 2017**). Processed by first collapsing the 3D ASDP tracer output field to a 2D field containing the max concentration over the water column at each timestep.

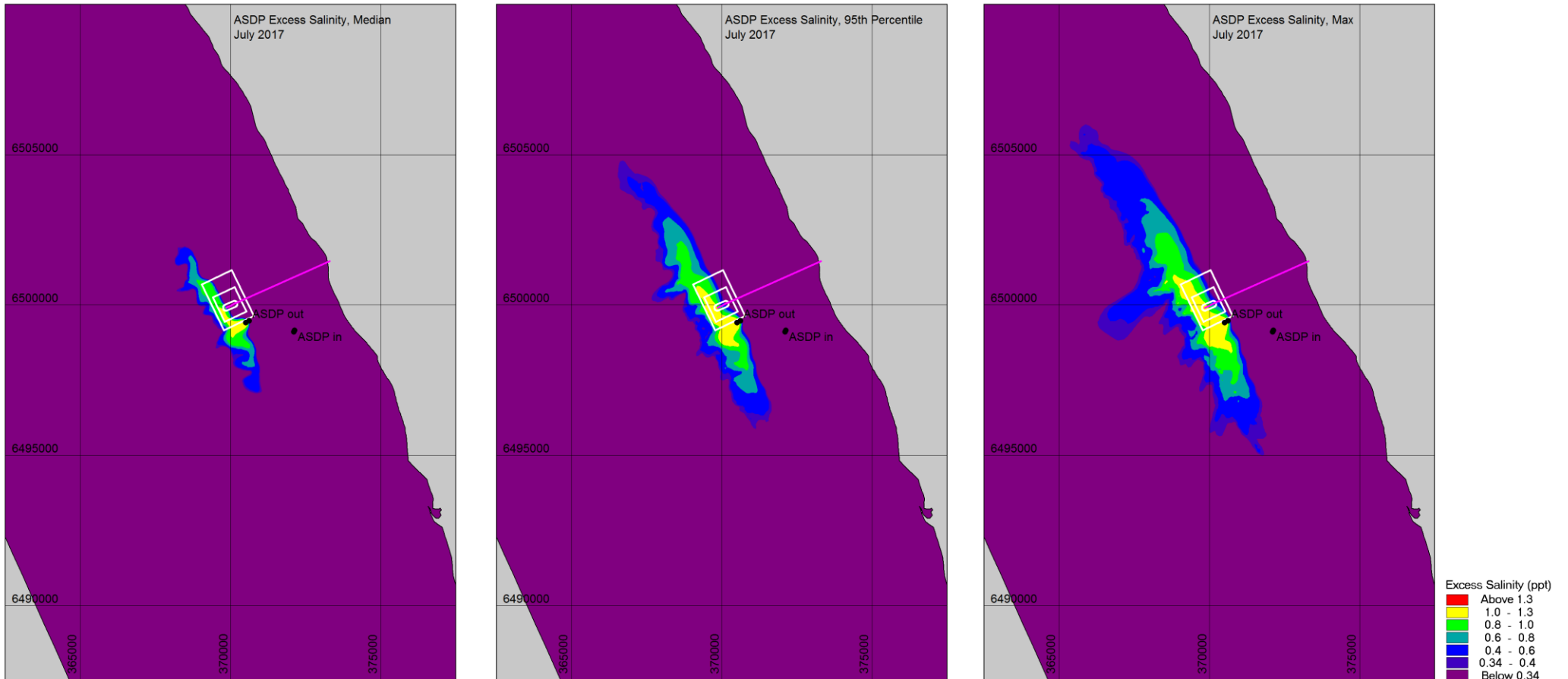


Figure B-5 Median, 95th percentile and maximum ASDP excess salinity. Monthly statistics (**July 2017**). Processed by first collapsing the 3D ASDP tracer output field to a 2D field containing the max concentration over the water column at each timestep.

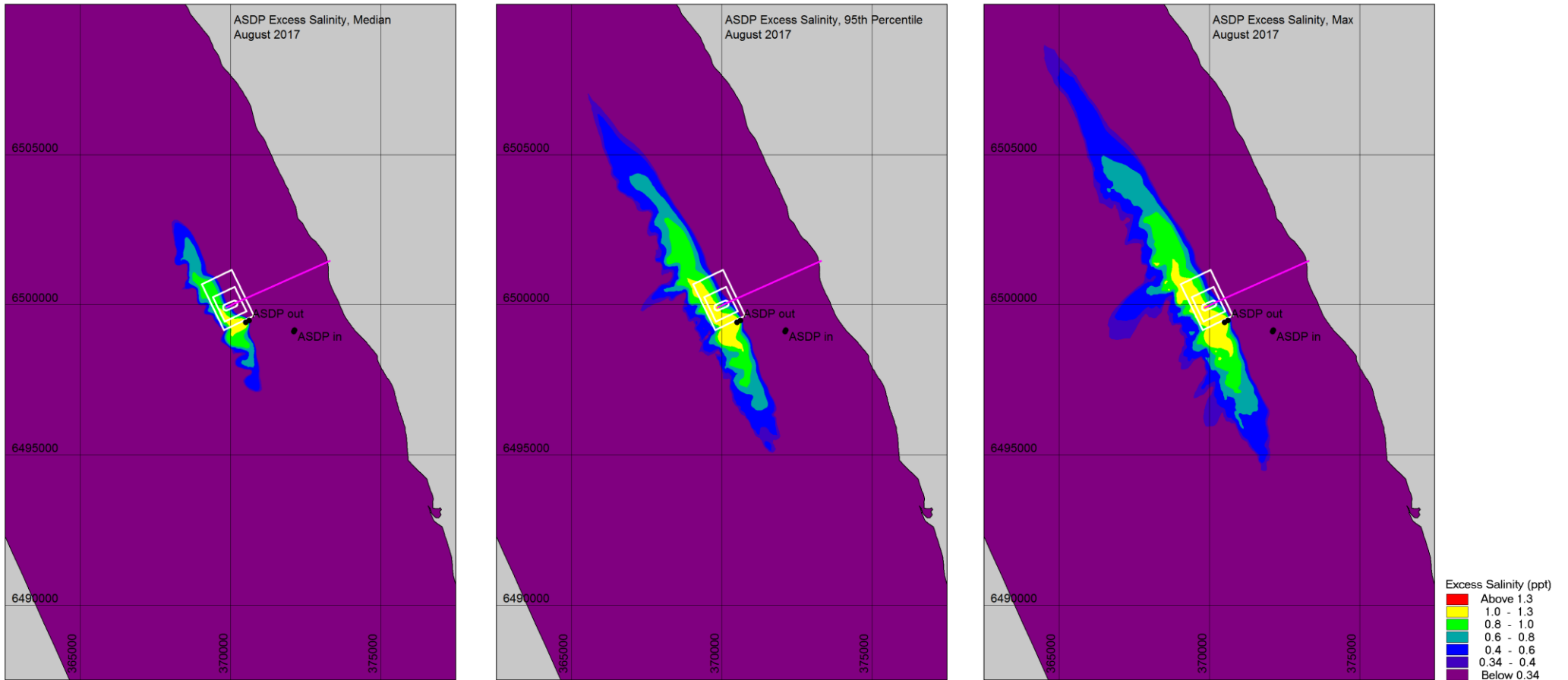


Figure B-6 Median, 95th percentile and maximum ASDP excess salinity. Monthly statistics (**August 2017**). Processed by first collapsing the 3D ASDP tracer output field to a 2D field containing the max concentration over the water column at each timestep.

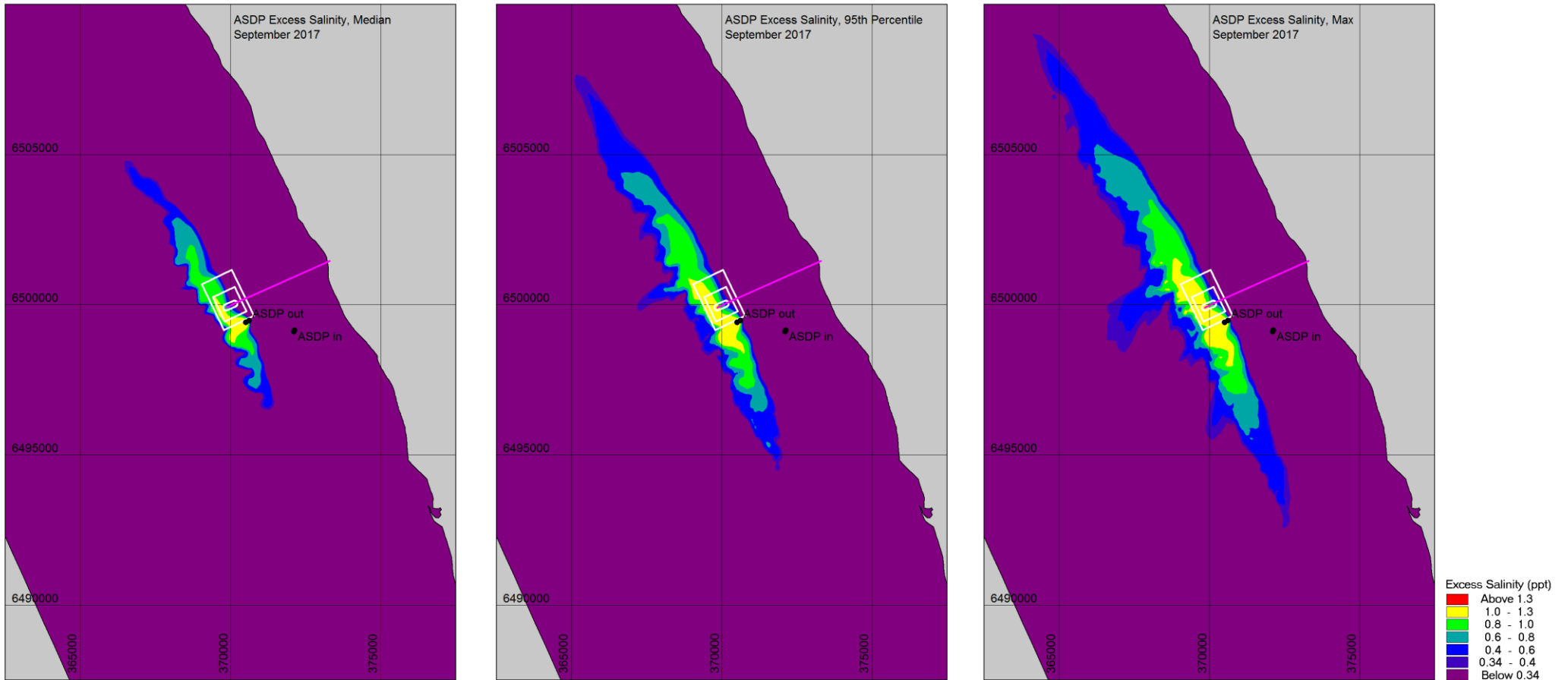


Figure B-7 Median, 95th percentile and maximum ASDP excess salinity. Monthly statistics (**September 2017**). Processed by first collapsing the 3D ASDP tracer output field to a 2D field containing the max concentration over the water column at each timestep.

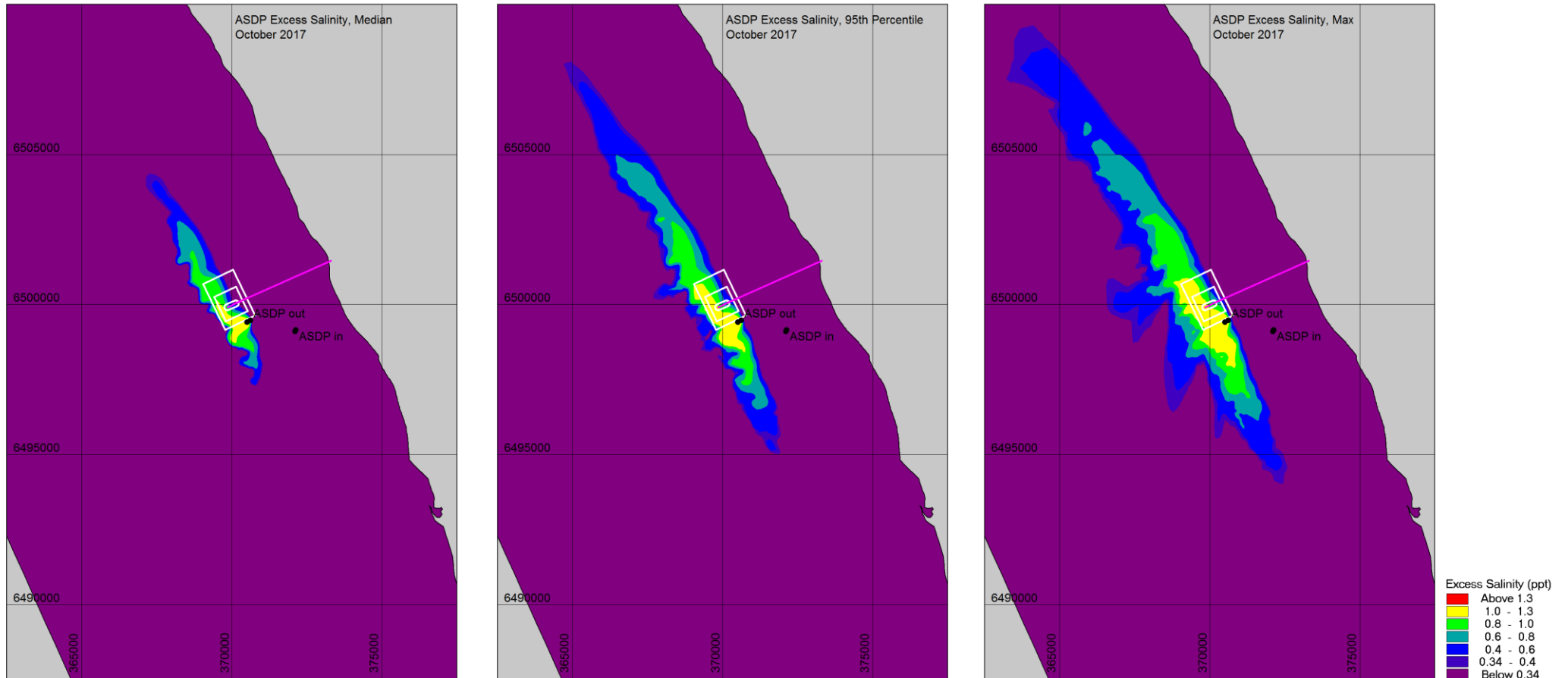


Figure B-8 Median, 95th percentile and maximum ASDP excess salinity. Monthly statistics (**October 2017**). Processed by first collapsing the 3D ASDP tracer output field to a 2D field containing the max concentration over the water column at each timestep.

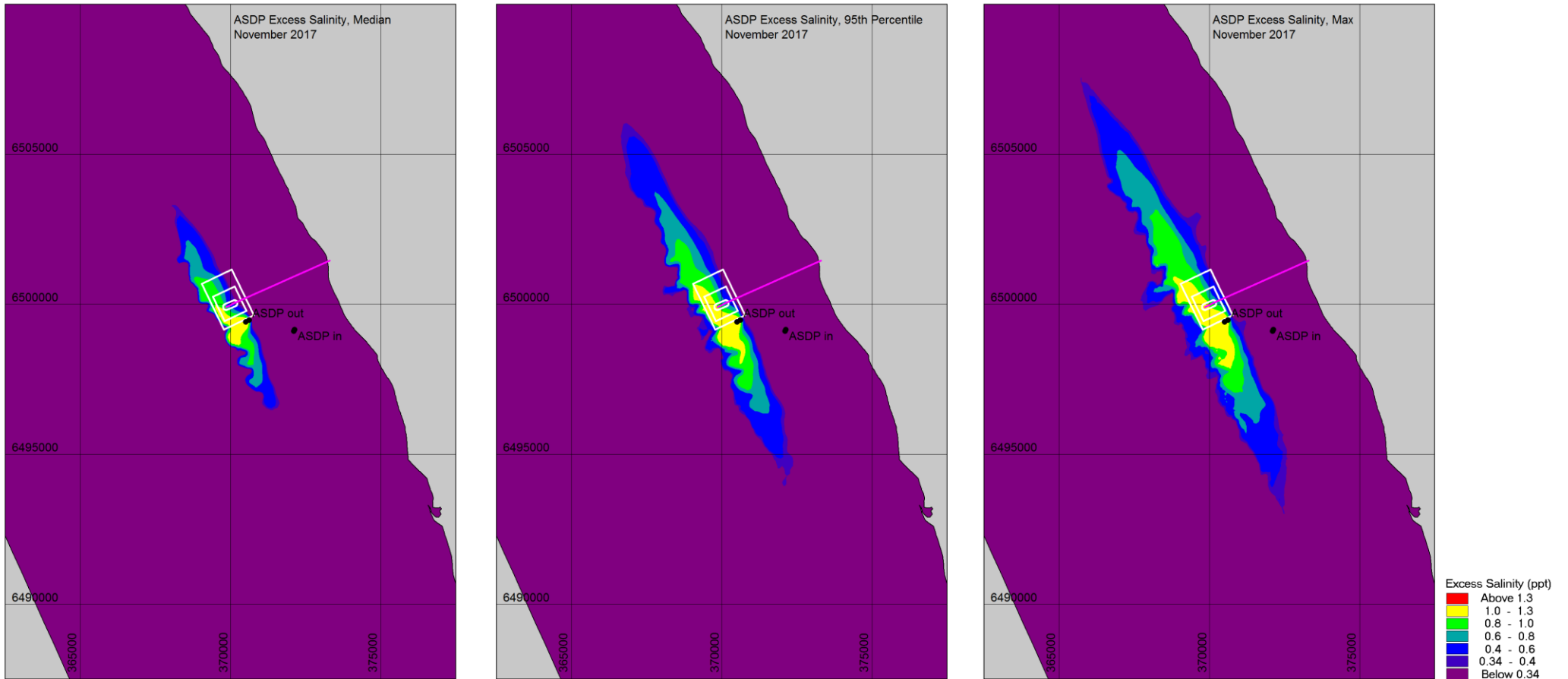


Figure B-9 Median, 95th percentile and maximum ASDP excess salinity. Monthly statistics (**November 2017**). Processed by first collapsing the 3D ASDP tracer output field to a 2D field containing the max concentration over the water column at each timestep.

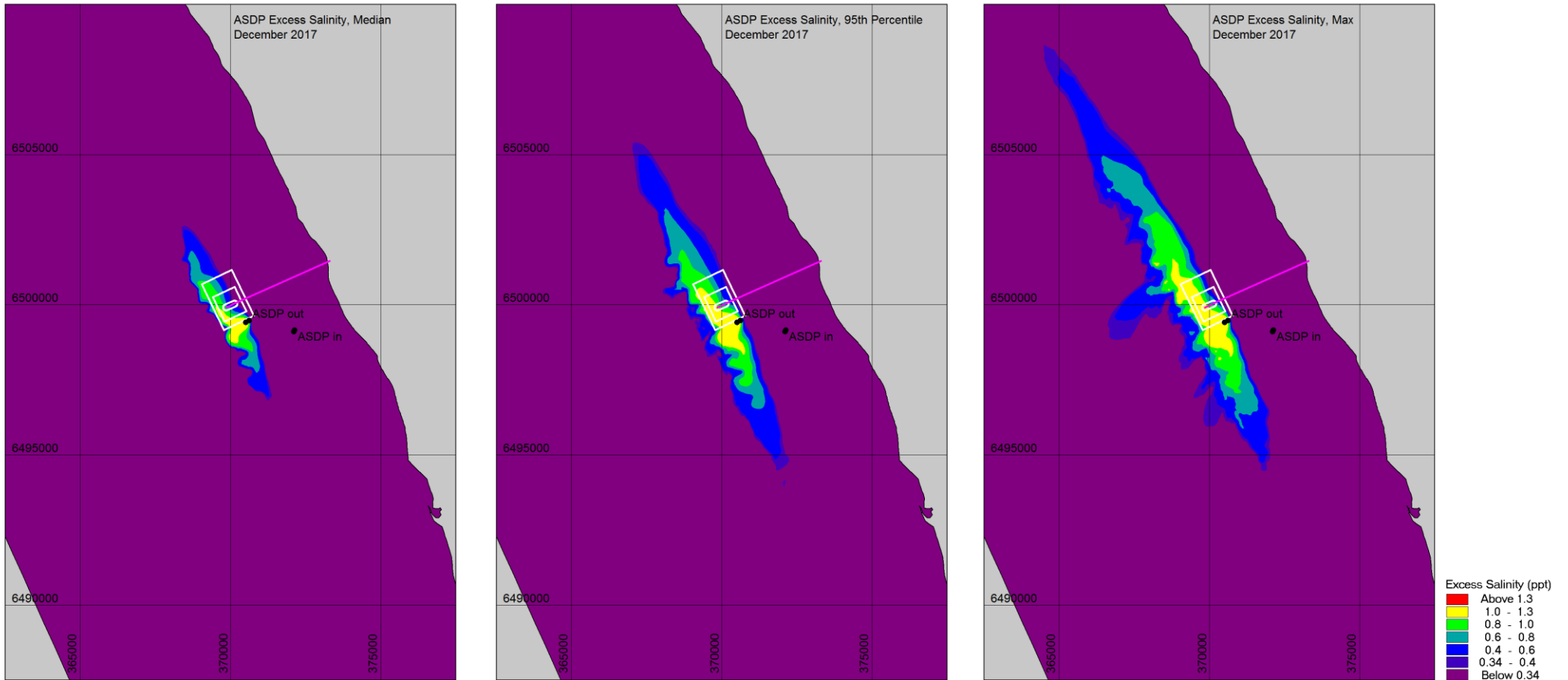


Figure B-10 Median, 95th percentile and maximum ASDP excess salinity. Monthly statistics (**December 2017**). Processed by first collapsing the 3D ASDP tracer output field to a 2D field containing the max concentration over the water column at each timestep.

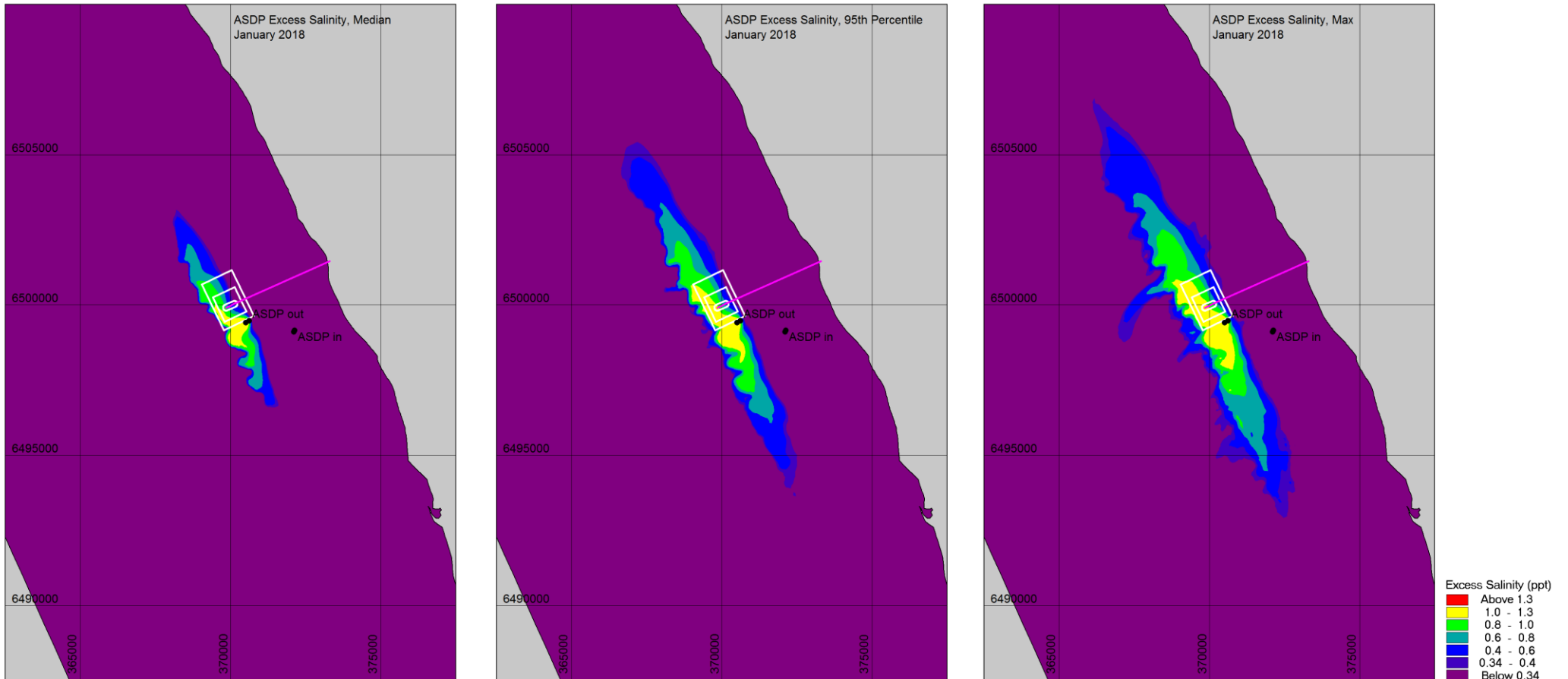


Figure B-11 Median, 95th percentile and maximum ASDP excess salinity. Monthly statistics (**January 2018**). Processed by first collapsing the 3D ASDP tracer output field to a 2D field containing the max concentration over the water column at each timestep.

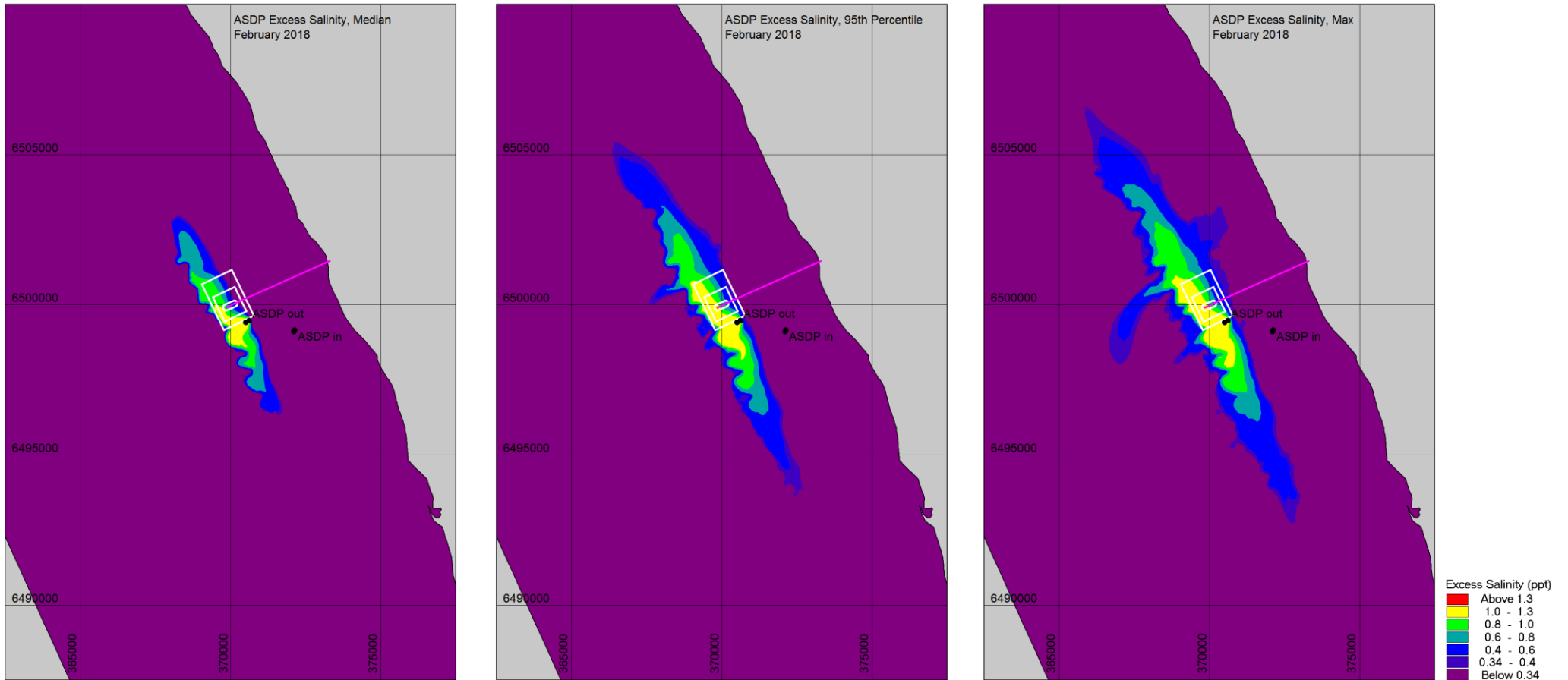


Figure B-12 Median, 95th percentile and maximum ASDP excess salinity. Monthly statistics (**February 2018**). Processed by first collapsing the 3D ASDP tracer output field to a 2D field containing the max concentration over the water column at each timestep.

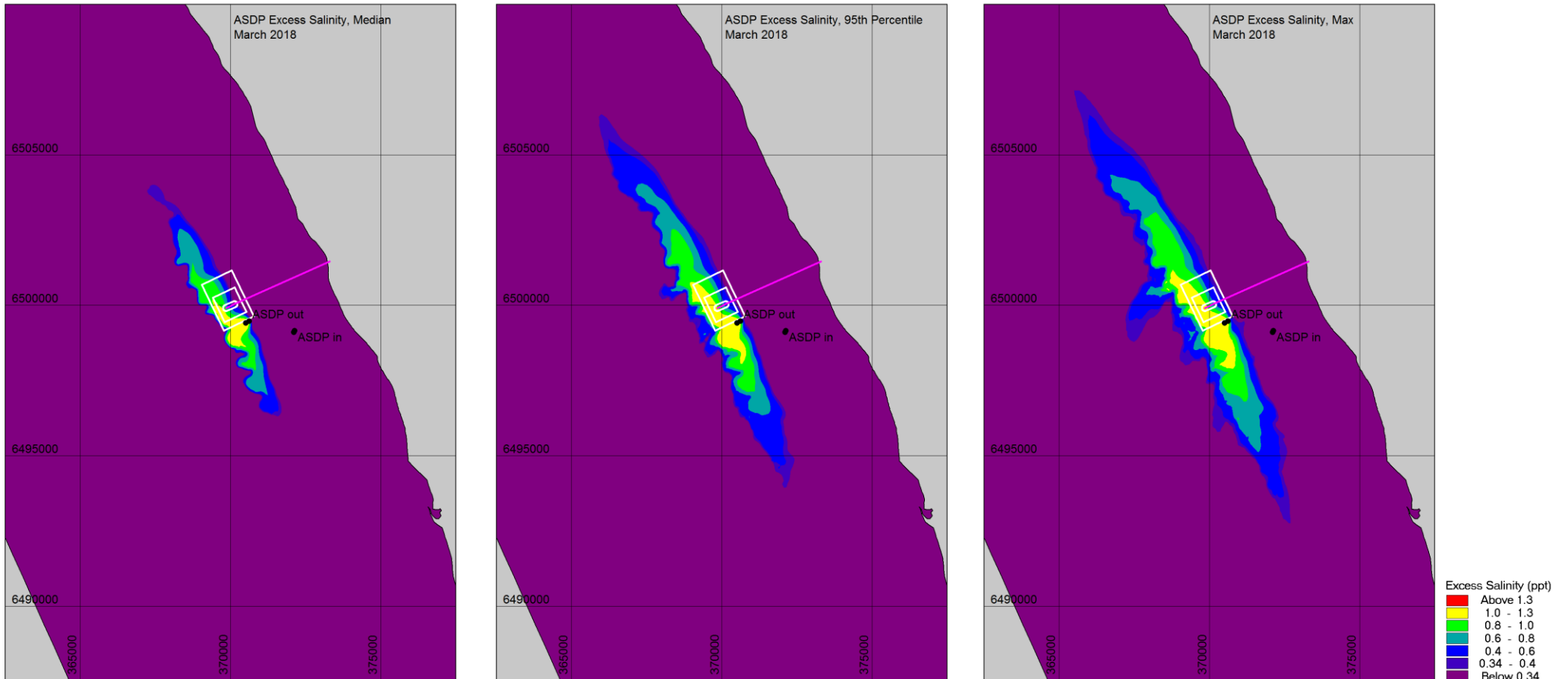


Figure B-13 Median, 95th percentile and maximum ASDP excess salinity. Monthly statistics (**March 2018**). Processed by first collapsing the 3D ASDP tracer output field to a 2D field containing the max concentration over the water column at each timestep.

APPENDIX C

WWTP S2 (Seafood Consumption) and S3 (Recreational) Mapping

C WWTP S2 (Seafood Consumption) and S3 (Recreational) Mapping

This appendix presents mapping of modelled WWTP-derived faecal indicator bacteria concentrations, with specific reference to the delineation of zones around the facility for safe consumption of seafood and recreation. Their specific definitions, per Water Corporation (2018) with subsequent clarification from BMT (2018).

- Consumption of seafood (Zone S2): median thermotolerant faecal coliform (TTC) bacterial concentration not to exceed 14 CFU / 100mL). This is to be assessed within 50cm of the bed, and so is calculated from the bottom layer of the model, with emphasis on the summer months of Dec-Mar.
- Primary or secondary recreational contact (Zone S3): maximum pooled Enterococci spp. must not exceed the NHMRC 'category A' guidance value of 40 Enterococci spp. MPN / 100mL). This is to be assessed within 50cm of the surface, and so is calculated from the top layer of the model, with emphasis on the summer months of Dec-Mar.

Figure C-1 provides mapping of the seafood and recreational criteria for the summer months of Dec – Mar. Figures C-2 through C-13 provide similar results by month in the sequence of the 12 month simulation, specifically April 2017 through March 2018.

All plots include overlays indicating the preferred ASDP intake and outfall locations.

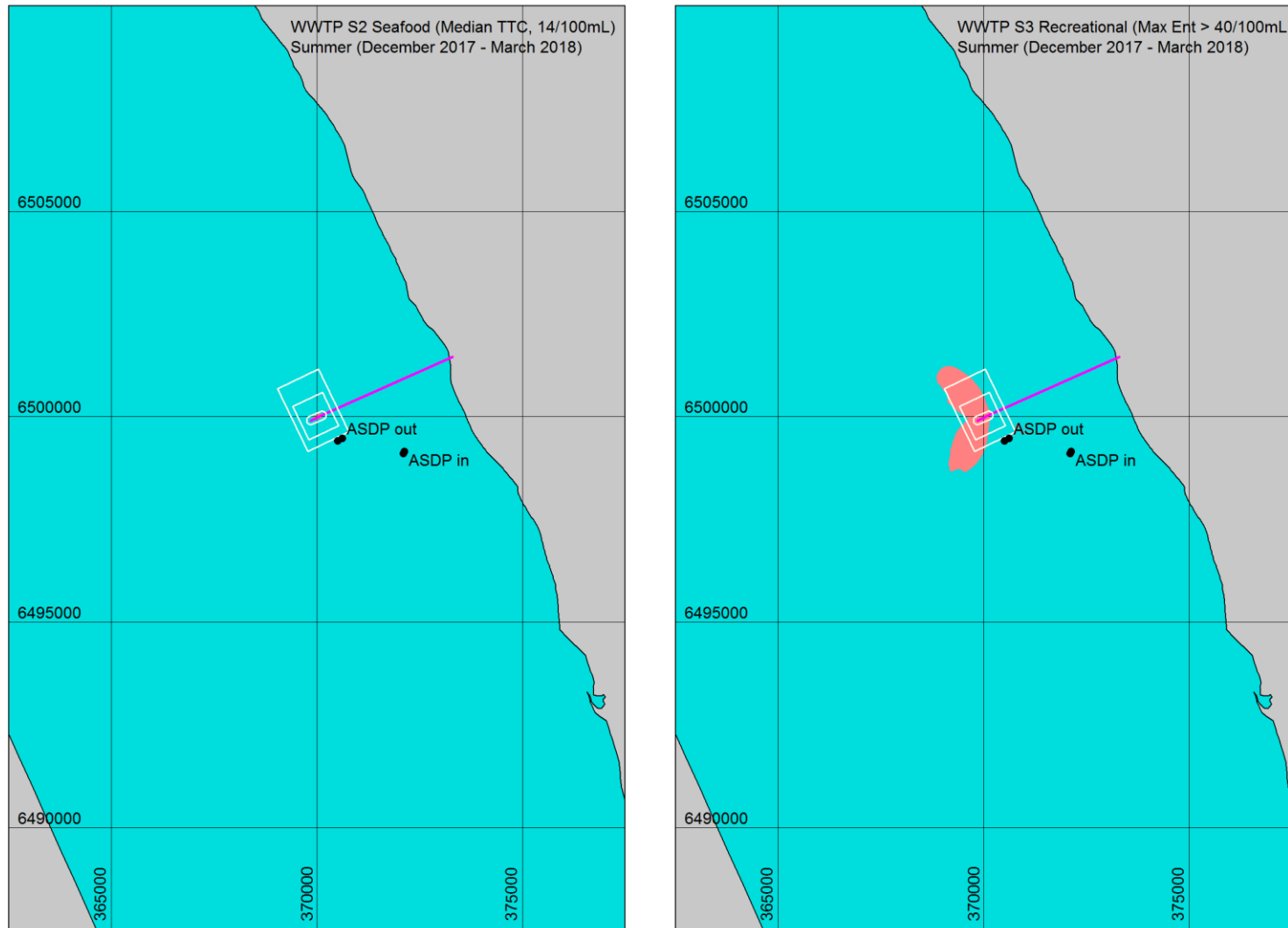


Figure C-1 Left: Exceedance of seafood consumption criteria (median TTC < 14 CFU / 100mL). Right: Exceedance of recreational criteria (max Enterococci < 40 MPN / 100mL). Summer statistics (Dec 2017 – March 2018).

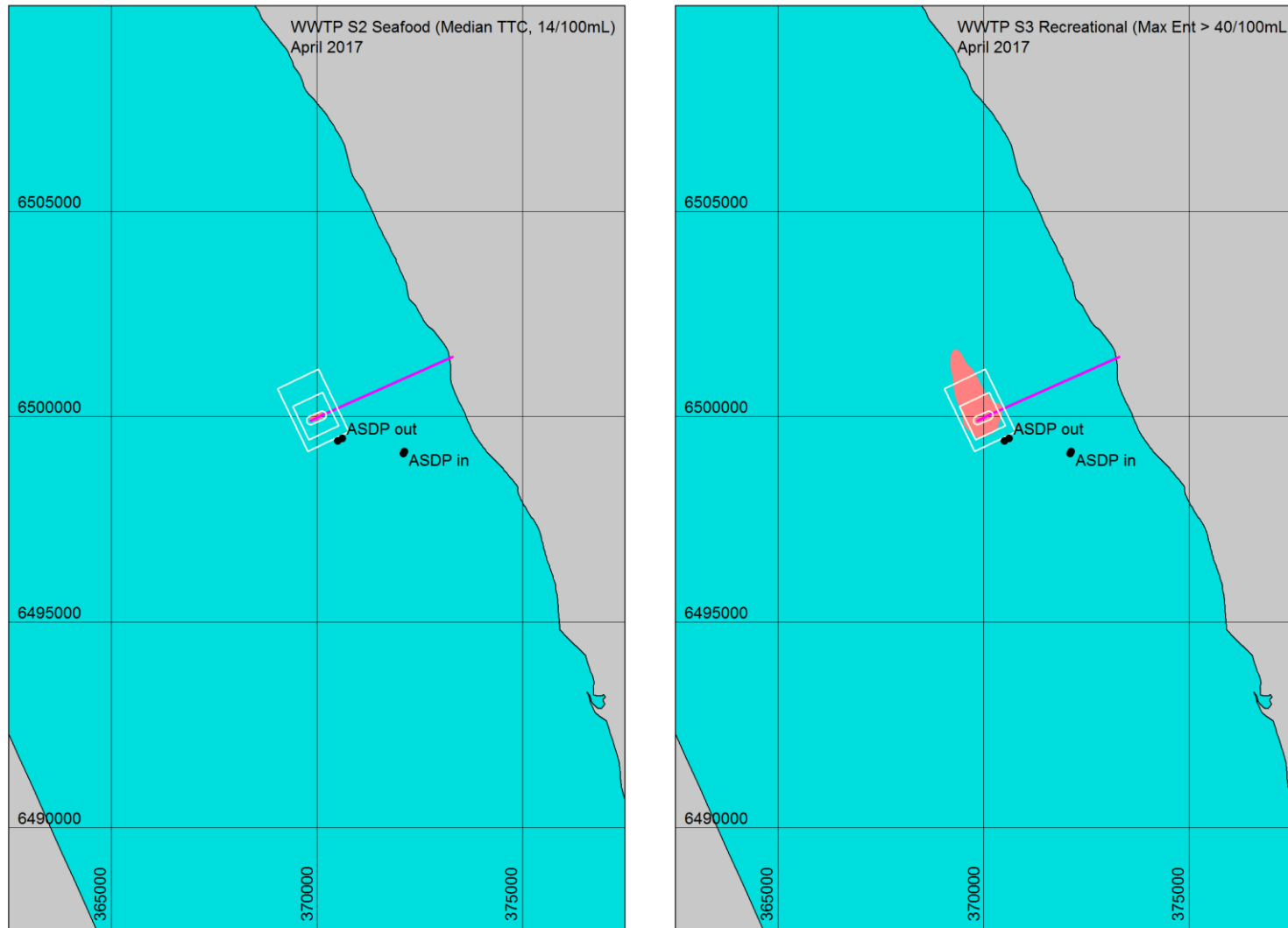


Figure C-2 Left: Exceedance of seafood consumption criteria (median TTC < 14 CFU / 100mL). Right: Exceedance of recreational criteria (max Enterococci < 40 MPN / 100mL). Monthly statistics (April 2017).

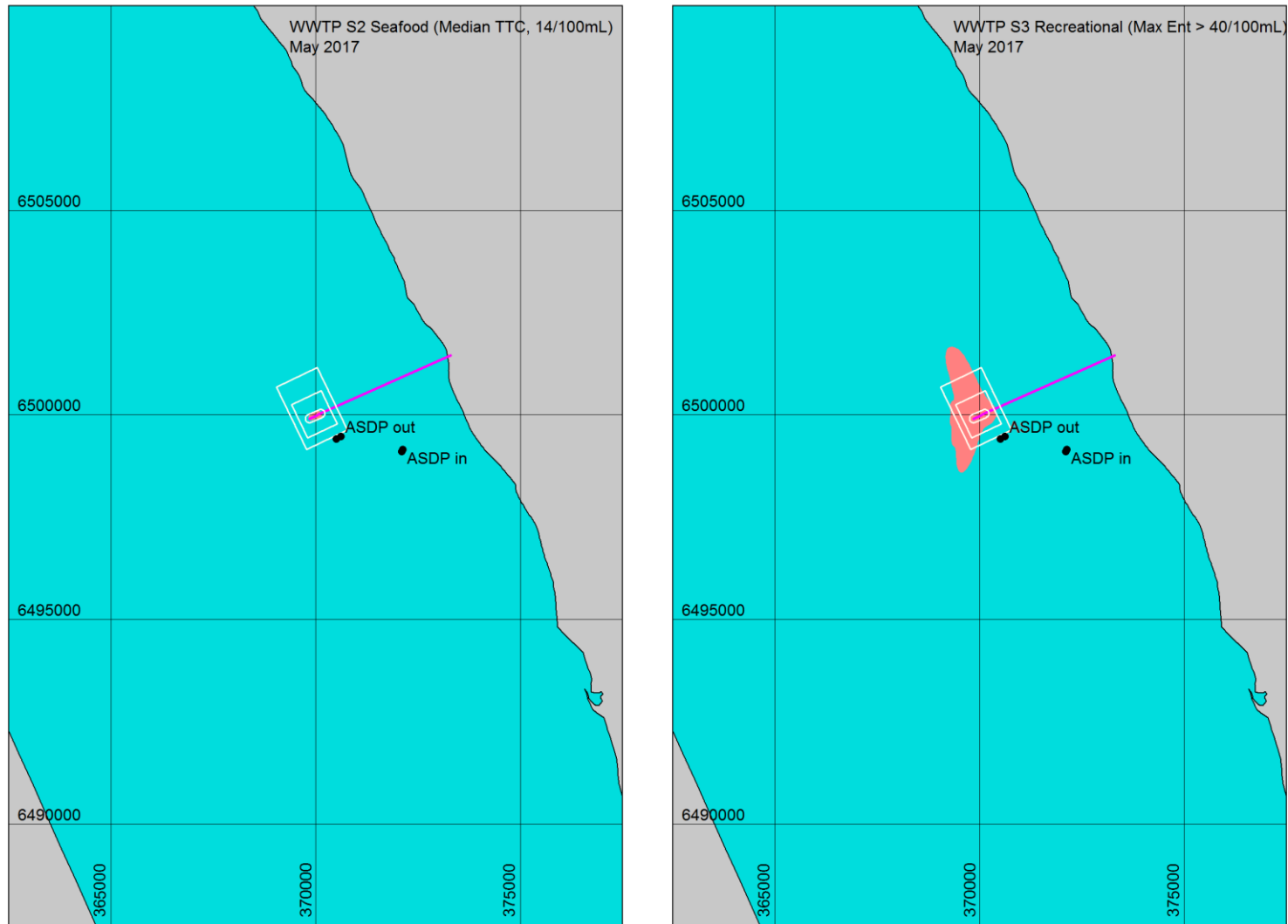


Figure C-3 Left: Exceedance of seafood consumption criteria (median TTC < 14 CFU / 100mL). Right: Exceedance of recreational criteria (max Enterococci < 40 MPN / 100mL). Monthly statistics (**May 2017**).

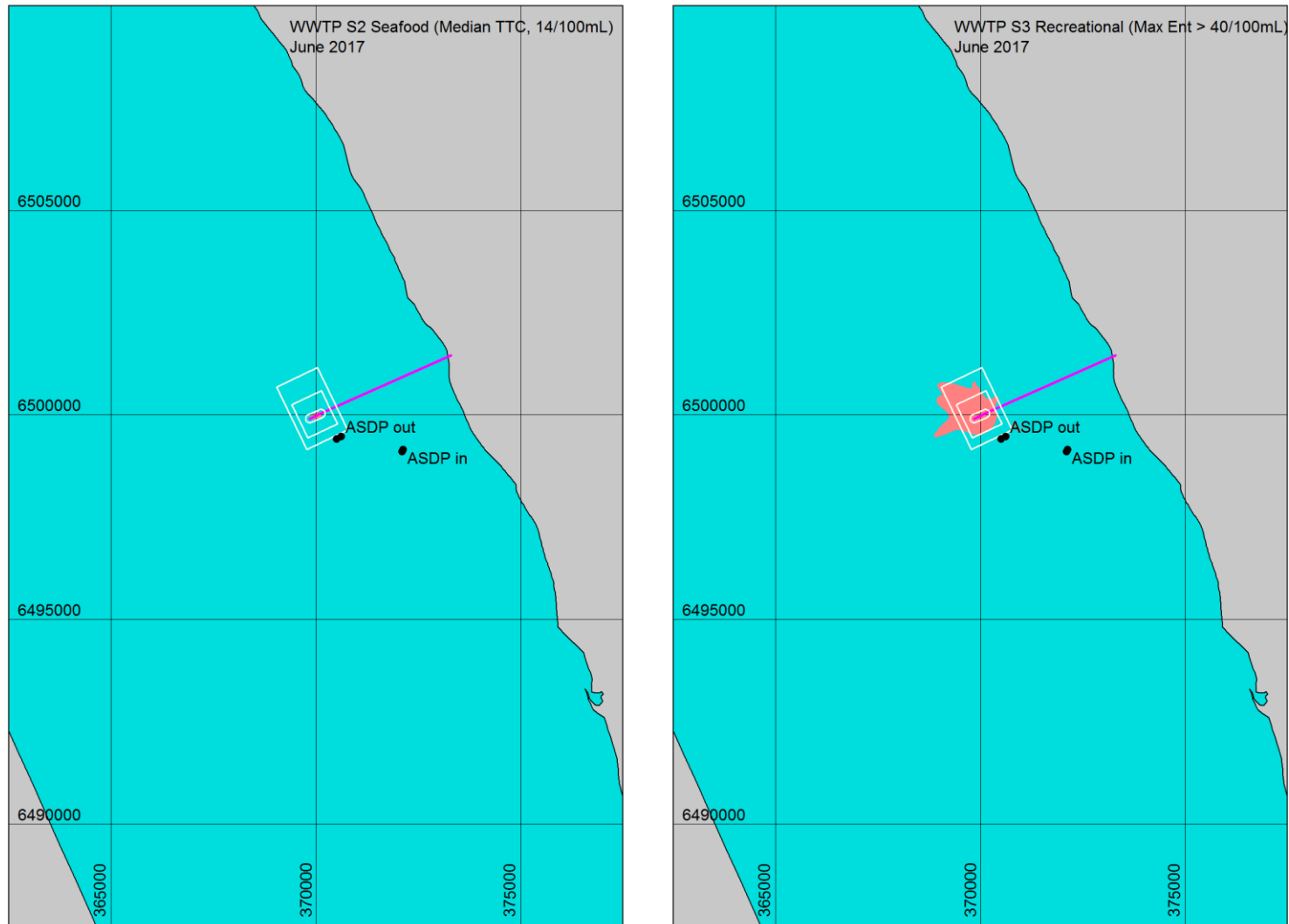


Figure C-4 Left: Exceedance of seafood consumption criteria (median TTC < 14 CFU / 100mL). Right: Exceedance of recreational criteria (max Enterococci < 40 MPN / 100mL). Monthly statistics (June 2017).

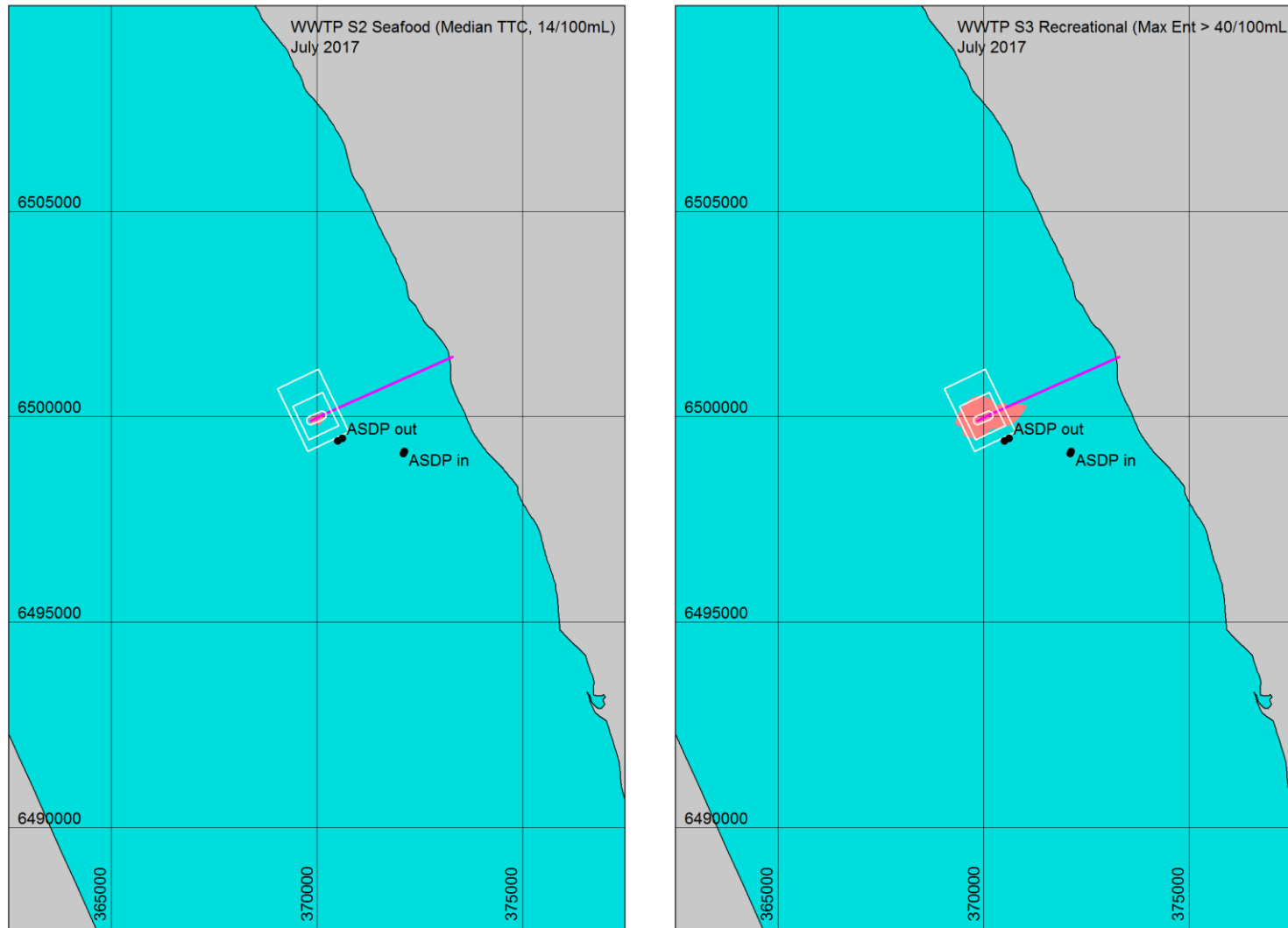


Figure C-5 Left: Exceedance of seafood consumption criteria (median TTC < 14 CFU / 100mL). Right: Exceedance of recreational criteria (max Enterococci < 40 MPN / 100mL). Monthly statistics (July 2017).

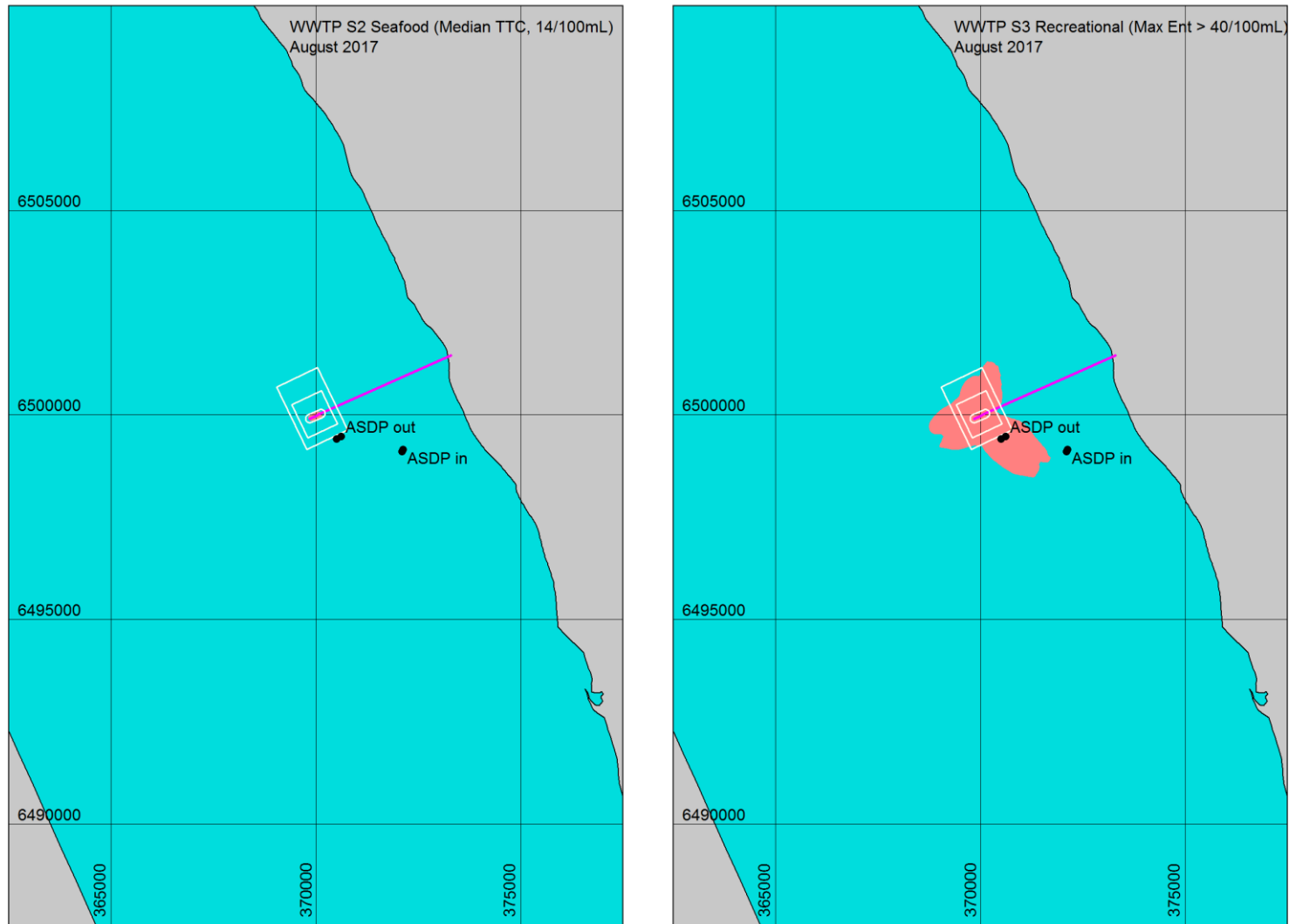


Figure C-6 Left: Exceedance of seafood consumption criteria (median TTC < 14 CFU / 100mL). Right: Exceedance of recreational criteria (max Enterococci < 40 MPN / 100mL). Monthly statistics (**August 2017**).

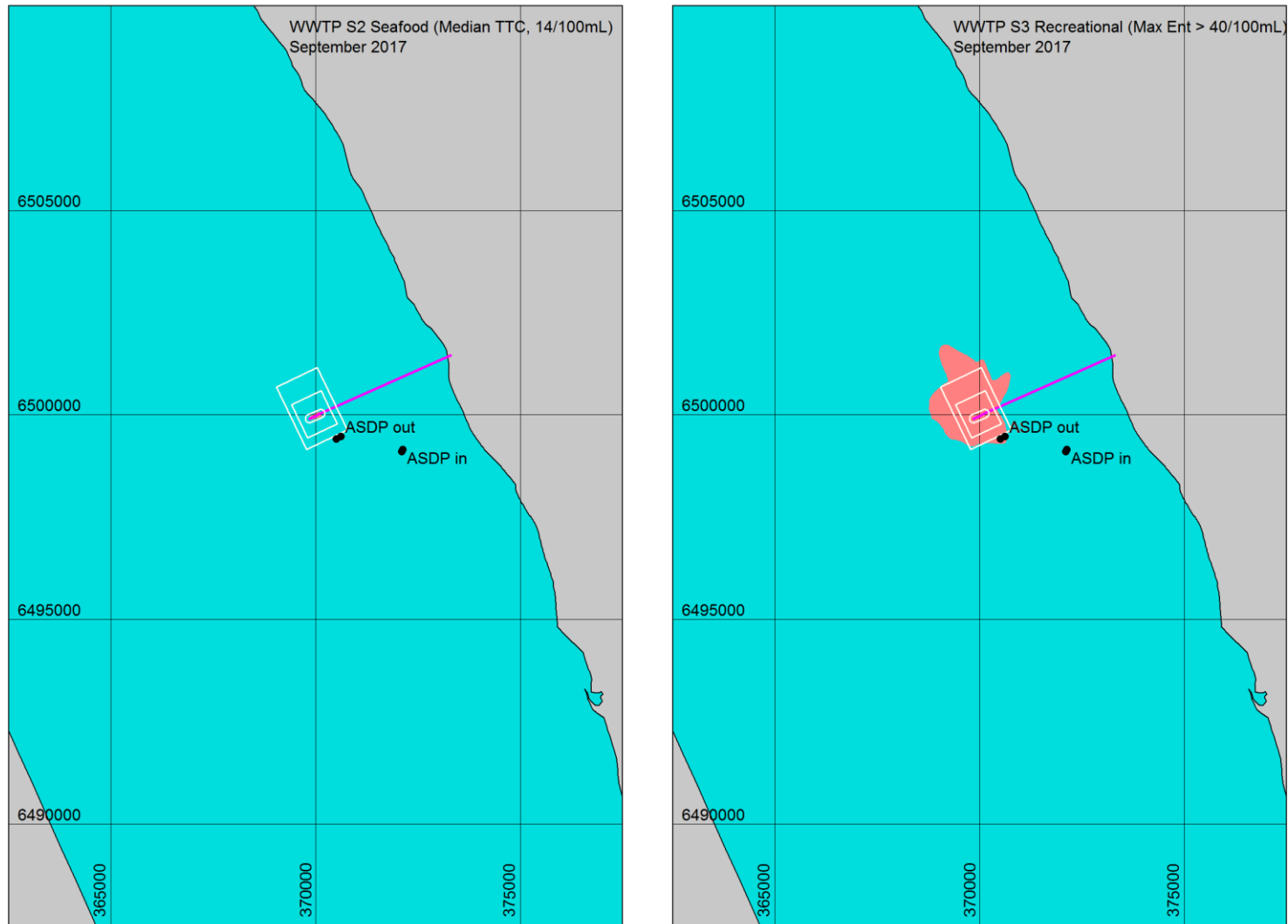


Figure C-7 Left: Exceedance of seafood consumption criteria (median TTC < 14 CFU / 100mL). Right: Exceedance of recreational criteria (max Enterococci < 40 MPN / 100mL). Monthly statistics (**September 2017**).

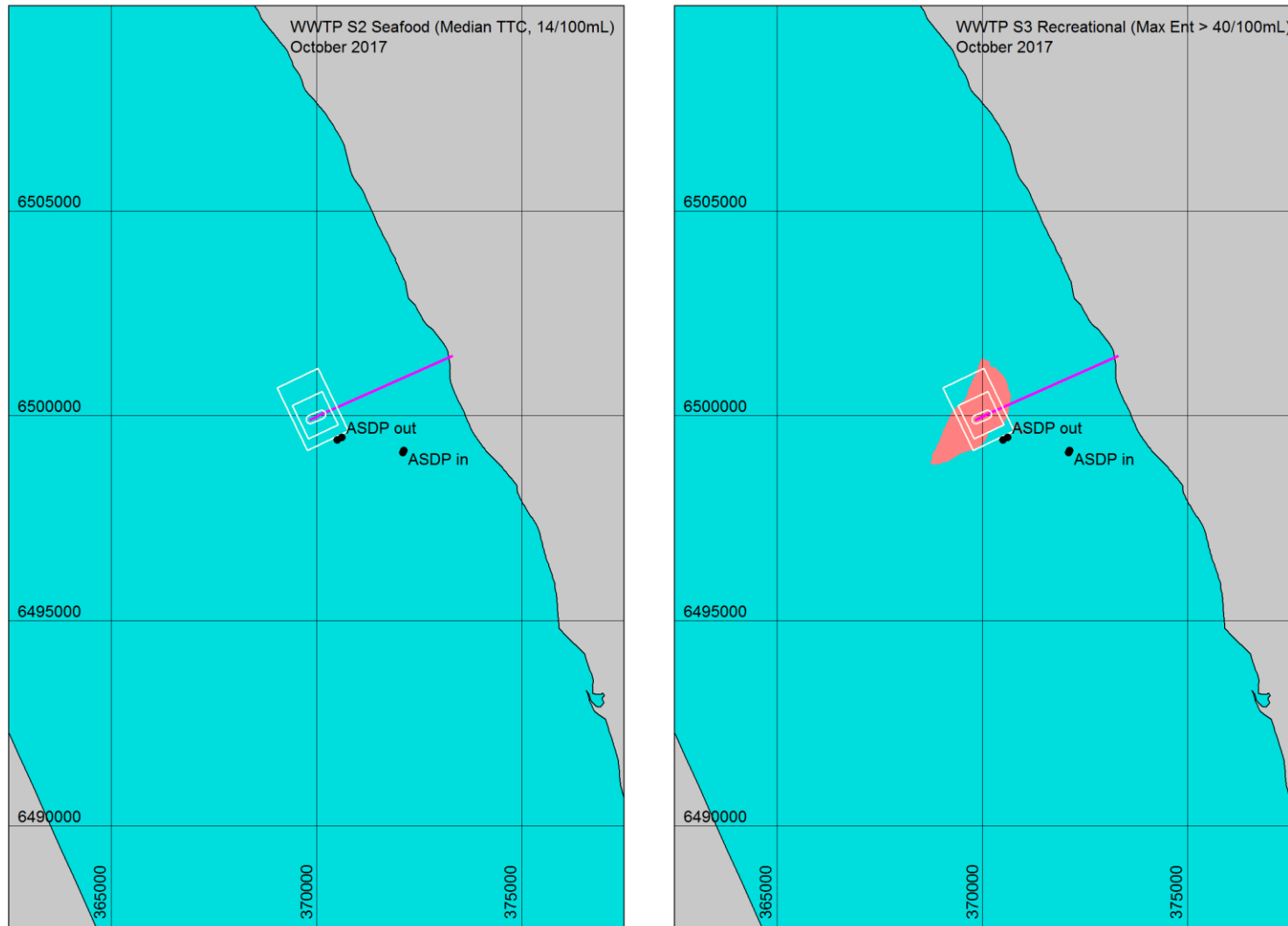


Figure C-8 Left: Exceedance of seafood consumption criteria (median TTC < 14 CFU / 100mL). Right: Exceedance of recreational criteria (max Enterococci < 40 MPN / 100mL). Monthly statistics (**October 2017**).

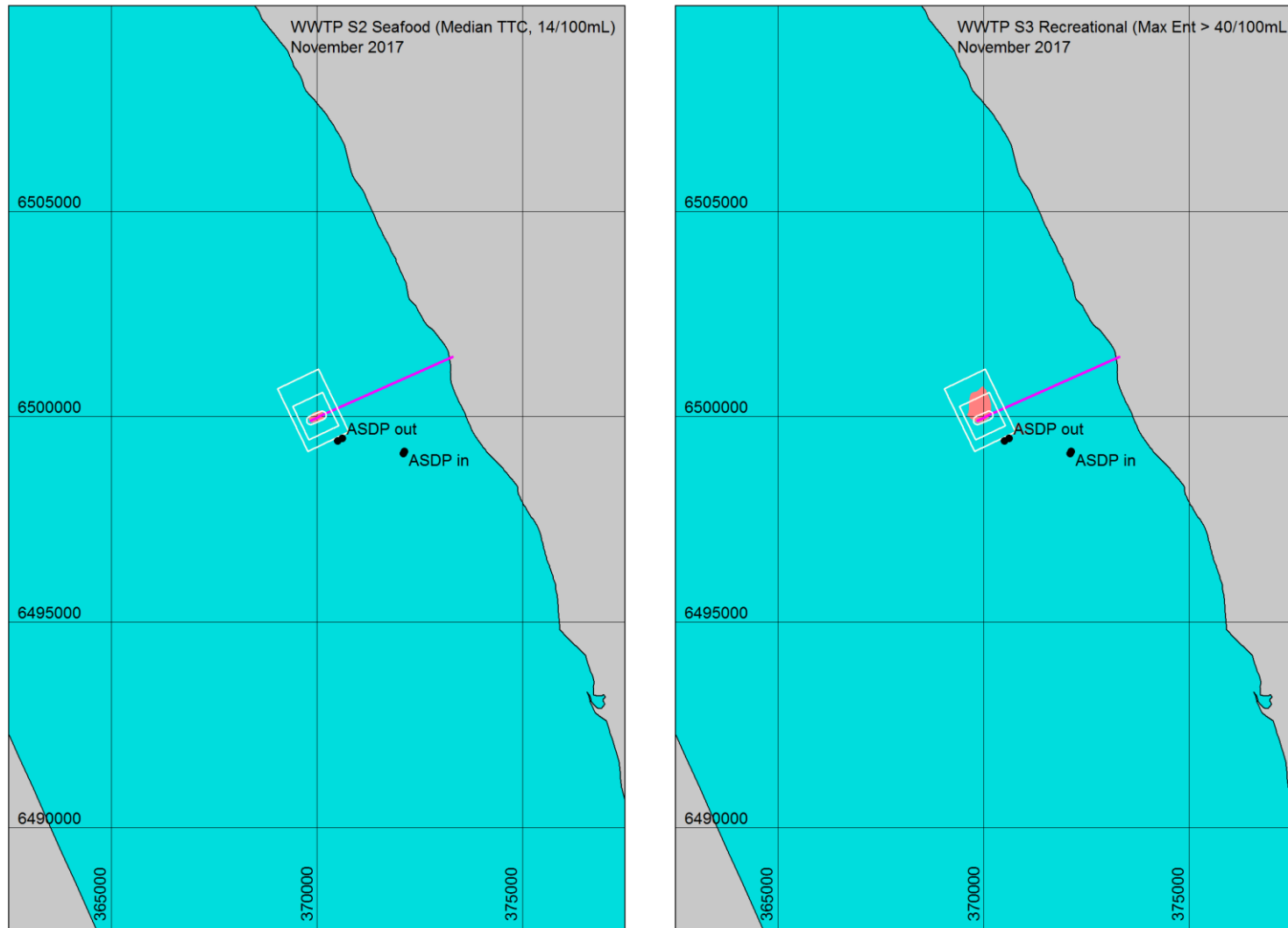


Figure C-9 Left: Exceedance of seafood consumption criteria (median TTC < 14 CFU / 100mL). Right: Exceedance of recreational criteria (max Enterococci < 40 MPN / 100mL). Monthly statistics (**November 2017**).

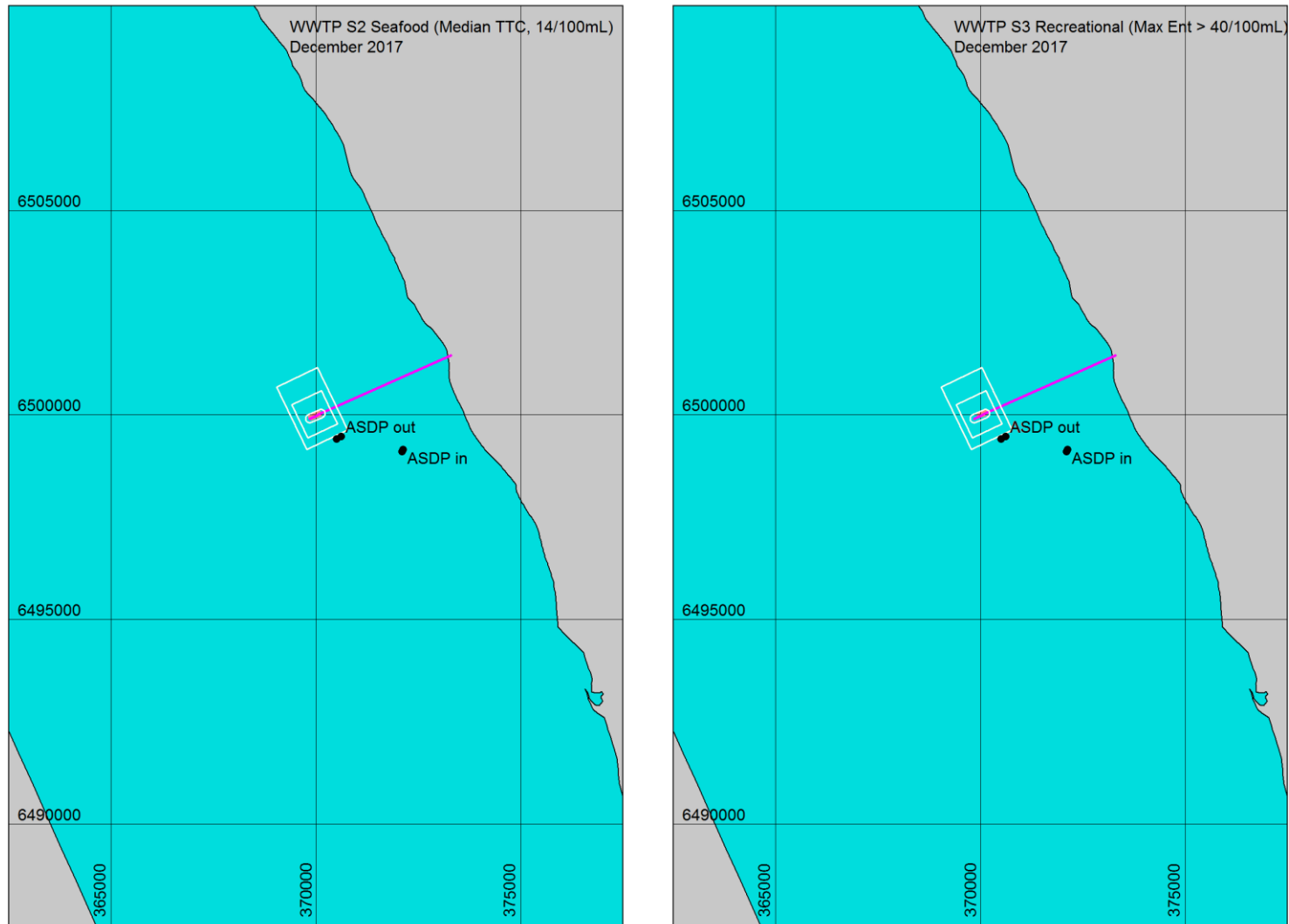


Figure C-10 Left: Exceedance of seafood consumption criteria (median TTC < 14 CFU / 100mL). Right: Exceedance of recreational criteria (max Enterococci < 40 MPN / 100mL). Monthly statistics (**December 2017**).

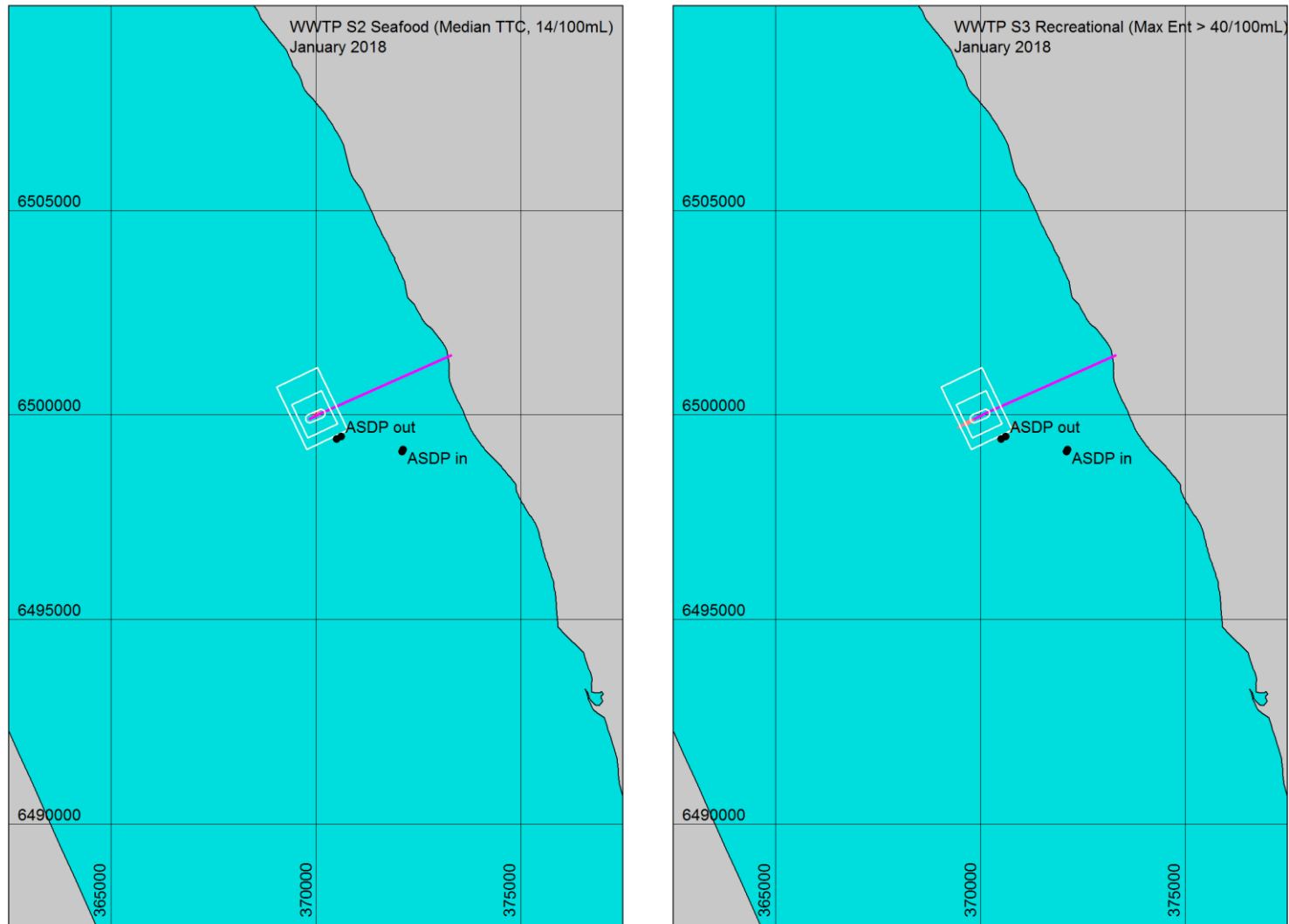


Figure C-11 Left: Exceedance of seafood consumption criteria (median TTC < 14 CFU / 100mL). Right: Exceedance of recreational criteria (max Enterococci < 40 MPN / 100mL). Monthly statistics (**January 2018**).

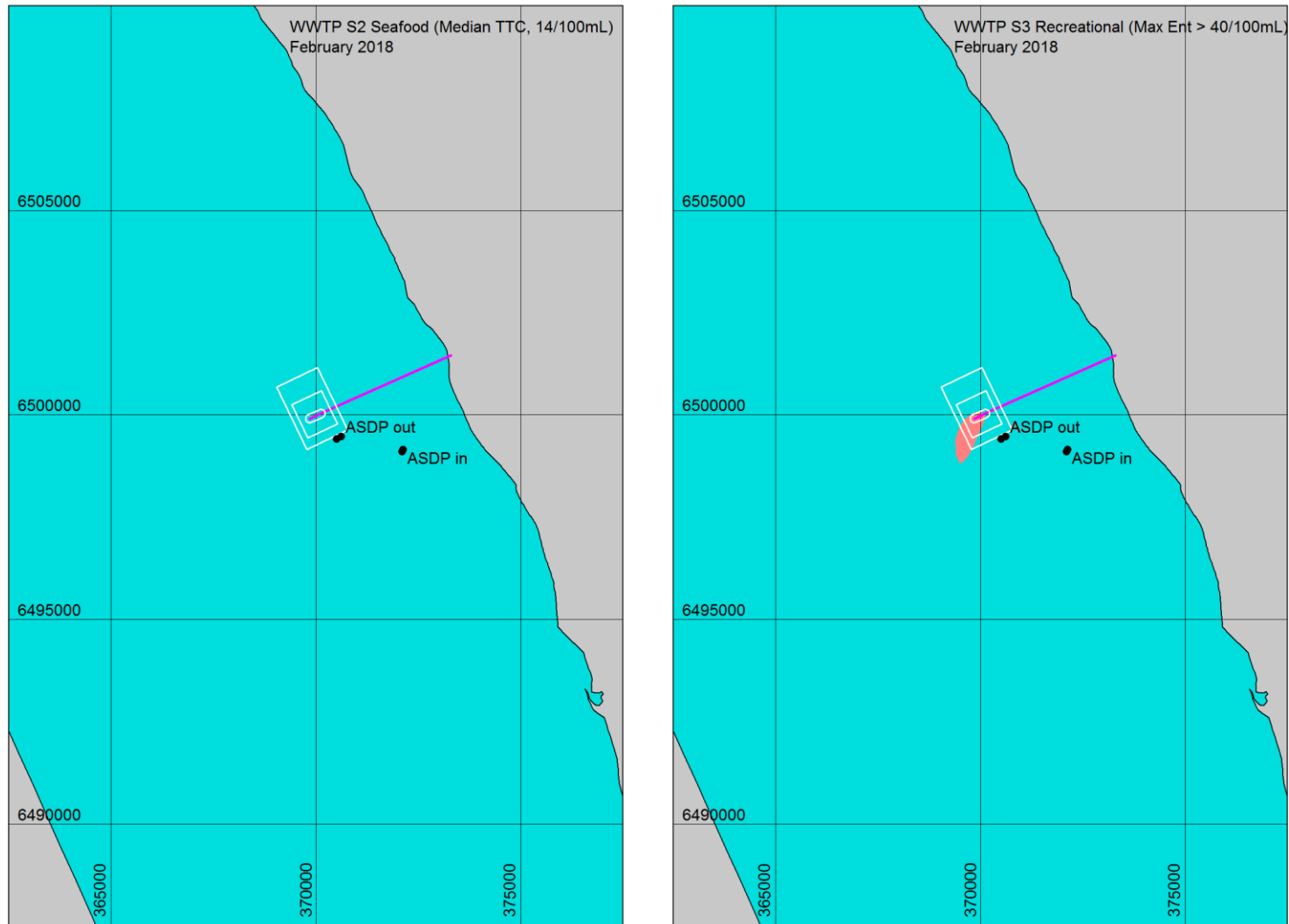


Figure C-12 Left: Exceedance of seafood consumption criteria (median TTC < 14 CFU / 100mL). Right: Exceedance of recreational criteria (max Enterococci < 40 MPN / 100mL). Monthly statistics (**February 2018**).

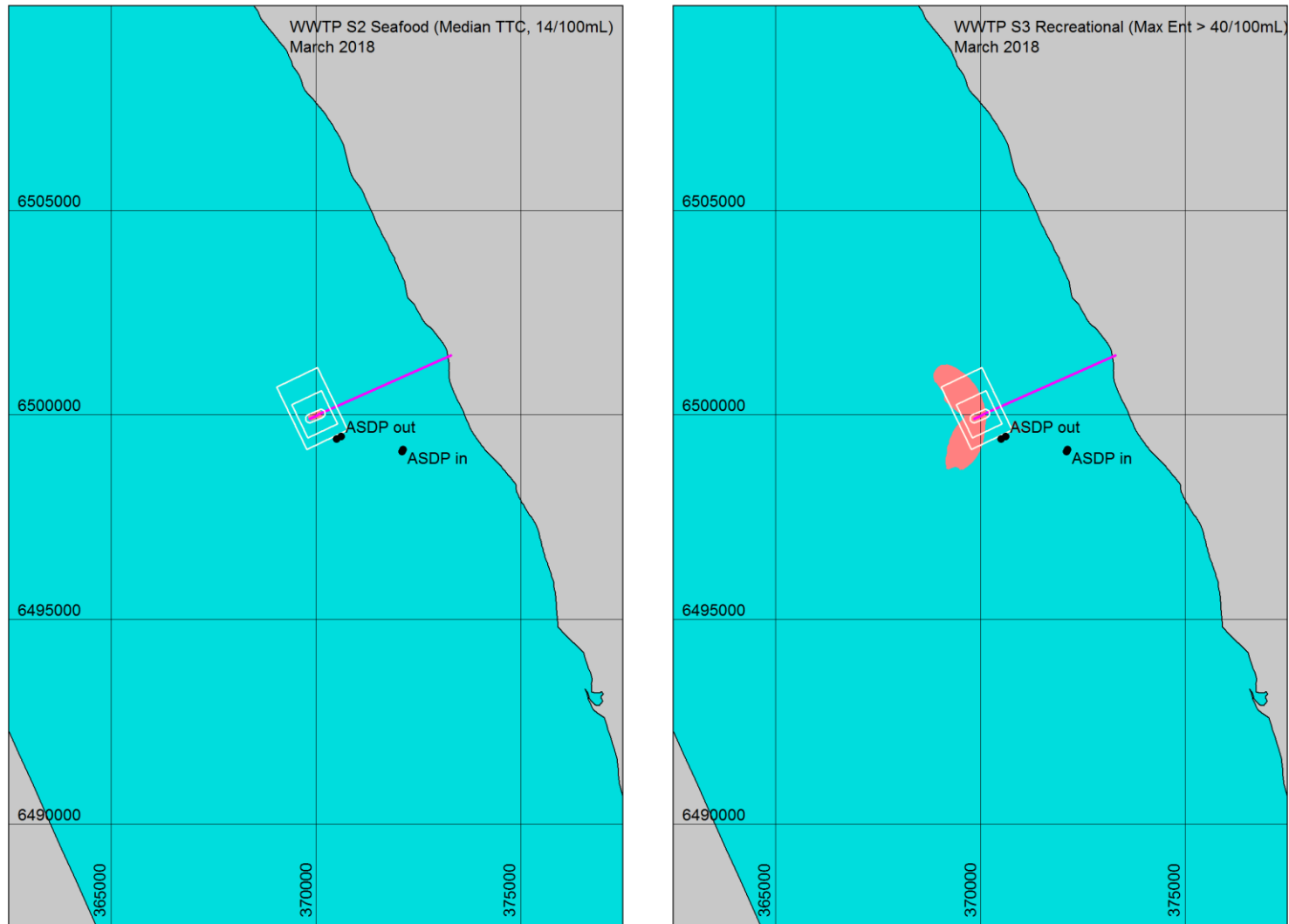


Figure C-13 Left: Exceedance of seafood consumption criteria (median TTC < 14 CFU / 100mL). Right: Exceedance of recreational criteria (max Enterococci < 40 MPN / 100mL). Monthly statistics (**March 2018**).

APPENDIX D

Dissolved Oxygen Saturation

D Dissolved Oxygen Saturation Fields

This appendix presents mapping of modelled fields of dissolved oxygen (DO) saturation. The anthropogenic aspect of this potential impact lies primarily with the additional near-bed residence time associated with stratification induced by the diluted brine wastefield of the ASDP. In terms of initial oxygen deficit, the WWTP discharge is far more significant than the ASDP. However, the initial dilution of the WWTP plume is far higher, its exposure to the seabed is far lower, and its mobility at the surface is far greater than is the ASDP discharge.

The result fields presented in this appendix are calculated from the bottom layer of the 3D model. The bottom layer is then assessed in terms of the non-exceedance of 90% DO saturation, evaluated as a median over a running 7 day window.

Figure D-1 provides a map of the exceedance of this criteria over the full annual simulation. These exceedances are seen to all occur within the three months of April, May and June 2017, the results of which are shown in Figures D-2, D-3 and D-4, respectively. The remaining months are blank fields and omitted for brevity.

It should be noted that the violations of the median 90% saturation criteria as plotted are only slightly below this threshold. The minimum 7-day median DO saturation over the year is 88%.

All plots include overlays indicating the preferred ASDP intake and outfall locations.

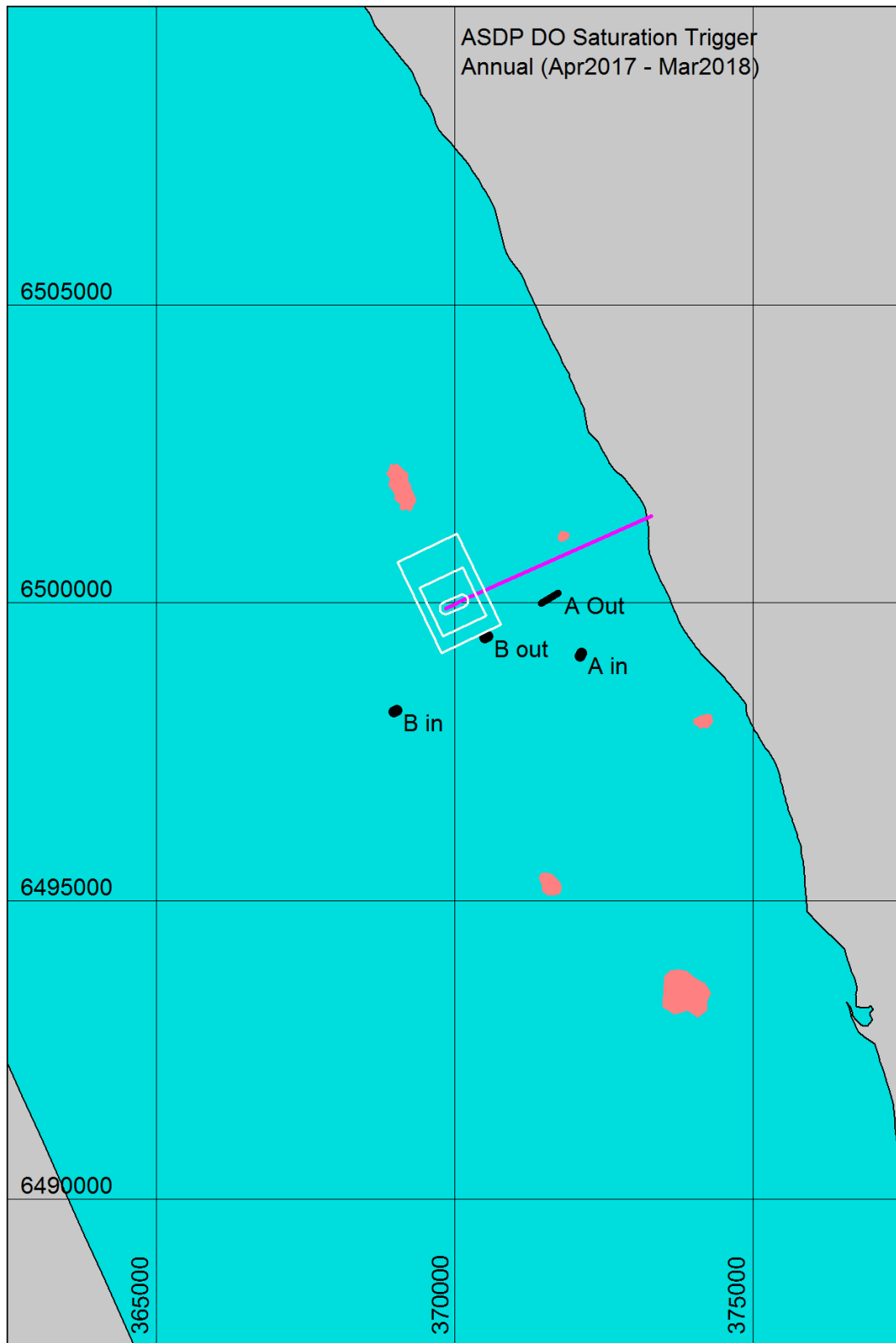


Figure D-1 Annual exceedances of the DO saturation > 90% criteria (as 7-day running median). Annual statistics (April 2017 – March 2018), bottom layer.

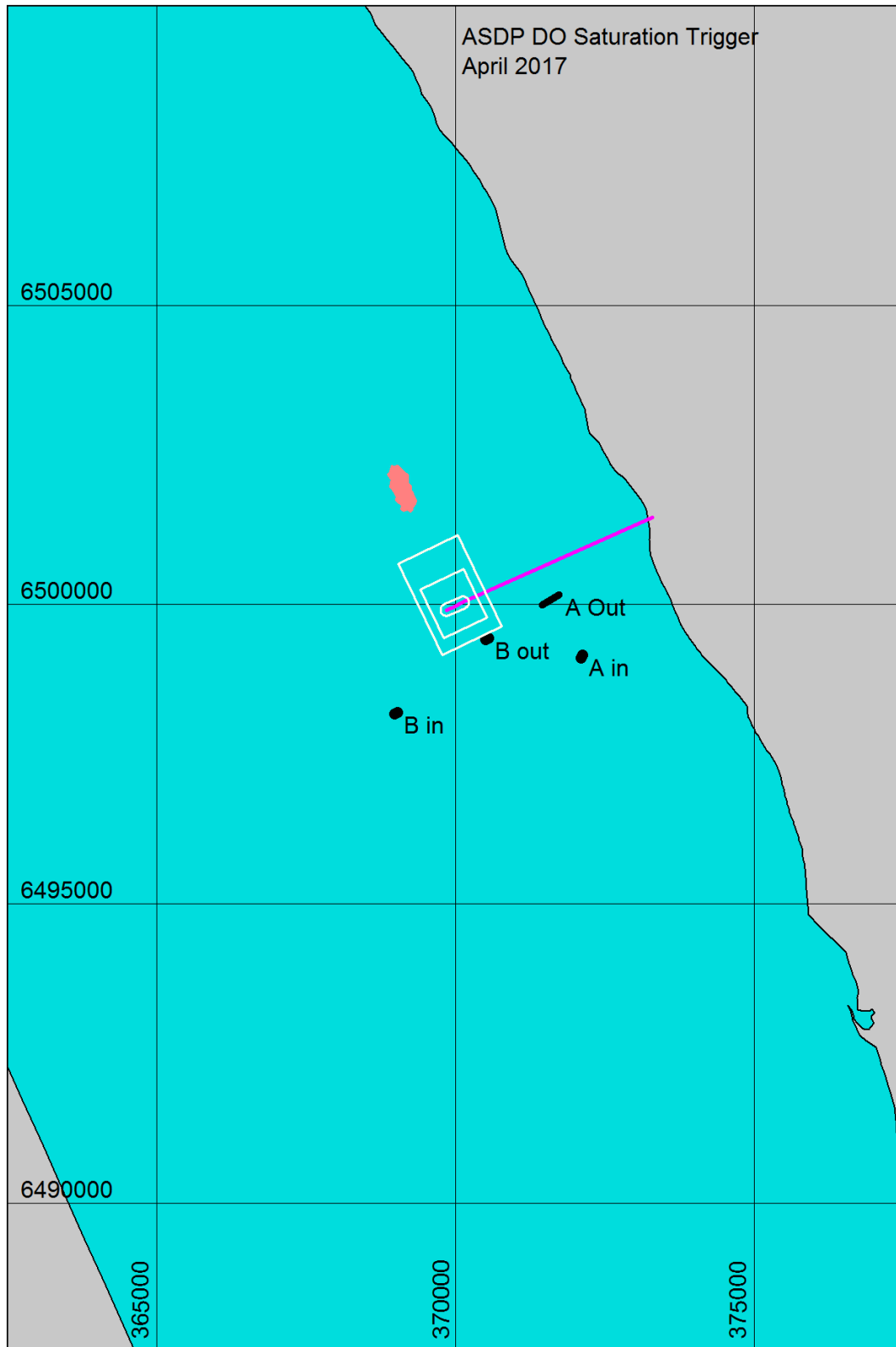


Figure D-2 Monthly exceedances of the DO saturation > 90% criteria (as 7-day running median). Monthly statistics (April 2017), bottom layer.

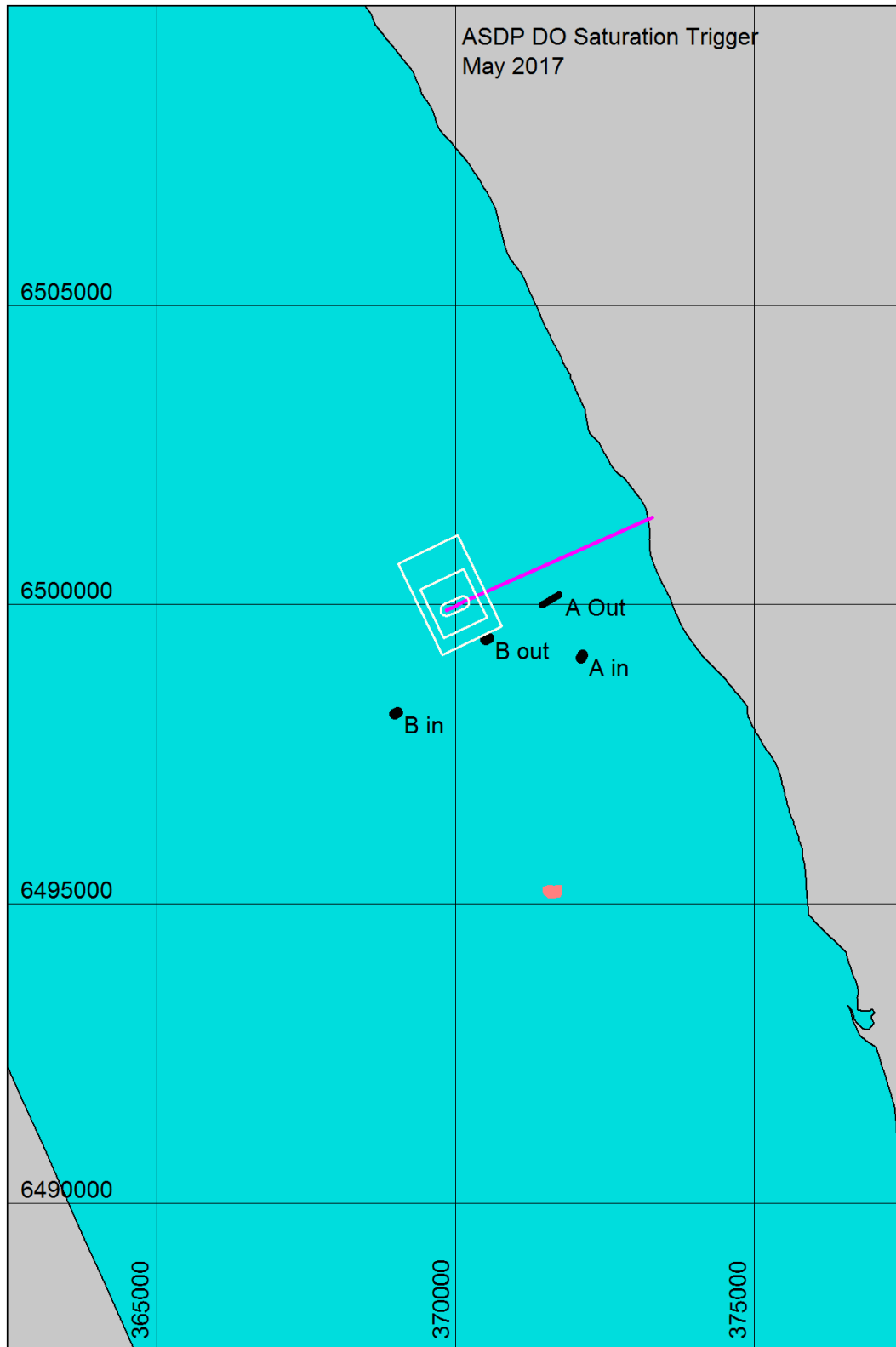


Figure D-3 Monthly exceedances of the DO saturation > 90% criteria (as 7-day running median). Monthly statistics (May 2017), bottom layer.

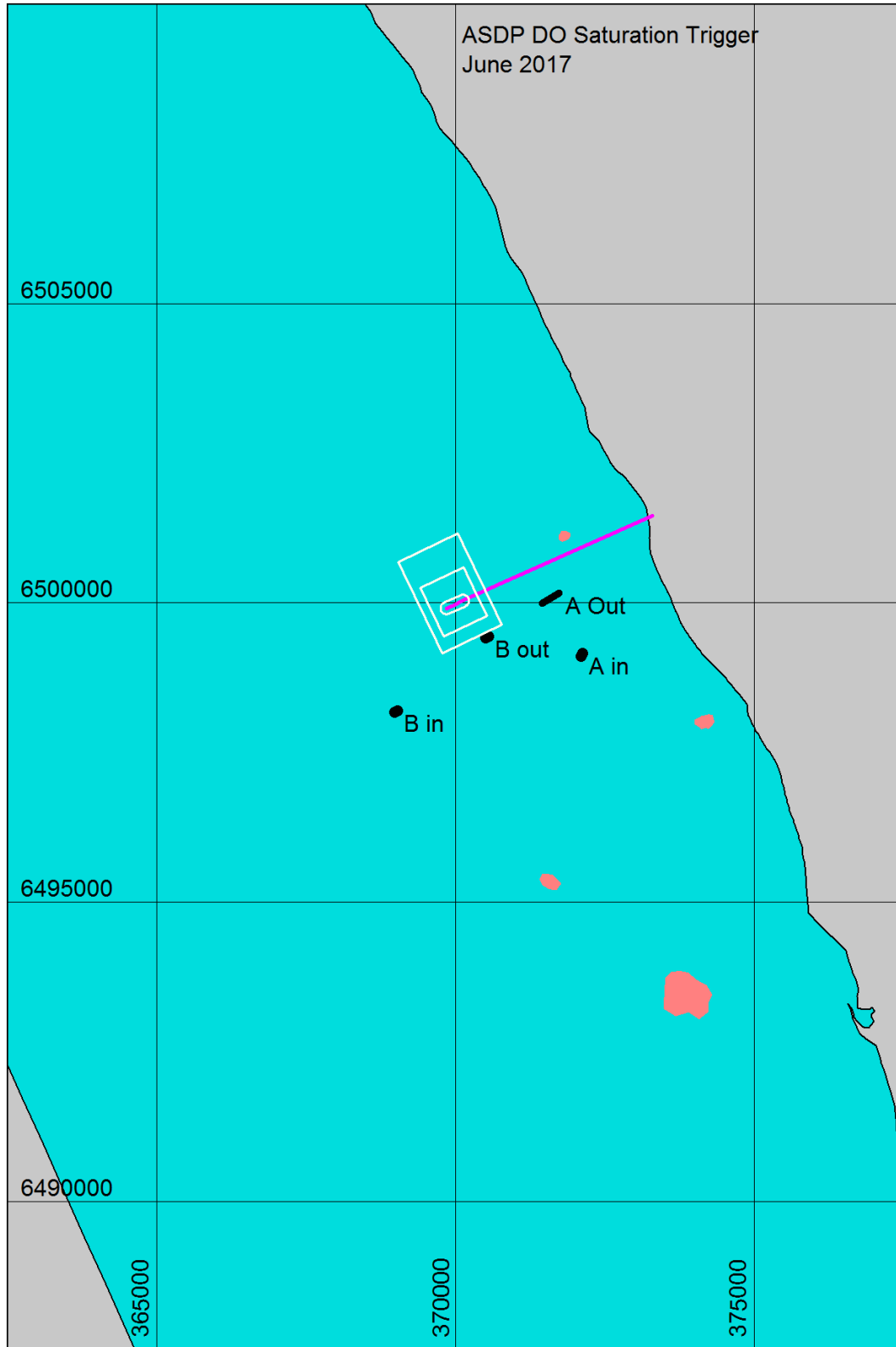


Figure D-4 Monthly exceedances of the DO saturation > 90% criteria (as 7-day running median). Monthly statistics (June 2017), bottom layer.